NUMERICAL MODELLING OF PIPELINE CONSTRUCTION

Alexander Dunstone

The University of Adelaide
School of Mechanical Engineering
South Australia 5005
Australia

Submitted for the degree Doctor of Philosophy, February, 2004

ABSTRACT

During the construction of pipelines, the girth welds, which join pipe sections, are placed under various stresses. The stresses are due to mechanical handling loads such as those that occur when lifting the front end of the pipeline to place it on supports as well as thermal stresses due to the welding thermal cycle. These stresses, combined with the presence of hydrogen from cellulosic electrodes, can produce hydrogen assisted cold cracking (HACC) in the root pass of pipeline girth welds. HACC can cause catastrophic failure of a pipeline girth weld. By reducing the residual stress and hydrogen concentration experienced in a pipeline girth weld, the risk of HACC is also reduced. The method used in this study to reduce the residual stress and hydrogen concentration is modification of the construction procedure.

A numerical model of the pipeline construction process has been created. After surveying the literature this appears to be the first model capable of modelling the process in a transient sense. This is extremely useful as the residual stress and hydrogen diffusion is not only dependant on the application of process parameters but also their timing.

In order to validate the modelling scheme developed, an experiment was conducted using the 'Blind Hole Drilling' strain gauge method of residual stress measurement. There was sufficient agreement between numerical and experimental results to indicate that the numerical modelling procedure was capable of conducting a study of pipeline construction.

The use of cellulosic electrodes for the welding of pipelines in Australia is preferred. Such electrodes possess certain favourable running characteristics suited to pipeline construction but unfortunately produce a very large amount of diffusible hydrogen, leading to saturation of the weld metal. The diffusion of hydrogen has been modelled using a scheme based on Fick's Second Law of Diffusion. The parameters reported to dominate the rate of diffusion are the timing of the weldment passes, the joint geometry, pre-heating and post-heating, all of which have been investigated in this thesis.

This study has highlighted the influence of process parameters on the resulting residual stress and hydrogen diffusion. By analysing the pipeline construction process in a transient sense, an understanding of the transient risk of HACC has been developed. This has enabled recommendations regarding procedural changes to be made to the pipeline industry.

STATEMENT OF ORIGINALITY

This thesis contains no material which has been accepted for the award of any other degree or diploma in any university or other tertiary institution, and to the best of my knowledge, contains no material previously published or written by another person, except where due reference has been made in the text.

I give consent to this copy of my thesis, when deposited in the University Library, being made available for loan and photocopying.

Alexander Dunstone, 1st of February 2004.

ACKNOWLEDGEMENTS

The work reported here was undertaken as part of a research project of the Cooperative Research Centre for Welded Structures. The Cooperative Research Centre for Welded Structures was established by and is supported under the Australian Government's Cooperative Research Centre Program.

I would like to thank my supervisors Dr Mike Painter, Dr Muhammad Wahab and Dr Ben Cazolato for their assistance and encouragement. I am particularly grateful for the guidance and support of Dr Mike Painter who was always my first port of call. Professor Valerie Linton and Ian Brown also provided useful comments on the work which was appreciated.

NOTATION

a, b, c Geometric parameters (width, depth and length) of Goldak's double ellipsoidal heat source

α Thermal diffusivity

A X-sectional area of pipe

A_C Area over which pipe line-up clamp is applied

A_i Inside area of pipe

A_o Outside area of pipe

$\bar{A}$ Residual stress rosette calibration constant

A_P Area of line up clamp plunger

$\bar{B}$ Residual stress rosette calibration constant

C Concentration of hydrogen

c_p Specific heat

d Diffusivity

D Diameter of hole drilled

D_i Inside diameter of pipe

D_{max} Maximum diameter caused by pipe ovality

D_{min} Minimum diameter caused by pipe ovality

D_0 Diameter of the gauge circle

D_P	Diameter of plunger
E	Young's modulus
F_C	Clamping force
F_H	Force on line up clamp plunger
F_n	Force on node
ΔH	Change in enthalpy
I	Current
$1/K_1$	Residual stress rosette sensitivity constant
n	Number of nodes in x-section
MF	Multiplication Factor
P	Pneumatic pressure
P_C	Clamping pressure
q	Heat generation
q_{de}	Heat generation applied to a node within a double ellipsoidal heat source.
q_{nodal}	Corrected nodal heat generation.
Q_{de}	Summation of nodal heat generation within a double ellipsoidal heat source.
Q_{total}	Total heat generation determined by welding heat input and arc efficiency.
R	Constant used to calculate diffusivity
R_i	Inside radius of pipe

R_m	Mean radius of pipe
R_o	Outside radius of pipe
t	Time
T	Temperature
V	Voltage
v	Welding velocity
W	Width over which clamp is applied
x, y, z	Coordinates
β	Angle between gauge one and principle stress
$\varepsilon_1, \varepsilon_2, \varepsilon_3$	Strain from gauges number 1, 2 and 3
ε_A	Total axial strain before drilling at applied load
$\Delta\varepsilon_A$	Total axial strain change after drilling at applied load
$\Delta\varepsilon_T$	Total tangential strain change after drilling at applied load
η	Arc efficiency
λ	Thermal conductivity
ν	Poisson's ratio
$\nu K_2/K_1$	Residual stress rosette Poisson's ratio
ξ	Position relative to moving arc
σ_{max}	Maximum principal stress

σ_{min}	Minimum principal stress
σ_n	Stress on node
∇	Operator
∇^2	Spatial distribution

LIST OF FIGURES

LIST OF TABLES

TABLE OF CONTENTS

Chapter 1

INTRODUCTION

A number of factors influence the tendency toward hydrogen assisted cold cracking (HACC) in ferrous weldments. It is generally recognised that the important factors are the presence of hydrogen, a hard susceptible microstructure and an applied stress. HACC is a phenomenon that is particularly relevant to the construction of gas pipelines, which exhibit all of these factors. Significant resources must be put into place to manage and monitor girth welding to avoid the possibility of HACC. Increased knowledge about the phenomenon and how it is influenced by construction parameters will have a major economic impact on pipeline construction.

The present study is motivated by three rationales. First, from past experience it is known that enormous expense in terms of loss of life, lost revenue and repair costs can result from HACC in girth welds during construction of gas pipelines. One such example occurred during the construction of the Moomba to Sydney pipeline in 1974. Today the occurrence of weld failure is low, however the potential risk and cost of hydrogen cracking still warrants further research.

Second, currently there is a push toward using higher strength pipe material. If X80 or X100 strength pipe can be safely used there will be a significant material saving through the use of thinner walled sections. The use of higher strength material will however require more stringent measures to avoid HACC. In order to implement these measures further research on HACC specifically related to pipeline construction is needed.

Finally, the speed of pipeline construction is the major determinant of pipeline construction cost. Methods are being considered by the pipeline industry to achieve an increase in construction speed; however they have implications with regard to increased risk of HACC as explained later in Chapter 2. It is clear that the prevention of HACC, while striving to reduce costs, requires further research.

The level of applied and induced stresses and their variation during the post weld period is particularly relevant to the possibility of HACC during pipeline construction. This has been recognised by a number of researchers, (Fletcher et al, 1999 and Glover et al, 1999), but determining these stresses and their relationship with process parameters is not a simple task.

A large amount of work has been done in the field of welding residual stress by researchers in the past. From the literature it is clear that while good progress has been made on numerical prediction and experimental measurement techniques, large discrepancies are often found between them. Experimental measurement techniques are also difficult to use to conduct a study over a wide variety of process parameters as they are very time consuming.

This type of study therefore lends itself to numerical prediction. Numerical modelling also offers the advantage that the transient stress field can be considered, which is important when studying a construction procedure heavily dependant on time. Numerical prediction can highlight trends which provide a greater insight into the stress evolution experienced by a girth weld.

The rate of hydrogen diffusion is also an important factor in the potential for HACC. The diffusion rate is highly dependant on the temperature cycle and geometry of the material. Numerical models of hydrogen diffusion, while difficult to verify, can highlight trends when considering various process parameters.

Establishing the transient response of the stress evolution, hydrogen diffusion, temperature cycle and the variation with construction variables, will help develop an understanding of the transient risk of HACC. This enables modification of the construction procedure which can reduce the chance of HACC while not inhibiting the progress of front end construction. Also restrictions placed on construction procedures such as the time of release of the line-up can be investigated for potential increases in the pace of construction (the major determinant of construction cost).

1.1 OBJECTIVE

The objectives of this work are to study the evolution of the temperature, stress and hydrogen concentration that occur in the root pass of a pipeline girth weld during construction. Furthermore, to investigate the influence of various process parameters and relate this knowledge to the likelihood of HACC.

1.2 SCOPE

This present study commences with the background behind the problem of HACC in pipeline girth welds. The welding technique used is explained and the pipeline construction procedure is described. The literature relating to:

- stress due to mechanical handling loads applied to pipelines,
- thermal modelling of the welding process,
- analytical, experimental and numerical calculation of residual stress in circumferential welds and
- hydrogen diffusion modelling of the welding process is reviewed.

The approach taken in this current study is to develop and experimentally verify comprehensive numerical simulations of the pipeline construction process and use these to study the stress evolution experienced in a pipeline girth weld during pipeline construction. The finite element method was used to calculate the thermal and the stress cycle due to thermal (weld related) and mechanical loads which are applied to the girth weld during

construction. It appears that this present study is the first time the stress cycle in a pipeline girth weld has been analysed in a transient sense, which allowed consideration of the timing of the process.

Numerical models of hydrogen diffusion throughout the weld piece after welding are developed, based on Fick's Second Law of Diffusion. Modelling of hydrogen diffusion allowed consideration of factors such as pre-heating the near weld region and the effect of the hot pass. The transient evolution of hydrogen concentration was able to be compared with that of the temperature and stress in a typical girth weld. This facilitated a transient view of HACC in pipeline girth welds to be developed.

Chapter 2

HISTORICAL OVERVIEW

2.1 INTRODUCTION

Hydrogen assisted cold cracking is a phenomena that can lead to great expense when constructing pipelines (Hart, 1999). In order for HACC to occur there are three essential ingredients; a hard susceptible microstructure, a source of hydrogen and an applied stress. All of these ingredients exist in the pipeline construction process.

By developing a thorough understanding of HACC through the investigation of the evolution of temperature, stress and hydrogen concentration that occurs in the pipeline girth weld during construction, the risk of HACC can be reduced. These days low alloy high strength steels are used which are able to resist cracking even with a fully hardened microstructure. Due to this evolution the focus of current research on HACC has been aimed toward reduction of residual stress and hydrogen content.

It is virtually impossible to investigate the relevant pipeline construction parameters by experimental means. For this reason numerical models of the construction process will be

developed. Current pipeline construction procedures have mostly been developed using full scale testing and past experience. If new materials such as high strength pipe, high strength welding consumables are introduced or if changes are made to the operational procedures used, the impact on the potential for HACC cannot be fully predicted. With the use of numerical modelling a more complete scientific basis for the construction procedures can be developed.

2.1.1 Occurrence of Hydrogen Cracking in Girth Welds

From past experience it has been found that HACC is most likely to occur within the root weld pass during front end pipeline construction. The girth weld is conventionally made using cellulosic electrodes, which introduces a high concentration of hydrogen into the weld pool. The large thermal mass of the pipeline causes rapid cooling thus producing a hard martensitic microstructure in the heat-affected zone (HAZ). Applied stresses are produced by transient thermal stresses in the weld and the lifting and lowering of the pipeline front end.

In the late 1960's the British Gas Corporation had to repair 10% of their girth welds due to HACC in the heat affected zone (Phelps, 1977). The problems experienced were largely due to the lack of pre-heating and the rapid cooling of pipes with large wall thicknesses. The rapid cooling rate had the effect of not allowing the hydrogen, which was introduced into the steel during welding, to diffuse out of the material before the HAZ had cooled.

It has been reported by Hart (1999) that in the Middle East in 1970, probably the worst accident to result from HACC in a pipeline girth weld in terms of human life occurred. Seventeen men were incinerated during pipe failure and explosion when pressure testing was conducted with gas rather than water. The pipeline which was made of X60 24-42" diameter with 0.5" wall thickness cracked and the gas was ignited. It was stated that, "*The failure investigation determined the initiating cause of the brittle fracture was an HAZ hydrogen cracking in the root of a girth weld from an internal back weld repair made with a cellulosic electrode*" (Hart, 1999 pp. 4). It was explained that contributing factors were the high hydrogen, low heat input welding process used for the root pass and failure to lay the hot pass immediately after welding of the root pass.

Australia has also experienced problems with HACC such as during the construction of the Moomba to Sydney pipeline in 1974 (Hart, 1999). The cost of the weld failures including restitution costs but excluding external consequential costs was A$15 million, which in todays terms is of the order of A$100 million as reported by Hart (1999). The cause of the HACC was attributed to the pipe's "*high carbon equivalent and poorer fit up*" (Hart, 1999 p 5).

In the UK during the 1990's problems were experienced in thicker walled pipes. It was stated that the contributing factors in that case were "*the use of a compound bevel (the wall thickness was 19 and 25mm) and the use of more alloyed consumables, selected to meet the more stringent Charpy requirements of the heavier wall thickness*" (Hart, 1999 p 5). It was

explained that the compound bevel would "*tend to increase the layer thickness and decrease the interpass time for each layer, compared to the shallower layers in a wider vee preparation*" (Hart, 1999 p 5). This has the effect of reducing the amount of hydrogen that can escape between passes and results in a higher residual concentration of hydrogen in the near weld region.

HACC typically occurs due to the root pass that is laid during front end construction. While there have been many other failures that have occurred due to HACC in other structures such as in the failure of the Kings Bridge in the early 1960s (Mansell, 1994), this thesis is primarily concerned with understanding how HACC that occurs during front end pipeline construction can be avoided by strict procedural measures. Although many of these problems are not experienced as frequently nowadays due to the development of more weldable steels, an improved understanding is essential to maintain the efficiency of the process. Improved knowledge of HACC in pipeline girth welds also increases the capacity to avoid such problems recurring as the industry moves toward thinner walled and higher strength pipe in the future.

2.1.2 Factors Influencing Transient and Residual Stress

The two important sources of stress that are applied to a girth weld during pipeline construction are:

- those generated by externally applied loads from mechanical handling, and

- those that are internally generated from the welding thermal cycle.

The most significant external loads occur during the lifting and lowering-off operations, which are part of conventional pipeline laying practice. The desire for increased productivity often means that lifting takes place before 100% completion of the root pass around the full pipe circumference. This clearly has implications for the stress levels applied to the welded joint. The forward pace of pipeline construction is important in terms of pipeline construction cost. Therefore after the root pass is completed the line-up clamps are immediately removed and are used to line up the next length of pipe. The capping passes are completed later.

The stresses induced in the root pass during construction are due to the lifting and lowering of the pipe, ovality in the pipe and thermal stresses caused during the welding of the girth. The lifting stress occurs after the root pass is complete when lifting the front end of the pipe in order to place skids under it for support. The relevant parameters influencing the stresses from lifting are shown in Figure 2.1.

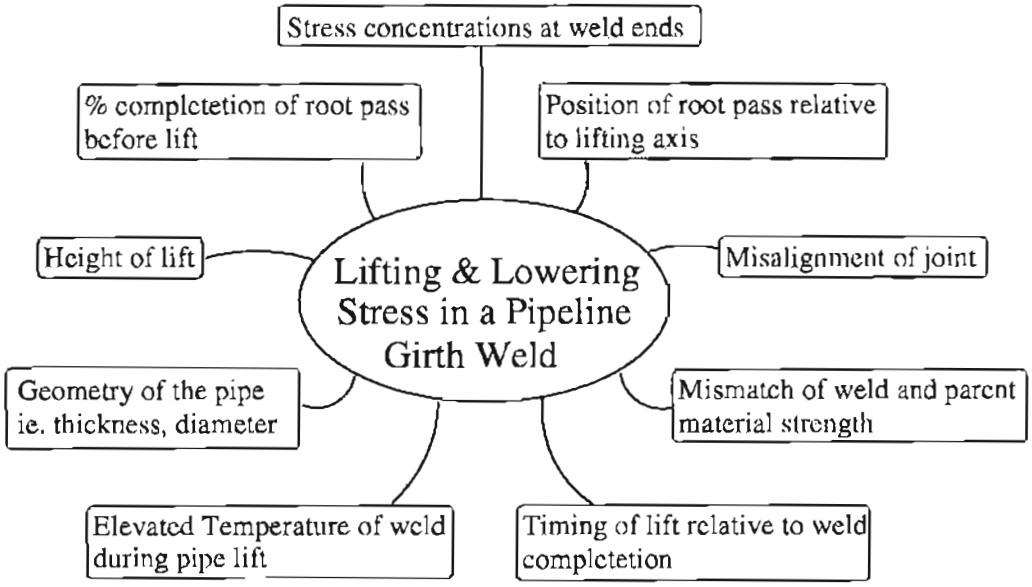

Figure 2.1: Factors influencing the stresses due to lifting and lowering operations.

Thermal stresses occur as a product of the non-uniform expansion and contraction resulting in local plastic deformation. Correcting any ovality in the pipe also produces stress since the line-up clamps are used to round the pipe before welding the root pass. When the clamps are removed the root pass is left under stress so ovality can affect the final residual stress field. Alternatively the pipes are not rounded before welding and as a result mismatch occurs in certain regions of the root pass. Mismatch results in stress concentrations in the root pass. The features controlling residual stress are shown in Figure 2.2.

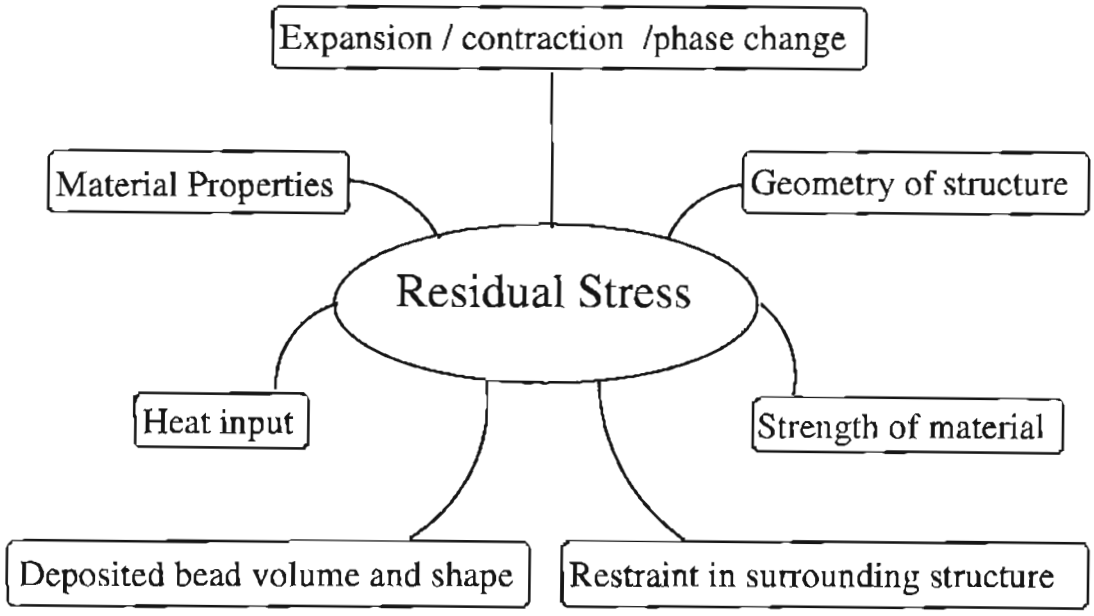

Figure 2.2: Factors influencing the residual stresses induced in the pipeline girth weld.

2.1.3 Overview of Thesis

The tensile residual stress developed during pipeline construction, which is dependant on process parameters, is the driving force behind the potential for HACC. By using numerical techniques the influence of a large number of process parameters can be considered quickly and cost effectively. Experimental measurement of transient and residual stresses during pipeline construction is difficult. In such a context, computer simulation is an extremely useful tool. It allows the calculation of variables such as the transient stress which are almost immeasurable experimentally and it may be used to provide a systematic evaluation of the influence of process parameters.

In order to completely study pipeline construction, a 3D modelling approach is required. Researchers such as Dong et al (2001) have conducted studies of 3D residual stress fields in girth welded pipes using the finite element method, however such work has not been directly related to the pipeline construction process. Studies of pipeline construction conducted in the past have ignored 3D effects in favour of 2D axisymmetric models for the computational speed they offer despite obvious 3D influences such as incomplete root welds.

North et al (1981) carried out a full scale experiment where pipeline construction was simulated while altering process parameters to determine what parameters led to HACC. While this provided insight into the tendency for HACC, it would be useful to also know the quantitative evolution of stress and hydrogen concentration, which are the fundamental drivers of HACC.

Work by Higdon et al (1980) related the construction process to residual stress and HACC. That work highlighted the impact of the construction process on the residual stress and hydrogen cracking. However, they were unable to consider the process in a complete transient manner due to the computational cost. Many simplifying assumptions were required due to the linear elastic modelling scheme used which prevented consideration of some of the most influential process parameters.

In this study 2D and 3D numerical models of pipeline construction were created. To validate these models, an experiment was conducted using the 'Blind Hole Drilling' technique of

residual stress measurement. This experiment gave confidence in the numerical results before embarking on a systematic study of process parameters.

Cellulosic electrodes have been traditionally used by the pipeline industry and even today they are preferred. This is because they allow robust field application with high productivity and the cost of building a pipeline is directly related to the speed of construction. Cellulosic consumables introduce high concentrations of hydrogen into the weld metal so in any study of HACC it is necessary to consider the evolution of hydrogen concentration during pipeline construction. In this work numerical models of hydrogen effusion were used to obtain this information.

After surveying the literature it appears that this investigation has been the first to analyse the effect of process parameters on the transient stress and hydrogen concentration with regard to the complete construction process. Increased knowledge of the evolution of stress and hydrogen concentration which resulted from this study has allowed a clearer understanding of the transient risk of cracking and hence in its control.

2.2 MECHANICAL HANDLING LOADS

Any fusion weld will generate a residual stress field due to non-uniform constrained expansion and contraction. However the resultant stress field experienced in a pipeline girth weld is influenced not only by the welding thermal cycle but also by the mechanical handling loads associated with pipeline construction. For example the application and removal of the line-up clamp and lifting and lowering of the front end of the pipeline while support skids are prepared. Also mismatch of oval pipes can have the effect of increasing the stress induced in the weld due to lifting of the pipeline.

2.2.1 Pipeline Construction Process

The pipeline construction process is highly time dependant. The reason for this is that the faster a pipeline can be constructed the lower the construction cost. Of particular concern is the pipeline front end speed which is the pace at which the pipeline can be constructed with only a root and a hot pass neglecting the capping passes as these are completed later by a second welding crew. In Figure 2.3 a photograph of front end pipeline construction is shown. A description of the welding process used and the timing of the construction operations that are typically used in the field follow.

Figure 2.3: Photograph of front end pipeline construction.

2.2.1.1 Welding Process

In Australia the welding process generally used for pipeline construction is manual metal arc-welding (MMAW) as shown in Figure 2.4. This process uses a covered electrode and an arc is formed between the work piece and the electrode. The electrode is covered in a flux which melts during welding, forms a slag on top of the weldment shielding it from the atmosphere and prevents oxidisation of the near weld region. The electrode and flux composition can be varied to allow a wide variety of materials to be welded using this process. The method generally used for pipeline welding is known as 'Stovepipe welding'.

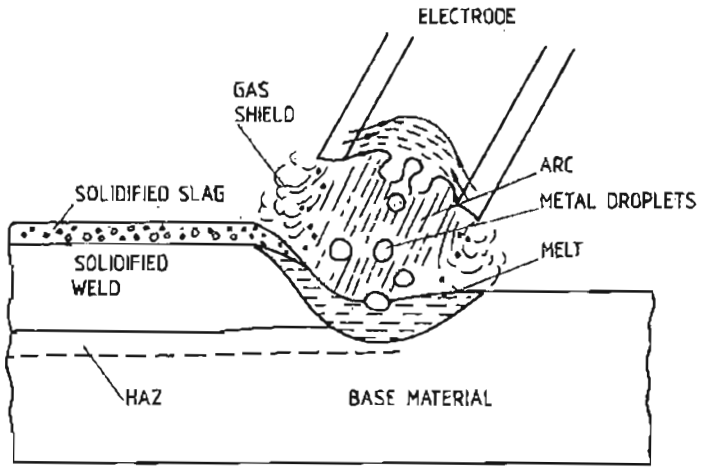

Figure 2.4: Manual metal arc-welding. Karlsson (1986)

The 'Stovepipe welding' process is favoured by the pipeline construction industry (Spiller, 1970). 'Stovepipe welding' involves two welders, welding in the vertical down position on either side of the pipe. Welding in the vertical down position rather than in the vertical up position allows much faster welding speeds to be achieved. The joint preparation that is generally used is a 60° included angle with a 1.6mm root face and a 1.6mm root gap.

In the past rutile type electrodes were used for pipeline welding in the vertical up position. In this position these electrodes produce acceptable welds as the fluid slag is left behind the arc. As explained in (Spiller, 1970), when rutile type electrodes are used in the vertical down position however the slag runs downward faster than the arc travels, flooding the arc, thereby making welding in the vertical down position impossible. High cellulose electrodes are generally recommended for stovepipe welding of pipelines as they allow welding in the

vertical down position. These electrodes produce a small volume of slag, a powerful arc and a gaseous shield of carbon-monoxide and hydrogen allowing rapid changes of electrode angle.

It was stated by Bailey et al (1993) that cellulosic electrodes contain a high moisture content causing them to introduce hydrogen into the material and that the cellulose itself contains a high proportion of hydrogen. This means baking the moisture out of the electrodes makes little improvement in terms of hydrogen reduction as compared to low hydrogen electrodes. However if the hydrogen concentration was to be reduced it would alter the desirable welding characteristics of the cellulosic electrodes such as reducing the weld penetration that can be achieved. The use of cellulosic electrodes does however have implications in terms of HACC.

During Stovepipe welding a number of different passes are laid. The first pass is known as the root pass or the Stringer bead. This pass is carried out by using no weaving and the electrode is pushed into the root of the joint, while holding the electrode at an angle of 60° in the direction of travel. This ensures a small weldment bead and controlled penetration.

A hot pass is laid after the root pass ideally while the root pass is still warm. An angle of 60° relative to the direction of travel is used with a short arc and a light drag with a forward and backward motion. This is done to prevent any undercut or wagon tracks occurring as a result of the root pass.

Filler beads are then carried out with the electrode initially 90° relative to the direction of travel, however the angle increases to 130° relative to the direction of travel at the 6 o'clock position. A rapid weave is used while travelling from the 12 to the 4 o'clock position and an up and down movement is used from the 4 to the 6 o'clock position. This is done to ensure that the filler beads leave flat faces and avoid any weld undercut.

Sometimes only Stripper beads are required rather than Filler beads. Stripper beads help fill the concave sections that occur in the 2 to the 4 o'clock position and the 10 to 8 o'clock position. These beads bring the weld up flush with the pipe outer surface before the capping passes are laid.

Capping passes complete the joint with the electrode initially angled 90° in the direction of travel, however the angle increases to 130° in the direction of travel at the 6 o'clock position. The tip of the electrode uses a lifting and flicking action with side to side motion and a medium to long arc length. The capping bead is generally limited to a width and depth of 19mm x 1.6mm.

2.2.1.2 Timing of Events

There is a number of activities associated with pipeline construction. These activities include preparing a right of way, joining of the pipe segments, covering the welds with a polymer coating, digging a trench for the pipeline, lowering the pipeline into the trench, pressure testing the pipeline and 'tying in' the joined sections. The rate limiting process however is

front end welding. A typical front-end construction process was outlined in Smart et al (1995). The sequence of events are described in Figure 2.5.

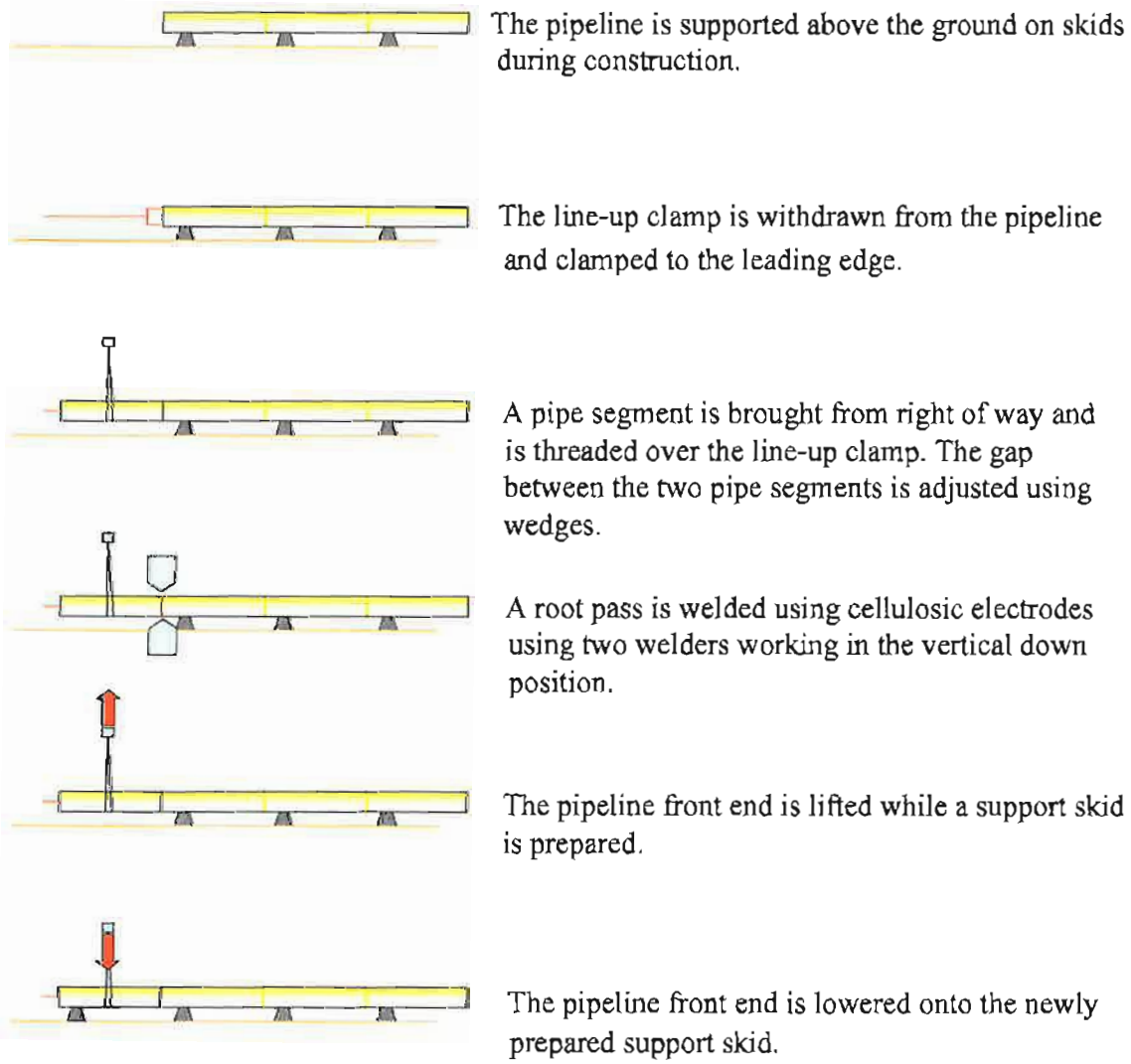

Figure 2.5: Sequence of operations in pipeline construction. (Smart et al 1995)

This process is designed so that the welders spend as much time welding as possible in order to maximise the front end speed. There are possibilities however to further increase the front end speed which have been identified by some researchers such as Smart et al (1995) and Henderson el at (1996). For example, Henderson el at (1996) showed that if the line-up clamp could be removed and the lifting and lowering off was conducted after only 50% completion of the root pass, the cycle time could be reduced from 6 minutes to 4.5 minutes.

However, possible increases to the forward pace are dependant on the process parameters. For example, if high strength pipe such as X80 or X100 were used the likelihood of HACC may be greater and so a more stringent procedure may be required which could limit the forward pace.

Henderson et al (1996) gave a schematic representation of the timing of the welding process for a procedure using two welders, a 100% completion of the root pass before lifting and no removal of the line-up clamp until completion of the root pass as shown in Figure 2.6.

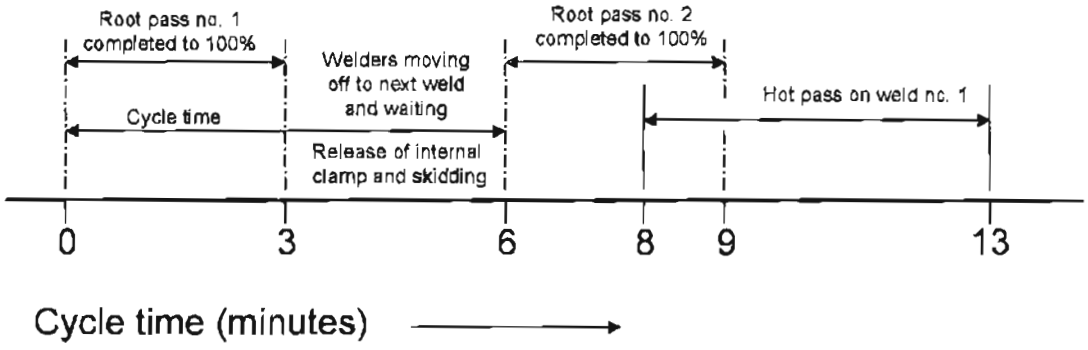

Figure 2.6: Schematic representation of welding of the root pass by two welders at 200mm/ min on a DN350 pipe. The clamp is released after 100% root pass completion. (Henderson et al, 1996)

2.2.2 Stress Due to Lifting Pipeline Front End

Lifting stresses are produced when the pipeline front end is lifted to place a skid under it for support. During lifting the number of pipe lengths that are lifted off the skids depends on the lift height as well as the terrain over which the pipe line is being constructed. While the terrain causes some variability, most studies in the past assume the pipeline is being constructed on flat ground. One such example is Smart and Bilston (1995).

Smart and Bilston (1995) reported that the line-up clamps which align the two ends of pipe during the welding of the root pass provide no moment against the lifting stresses that are induced during the lifting and lowering operations. No reason was given for this assumption other than to state, "*It is clear that the clamp does not provide an effective moment*

connection between the pipes" (Smart and Bilston, 1995 P6-3). They suggested that the line-up clamps should therefore be removed before this operation and joined to the new front end to increase the rate of construction.

The effective moment connection between the pipes is also affected by the proportion completed and location of the root pass. In the Figure 2.7 the section modulus is plotted against the percentage of the root pass that is completed for different weld starting positions. From this graph, the dependence of the section modulus on the weld starting position can be seen. It was stated by Smart and Bilston (1995) that if 70% of the girth is welded, the stress in the root pass will be 25% greater if welding begins 20^{o} after top dead centre rather than if welding begins at 20^{o} before top dead centre. They therefore suggested that a partially completed root pass will not be significantly more stressed than a fully complete root weld provided that the weld segments are correctly located.

Lifting the pipeline front end before the root pass was completed would have the benefit of increasing the forward pace of construction and thereby reducing cost. Smart and Bilston's (1995) justification for this was the section modulus is not greatly reduced provided that certain portions of the root pass are welded. However, the lifting process often occurs while the near weld region is at an elevated temperature. This has the effect of reducing the strength of the material in this region. Also it is known that stress concentrations occur at the weld ends due to the welding thermal cycle, which will influence the resulting stress field. The

simple analytical model used by Smart and Bilston (1995) to develop the results presented in Figure 2.7 was unable to account for these effects.

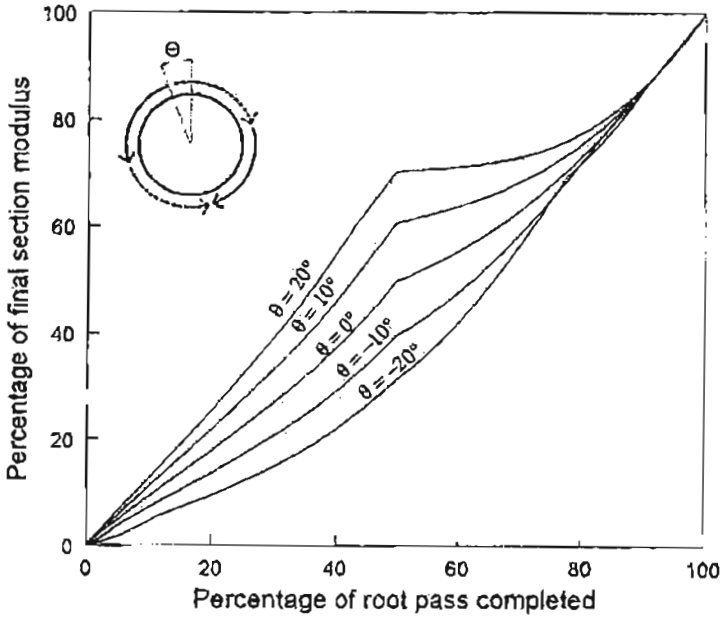

Figure 2.7: The variation of rate of development of section modulus with start position. (Smart and Bilston, 1995)

Pipe body stresses were calculated using classical beam theory by Higdon et al (1980). In Figure 2.8(a) and Figure 2.8(b) the bending stress has been plotted against lift height for different joint locations. The local geometry of the root passes has been ignored, however these graphs show the joint which contains the greatest bending stress for a given lift height. Joint 1 is closest to the front end, joint 2 is second from the front end and so forth. The

bending stress versus the distance from the point of lift was also plotted as can be seen in Figure 2.8(c).

It is assumed by Higdon et al (1980) that the pipe is lying on flat ground rather than on support skids that are placed near each girth weld along the pipeline. Making this assumption allowed simple analytical calculations to be made however the use of support skids would cause the pipe body stress to be greater than is shown in Figure 2.8 at certain lift heights. This needs to be taken into account when considering the influence of lift height on the stress induced in a pipeline girth weld. Another factor not taken into account is the variation in terrain. For example when constructing a pipeline over a hill the lifting stresses will be increased.

In order to examine the interaction between lifting and lowering and residual stress, Higdon et al (1980) took the analytic lifting stresses and superimposed these onto a residual stress field as described later in Section 2.3.1.

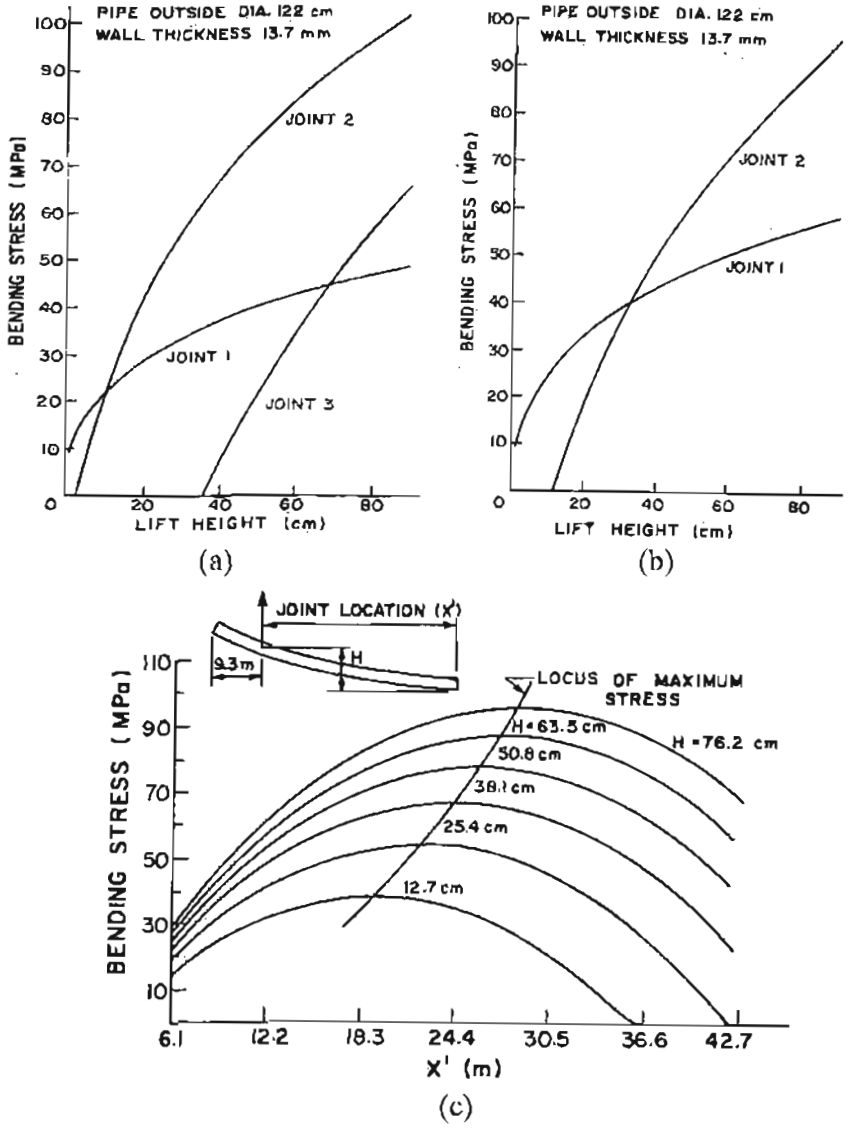

Figure 2.8: (a) Lifting stresses for pipe length of 18.3m. (b) Lifting stresses for pipe length of 24.4m. (c) Bending stress verses joint location for pipe with 122cm outside diameter and 13.7mm-wall thickness. (Higdon et al, 1980)

2.2.3 Experimental Analysis of Lifting Stress

Whilst no research has been undertaken to measure the stress in a girth weld due to the lifting and lowering process, some work on simulating the lifting process to investigate the effect of lifting and other process variables on the occurrence of hydrogen cracks has been carried out. An experimental test rig was developed by North et al (1980) in order to carry out full scale testing of the pipeline construction process. North et al (1980) decided to produce a full-scale rig due to the large number of field variables, which make it very difficult to produce laboratory techniques, which simulate the construction process.

The test rig consisted of two 6.5m pipe lengths, which were hydraulically loaded, in four point bending. A series of tests were carried out whilst controlling the pre-heat, the holding time, pipe misalignment (high-low at 6 o'clock position) and the equivalent lift height. The pre-heat was applied using six external gas burners to a region approximately 150mm wide on either side of the weld region. Typical results are shown in Table 2.1.

Test no.	Pipe no.	Preheat before welding (Celsius)	Weld temperature at loading (Celsius)	High-low at 6 o'clock position (mm)	General pipe stress at weld joint (Mpa)	Jack Pressure (Mpa)	Equivilent lift height (mm)	Holding time under load (seconds)	Test results
11	3A	none	-	none	43.78	14.74	160	15	no cracking
22	3A	none	<68	none	60.78	20.69	333	15	no cracking
33	3A	none	-	none	81.04	27.58	673	2.9	complete weld failure
44	3A	none	<68	2.38	60.78	20.69	333	4.5	complete weld failure
55	3A	none	49	2.38	60.78	20.69	333	8.3	complete weld failure
66	3A	56	75	2.38	60.78	20.69	333	15	limited cracking at 6 o'clock position
77	3A	75	85.5	2.38	60.78	20.69	333	15	limited cracking at 6 o'clock position
88	3A	100	117	2.38	60.78	20.69	333	15	no cracking
99	3A	121	108	2.38	60.78	20.69	333	15	no cracking
10	3A	101	94	2.38	81.04	20.69	660	15	no cracking
11	3A	94	118	2.38	81.04	20.69	660	15	no cracking
12	45	54	82	2.38	60.78	20.69	333	0.6	complete weld failure
13	45	75	102	2.38	60.78	20.69	333	15	no cracking
14	45	75	92	2.38	60.78	20.69	333	15	no cracking
15	57	98	116	2.38	60.78	20.69	333	15	no cracking
16	57	75	100	2.38	60.78	20.69	333	15	no cracking

Table 2.1: Experimental results which where obtained from the full-scale weldability program. (Glover et al, 1981).

A reasonably severe criterion was used to determine whether HACC would occur. For example a 15 minute holding time was used, whereas in reality the pipe is only lifted for a few seconds. North et al (1980) did however give an indication of the parameters required to induce cracking. They concluded that provided no mismatch of the pipe segments existed cracking was unlikely to occur and if considerable mismatch existed pre-heats of 75°-100°C were required to avoid HACC. These days however mismatch is rarely a problem due to the line-up clamp used. Also the stress induced in the root pass is increased by factors such as incomplete root passes, which was not taken into account in this study.

The British Gas Corporation has also used full-scale pipe bending, to test pipe root pass weld integrity. The procedure for the weldability testing which is outlined in Phelps (1977) is as follows. Two pipes greater than 10m in length have a root pass welded around the girth at a starting temperature of 0°C using celluosic electrodes. Then a third and a fourth pipe are also joined by completing a root pass at a starting temperature of 20°C. Then one end is lifted to simulate the lifting and lowering operations. The welds are mechanically tested and X-rayed to see if they meet British Gas Specification PS/P2 'The Field Welding of Steel Pipelines'. The welds are microscopically examined at a magnification of 250X in order to determine the presence of cracking in the HAZ.

One of the major reasons the British Gas Corporation had for rejecting a weld was cracking in the HAZ. They found two types of cracking occurred; hydrogen-embrittlement cracks and decarburisation cracking. It was found that hydrogen-embrittlement cracks generally occur

on the inside surface of the pipe where the greatest stress concentration occurs. It was suggested that a typical hydrogen concentration of 90mL per 100g of weld was generally required for hydrogen cracking to occur.

Henderson et al (1996) also investigated the effect of lifting the pipeline front end. They measured the displacement across the root pass in the 6 o'clock position during the lifting and lowering process. It was found that there was a greater displacement when the pipe was lifted than when the pipe was lowered. This suggested that plastic deformation occurred at the root pass in the 6 o'clock position which would have the effect of altering the final state of residual stress.

The experimental methods which have been used in the past with regard to lifting and lowering of the pipe have focused on whether it caused the weld to crack. It has been shown that it can cause enough stress in the girth weld to induce cracking. However the manner in which the lifting process actually alters the final state of residual stress has not been demonstrated.

2.2.4 Ovality Stress

Ovality in the pipe can cause stress concentrations, which magnify the effect of the lifting process. Pipes have a specified allowance of 1% ovality in relation to the total diameter (Pick et al 1982). Ovality stresses are also caused by the spring back of oval shaped pipes, which

have been temporarily rounded by the line-up clamp. After welding is completed, additional stresses are produced in the root pass due to the spring back of the rounded pipes.

Wiekcrcrt et al (1984) used finite element analysis to investigate the increase in stress that resulted from lifting ovalised pipes that have their major axis 90^{o} apart as shown in Figure 2.9. It was found that the increase in stress that resulted was less than the stress induced by the lifting and lowering process itself. North et al (1981) found that the stress concentrations produced by oval pipes being joined without being rounded is greater than the residual stress that is produced by rounding the pipes before welding.

Generally the use of a line-up clamp prevents any weld mismatch during pipeline construction. It is worth noting that while there is potential for stress concentrations to be produced due to ovality, consideration of ovality in studies conducted may have the effect of giving an inaccurate view of the stress that exists in a pipeline girth weld. This inaccurate view is because the line-up clamp will generally remove any ovality during welding. Of greater concern is the timing of the line up clamp release.

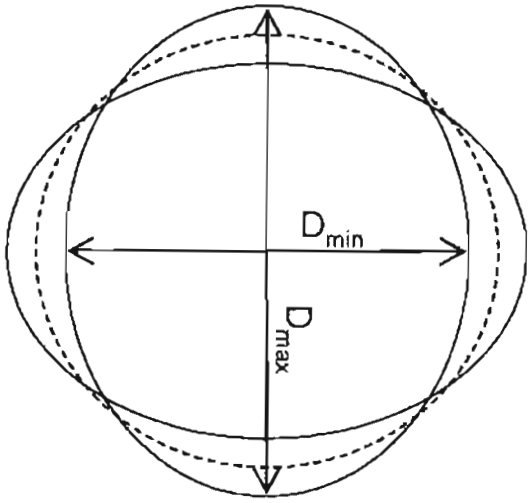

Figure 2.9: The maximum pipe ovality occurs when major axes are at right angles.

2.2.5 Summary

It has been recognised by a number of researchers that the mechanical handling loads influence the propensity toward HACC. This finding has been based on full scale testing and limited numerical analysis. While experimental studies have demonstrated what combination of parameters are likely to cause HACC, they do not allow a quantified understanding of the phenomena. For example it is difficult based on limited experimental data to estimate the variation in risk of HACC that may arise from, say a change in welding heat input, an increase in pipe yield strength or a reduction in pipe wall thickness.

Numerical analyses are also made on many simplifying assumptions. Many of these simplifications are due to inability to create adequate 3D simulations and as a consequence

these assumptions were unable to be tested. Using 2D residual stress fields from butt welds and superimposing the results from analytic lifting models have some inherent limitations. Some of these limitations include:

- it is assumed the lifting and lowering process has no effect on the final state of residual stress,
- the residual stress field is assumed to be axisymmetric,
- material properties are not temperature dependant,
- the result of incomplete root passes and stress concentrations at the weld start and stop position are ignored,
- the temperature of the material is assumed to be ambient during lifting.

2.3 RESIDUAL STRESS

Residual stresses are produced in welds due to non-uniform temperature gradient produced by the heating and cooling of the near weld region during welding. As the near weld zone expands and contracts it produces local stresses. Some of these stresses reach the yield strength of the material and plastic deformation occurs. When the weld metal has completely solidified, elastic unloading stresses in the elasto-plastic region lead to the development of residual or internal stresses. To simply explain the concept of residual stress, consider the case of a bar of elastic-perfectly plastic material shown in Figure 2.10, which is restrained at the weld ends using rigid platens.

When the bar is heated in the middle it expands producing a compressive stress, and eventually it reaches the yield strength of the material (0-1). As the bar is heated further it continues to expand, the stress induced in the bar could reached the yield strength of the material and plastic deformation occurs (1-2). Then the bar is allowed to cool and contract relieving the compressive stress. The unrestrained length of the bar is now shorter than it was (due to the plastic strain that occurred during (1-2)) causing a tensile stress in the bar to develop as it cools (2-3). As the bar continues to cool the tensile stress in the bar reaches the yield strength of the material and then plastically deforms until the temperature returns to ambient leaving the bar with a residual tensile stress (3-4). The residual tensile stress approaches the yield strength of the material. This same phenomena occurs during the

welding process as the material expands and contracts at different rates due to temperature differential in the material.

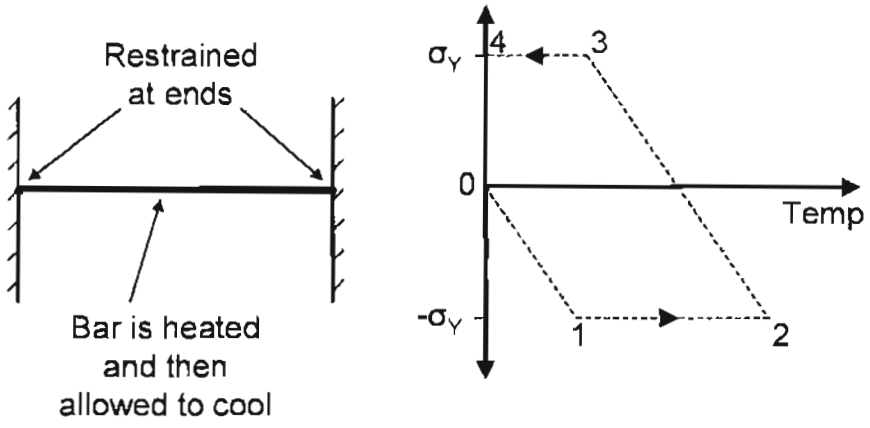

Figure 2.10: A bar is restrained at the ends, heated in the middle and allowed to cool. It goes through a stress cycle, which leaves it with a tensile residual stress. (Wells 1953)

Extensive data is available on residual stress distributions in pressure vessels, however comparisons of geometries and process effects are difficult due to non-uniformity of materials and methods for determining residual stress (Scaramangas, 1984).

Chandra (1985) conducted a review of the work in the field of residual stress in butt-welded pipes. The paper considered analytical, experimental and finite element techniques including the thermal modelling required for this analysis. His review is now some what out of date however, as developments such as the use of 3D models have occurred since that review. Another review was collated by Mohr (1996) relating to the influence of some parameters on

the residual stress in circumferential welds rather than the modelling techniques themselves. This review highlighted the large variability in results mainly due to the different welding parameters used by different researchers. To address this problem this thesis will consider a large variety of construction parameters while using the same model.

2.3.1 Analytical Residual Stress Models

Wells et al (1953) developed a residual stress model for a butt weld in a flat plate. This model used a heat flow model due to moving heat sources to predict a temperature distribution in the plate. The equations used to calculate the temperature distribution were developed by Roberts (1923) and were first applied to welding problems by Rosenthal (1935), however, there were many simplifying assumptions, which are summarised in Myers (1967).

The approach that is generally used when producing analytical models of residual stress in circumferential welds was first undertaken by Vaidyanathan et al (1973). The method was based on the previous work by Wells et al (1953) for a residual stress model for a weld in a flat plate. Vaidyanathan et al (1973) proposed to consider the pipe as a flat plate, which had been rolled into a cylinder. They used thin shell theory to evaluate the stress caused by the deformation.

The direction of the principle stresses for the analogy between a weld in a flat plate and a weld in a cylindrical shell can be seen in Figure 2.11. The flat plate model predicts high

longitudinal stresses near the weld, low longitudinal stresses away from the weld and negligible transverse stresses as can be seen in Figure 2.12. When these stresses are transposed into the circumferential direction and the material is allowed to deform the residual stress pattern changes. This is because the cylindrical weld and the region away from the weld can displace in the radial direction. This has the effect of reducing the hoop stress to less than the longitudinal stress predicted by the flat plate model. The deformed shape of a circumferential weld is shown in Figure 2.13.

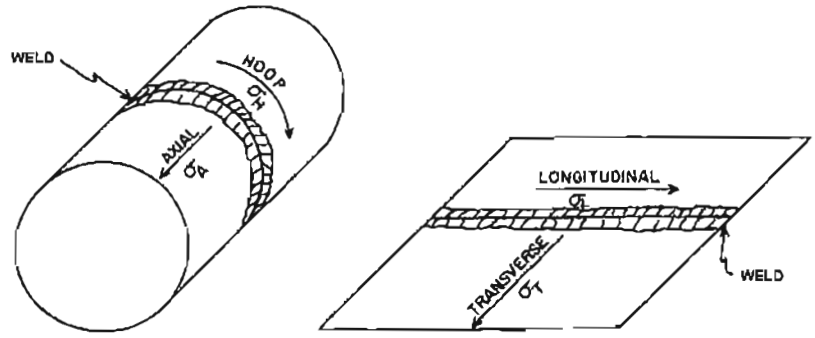

Figure 2.11: Definitions of stress directions. Vaidyanathan et al (1973)

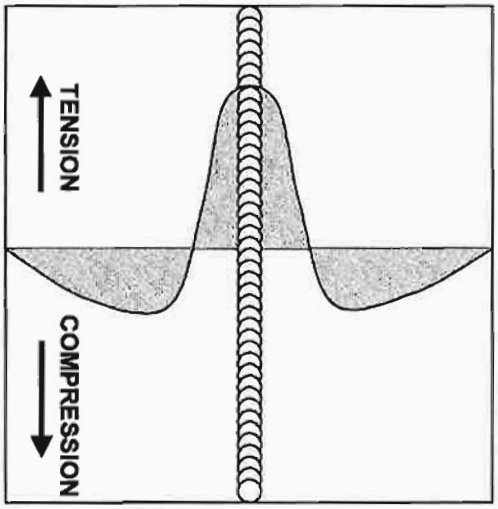

Figure 2.12: Typical distribution of the stress parallel to the weld direction in a butt welded plate. Koichi Masubuchi (1980)

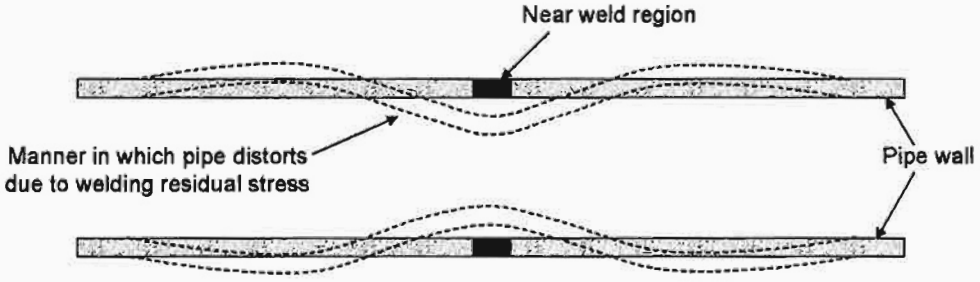

Figure 2.13: The manner in which a tube distorts to relieve residual stresses due to circumferential welding. Masubuchi (1980)

This model was useful in highlighting the residual stress patterns to be expected in a circumferential weld, at a time when computer speed inhibited the use of economical

numerical solutions. Analytical solutions however do not account for temperature dependant material properties and the effect of phase transformation.

Weickert et al (1984) used the analytical technique developed by Vaidyanathan et al (1973) to calculate the residual stress field in a cylinder. The results were superimposed with pipe body lifting results as described in Section 2.2.2 to calculate the resultant stress due to lifting and residual stress on the root pass. They looked at the resultant stress for two stress concentrations in the root pass, which were labelled, region A and region B. These areas can are shown in Figure 2.14(a) and Figure 2.14(b) and the stress due to lifting the pipeline front end, the stresses due to ovality and the residual welding stress can also be seen.

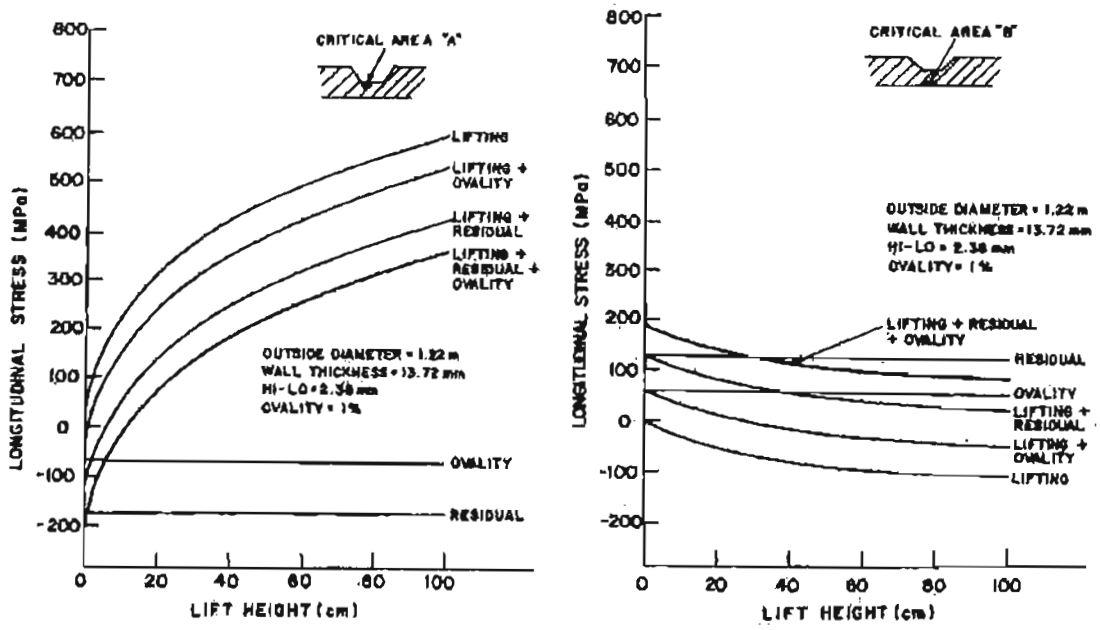

Figure 2.14: (a) Residual, ovality and lifting stresses (Region A). (b) Residual, ovality and lifting stresses (Region B). Weickert et al (1984)

In Figure 2.15 the combined stress in regions A and B are plotted on the same axis. From this graph it can be seen that for this size of pipe the lowest maximum stress was calculated to be where the two lines meet at an approximate lift height of 30cm.

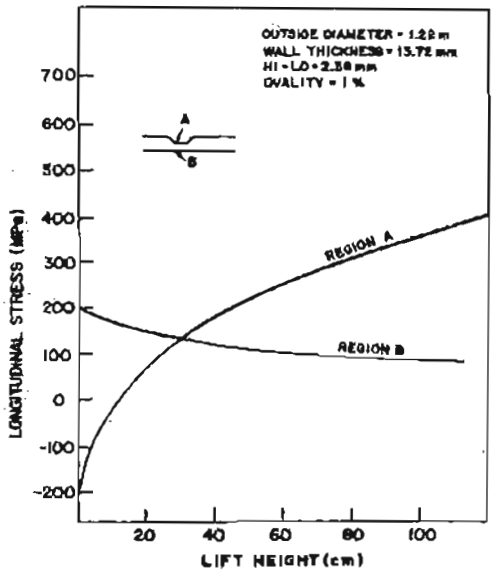

Figure 2.15: Combined residual, ovality and residual stresses. Weickert et al (1984)

The residual stress field was created by taking a typical two-dimensional residual stress field in a flat plate (which is calculated analytically) and wrapping it into a cylinder. The stresses due to lifting and ovality were then superimposed onto the residual stress field. Clearly this approach does not account for the transient development of residual stress. It was assumed that the final state of residual stress is unaltered by the lifting and lowering process since simple linear elastic models were used (to superimpose the residual stress and lifting stress results) which cannot simulate any plastic deformation.

Consequently part of the investigation carried out by the author of this thesis is to assess whether the lifting of the pipeline front end does have an effect on the final state of residual stress. In order to consider this, the mechanical handling loads that occur during construction

need to be incorporated into a thermo-elastic plastic model of the complete construction process. Other limitations of the work conducted by Weickert et al (1984) prevent consideration of many important process parameters that affect the welds propensity toward hydrogen cracking. For example, the timing of the lifting process, the heat input, the welding speed and pipe and weld metal properties are among the many process variables not considered in their work.

2.3.2 Numerical Residual Stress Models

Analytical models have been shown to produce results of a reasonable accuracy (Easterling, 1992). These models however are limited to single passes with welds of simple geometries. Experimental methods of measurement are useful but are also limited as described later in Chapter 4. Due to the complexity of the geometry of most welds, the ability to consider effects such as latent heat of vaporisation and temperature dependant material properties, finite element techniques have proved extremely useful.

When modelling residual stress the approach that is generally taken is to use a numerical thermal model to calculate a temperature history for input into a mechanical model. The two models are assumed to be de-coupled. A typical procedure is given in Figure 2.16.

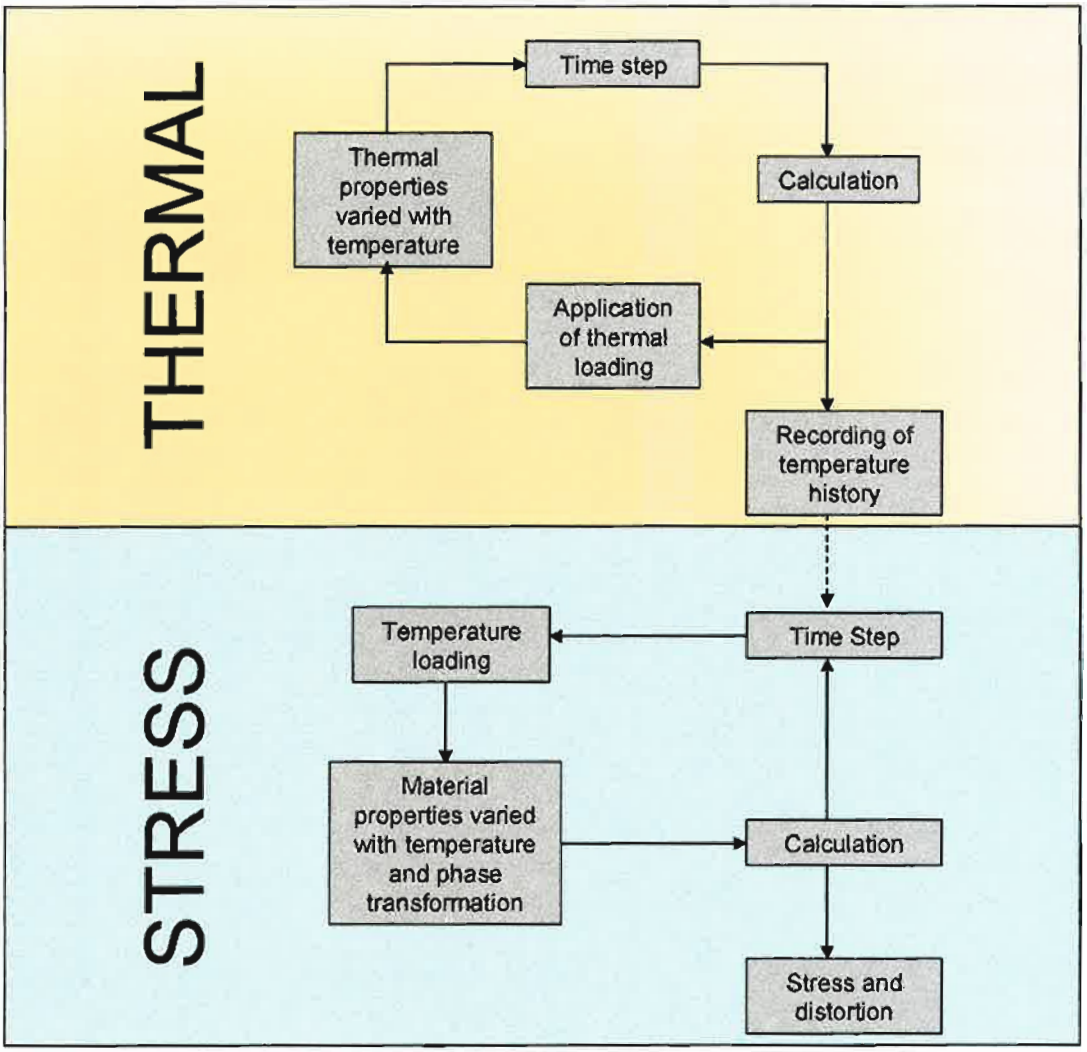

Figure 2.16: Typical procedure used when numerically modelling residual stress.

2.3.3 Thermal Modelling

Residual stress, distortion and the reduction of strength in the near weld zone are directly related to the thermal cycle of the welding process. For this reason it is important in a

numerical analysis of transient stress that the thermal cycle should be modelled accurately. The calculation of the thermal cycle during welding can be achieved by considering the process to be a transient thermal analysis with a moving heat source. The method by which the heat source is modelled greatly affects the accuracy of the thermal model. This is important for both closed-form and numerical solutions.

The majority of work in this area has simplified the calculations by assuming that conduction is the only means of heat transfer through the material. The calculation of the flow and heat transfer in the welding arc is usually ignored and such phenomena are approximated. These simplifying assumptions make modelling the welding process feasible. As stated in Davies (1995), without these assumptions a complete model of the welding process would have to include drag, gravity force, surface tension, electromagnetic forces, plasma pressure and shear on the weld pool surface, buoyancy, impact force of the droplet, flow of molten material carrying heat and momentum, radiation, conduction, convection, evaporation of molten metal.

2.3.3.1 Heat Flow Equations

Solutions to heat flow equation applied to the welding process were first developed by Rosenthal (1935). These are generally expressed as a heat flux:

$$\text{Heat Flux} = \frac{\eta VI}{v} \text{ MJm}^{-1} \tag{2.1}$$

where

η = Arc efficiency

V = Voltage

I = Current

v = Welding velocity

The differential equation of heat flow is:

$$\frac{\partial^2 T}{\partial x^2} + \frac{\partial^2 T}{\partial y^2} + \frac{\partial^2 T}{\partial z^2} = 2\lambda \frac{\partial T}{\partial t} \qquad (2.2)$$

where

T = Temperature

x, y, z = Cartesian coordinates

t = Time

λ = Thermal conductivity = $\frac{\rho c_\rho}{\alpha}$

ρ = Density

c_ρ = Specific Heat

α = Thermal diffusivity

As the arc passes over the material being welded at a constant velocity, a constant unchanging temperature field in relation to the welding arc develops. This occurrence allows simplification of the analysis so that a temperature profile can be developed more economically by using what is known as the 'quasi-steady state' assumption. Equation 2.2 relates to a fixed coordinate system. However if x is replaced with ξ where:

$$\xi = x - vt \tag{2.3}$$

where

ξ = Position relative to moving arc

then a quasi-stationary temperature profile exists. This allows Equation (2.2) to be simplified as shown in Equation (2.4).

$$\frac{\partial^2 T}{\partial \xi^2} - \frac{\partial^2 T}{\partial y^2} + \frac{\partial^2 T}{\partial z^2} = -2\lambda v \frac{\partial T}{\partial \xi} \tag{2.4}$$

Its difficult to make experimental measurements of welding temperature fields due to the high temperatures experienced in the fusion zone. However in the past, measurements of temperatures in the fusion zone have been made using embedded thermocouples. This demonstrated that Rosenthal's (1935) analytic model and point heat source can predict temperature distributions away from the fusion zone with good accuracy, however it is limited for describing temperature distributions in the fusion zone.

This inaccuracy in temperature prediction in the fusion zone is primarily due to the assumptions made in order to develop an analytical solution. The material property data used is assumed to remain constant with changing temperature and the latent heat due to phase transformation is ignored. The heat loss from the surface of the material is also neglected. More refined heat source models are required to predict temperature distributions in the region about the arc with reasonable accuracy.

Due to the simplifying assumptions required to develop closed form solutions which limit their application to restricted scenarios, the process lends itself to numerical methods. Numerical modelling allows the use of complex heat sources, complex material property definitions and allows convection and radiation from the surface of the material to be accounted for.

2.3.3.2 Heat Sources

The geometries that have been used to model the welding arc vary from point sources to complicated shape functions depending on the application. Much work has been done on modelling the geometry of heat sources.

Pavelic et al (1969) first suggested the idea of a distributed heat source. A disc model was proposed that had distributed the heat flux (W/m^2) with a Gaussian distribution. In Krutz et al (1978), Chong (1982), Westby (1968), Anderson (1978), Paley et al (1975) and Friedman (1975) the disc model was combined with finite element analysis to produce temperature

distributions which were significantly better than those calculated using the Rosenthal (1935) point source analytic solution.

Goldak et al (1984) proposed a mathematical model for the geometry of a heat source. This model uses a double ellipsoidal geometry with a Gaussian distribution of the heat flux. This model has the advantage that the geometry of the heat source can be easily altered. It also has the capability to model asymmetric heat sources such as strip electrodes. The result is Equation 2.5.

$$q(x, y, z) = q_0 e^{-(Ax^2 + By^2 + Cz^2)} \tag{2.5}$$

where

q = Heat generation/unit volume

x, y, z = Coordinates

Constants A, B and C are calculated so the total heat input is ηVI and the source decays to 5% of the peak value at the extremities and $x = \pm a$, $y = \pm b$, $z = \pm c$. The geometric parameters are shown in Figure 2.17 as taken from Goldak et al (1984):

$$q(x, y, z) = \frac{6\sqrt{3}\eta VI}{abc\pi\sqrt{\pi}} e^{-3\left(\frac{x^2}{a^2} + \frac{y^2}{b^2} + \frac{z^2}{c^2}\right)} \tag{2.6}$$

where

η = Arc efficiency

V = Voltage

I = Current

a, b, c = Goldak's double ellipsoidal heat source geometric parameters

As it is a double ellipsoidal heat source, Equation (2.6) is used for both the front and the rear sections of the heat source. This model has the advantage that the geometry of the heat source can be easily altered. It has been suggested that the best results are obtained when the ellipsoid size and shape are approximately equal to that of the weld pool. This heat source model has been shown to produce accurate results for both shallow and deep penetration welds.

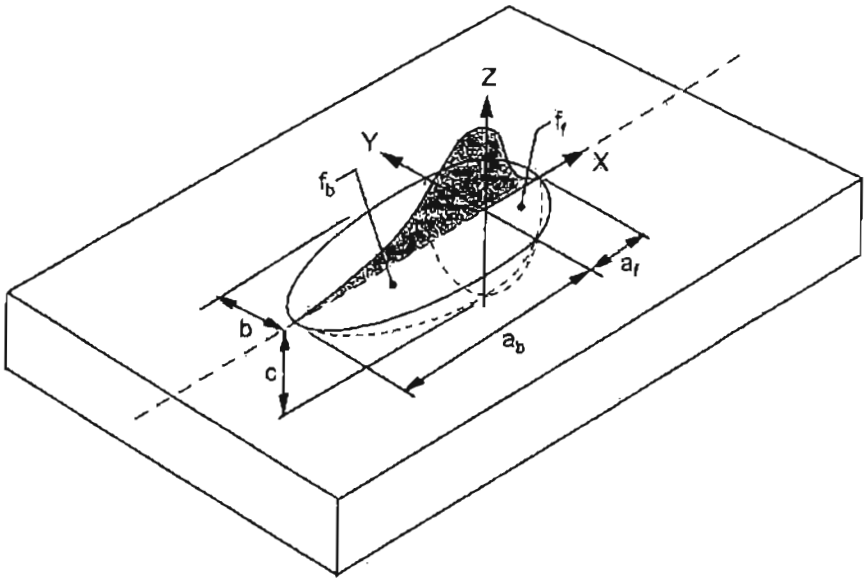

Figure 2.17: Goldak's double ellipsoidal heat source. Goldak et al (1985)

A closed form solution of Goldak's double ellipsoidal heat source has been developed by Nguyen et al (2000). This has allowed increased accuracy of temperature field prediction using analytical techniques. It is however still constrained to conduction only heat transfer and the effect of latent heat of vaporisation cannot be accounted for.

Much work since 1985 has been carried out testing and evaluating Goldak's double ellipsoidal heat source for varying welding processes and modelling techniques by a number of researchers such as Mahin et al (1986), Weckman et al (1988), Mangon and Mahimkar (1986), Terkriwal and Mazumder (1988) and Pardo and Weckman (1988).

While Goldak's heat source is still the most popular heat source used for welding simulation, modifications to it have been made in the past to produce more accurate results in certain welding processes. For example, Sabapathy et al (2001) modified the shape of the heat source to account for the weaving action used during in-service welding on gas pipelines. Also Nguyen et al (2001) developed what was described as a hybrid heat source. This was a modification of the double ellipsoidal heat source in an attempt to increase the accuracy of temperature predictions in relation to the depth of the weld.

2.3.3.3 Summary

A common simplification that is made in heat transfer analysis is the 'quasi steady state' assumption. This allows efficient predictions to be made by only considering the one time interval. This assumption is possible as the welding arc generally travels at a constant speed causing the temperature of the material to be constant in relation to the arc position away from welding start and stop positions.

Both numerical and analytical methods of heat transfer analysis have been used in the past, however modelling of the welding process is best suited to the use of numerical techniques. This is primarily due to the ability to account for the effect of latent heat of vaporisation. Also analytical models generally consider the heat transfer as conduction only and do not use temperature dependant material properties.

The accuracy of temperature field prediction in the region about the arc is highly dependant on the type of heat source used. Some of the heat sources that have been used in the past include point sources, disks, ellipsoids and double-ellipsoids. Although some researchers have made modifications to Goldak's double ellipsoidal heat source, it still remains the most popular heat source used for welding simulation today.

2.3.4 Thermal Stress Modelling of Welding

By de-coupling the thermal and mechanical models the complete temperature history calculated can serve as input for the mechanical model. As the transient stress is calculated the material properties are altered with temperature and effects such as phase transformation need to be accounted for.

When modelling circumferential welds the approach that has been commonly used is to assume the welding process is axisymmetric. This allows the use of 2D models which significantly reduce the computation time. Although three dimensional models have been used by some researchers, most work conducted to date has focused on the ability to achieve 3D simulations and efficient methods for doing so. Such work has also highlighted the ability and deficiencies of 2D axisymmetric simulation.

2.3.4.1 Transformation Plasticity

Transformation plasticity occurs during the phase change between austenite to banite and martensite. During this change, the crystal structure of the material changes, and there is a resulting reduction in material strength. This reduction in strength occurs during the expansions and contractions that occur in the near weld region after welding, and allows increased plastic deformation, producing an alteration in the residual stress field.

A number of analytical and numerical models have been developed for the calculation of residual stresses due to welding. The numerical models generally include a thermal model and a mechanical residual stress model. Friedman (1975) concluded that when creating such models there are only estimated welding parameters so the accuracy of the model will be limited. For this reason generally only simple finite element models were used rather than more complicated elastic-plastic models. However more accurate material data and welding parameters are now available so effects such as transformation plasticity can be considered.

When creating numerical models of residual stress it is often difficult to include the effect of transformation plasticity. The literature generally agrees that the plasticity produced in the material during the phase change from austenite to bainite and martensite does have an effect on the residual stresses left in the heat affected zone (HAZ). Josefson (1985) demonstrated this by using the simplifying assumption that the yield strength is reduced at the transformation temperature as shown in Figure 2.18. The dotted lines show the alterations made to the material strength curve which is used to simulate transformation plasticity.

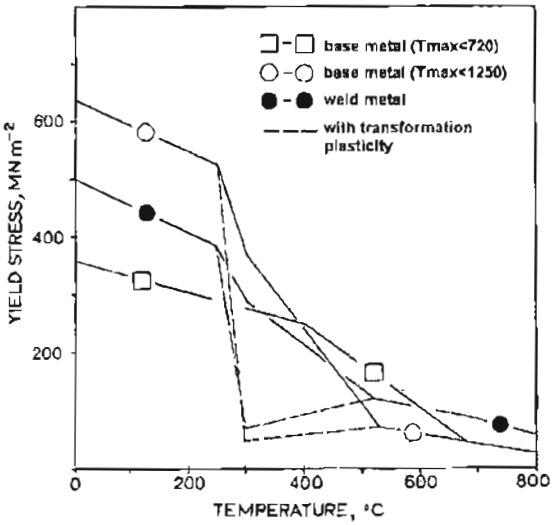

Figure 2.18: Temperature dependence of yield strength for C-Mn steel and the manner in which the definition was altered in order to allow for the effect of transformation plasticity. Josefson (1985)

Later Oddy et al (1990) also demonstrated the effect of transformation plasticity. In their investigation three transformation effects were considered. First, the effect of yield stress hysteresis which is where the yield stress of the material changes during the phase change of the material. This effect causes the relationship between yield strength and temperature to be different depending on whether the material is being heated or cooled as shown in Figure 2.19.

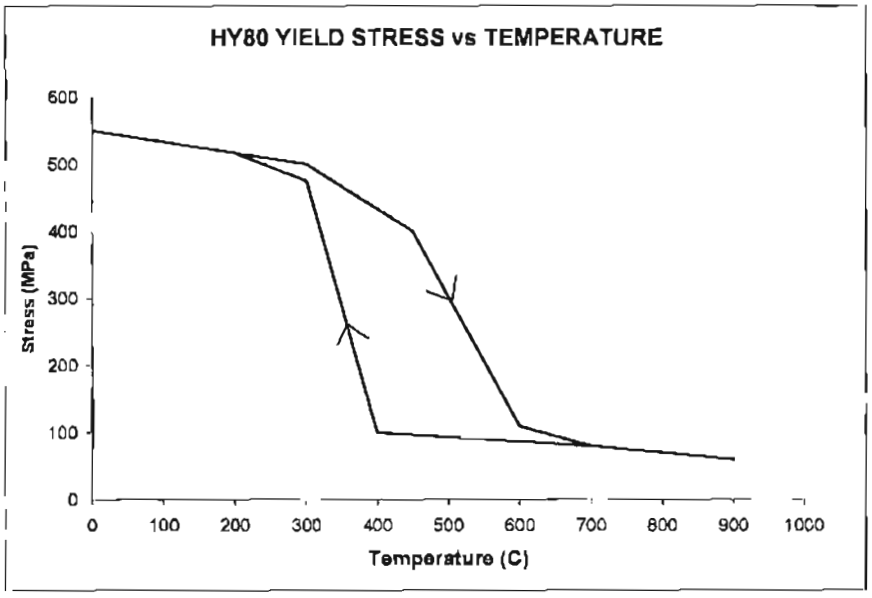

Figure 2.19: Yield strength verses temperature for HY80 steel, including yield hysteresis. Oddy et al (1990)

Second, the effect of the volume change that occurs during the phase change from austenite to bainite or martensite was considered. Oddy et al (1990) measured these volume changes using dilatometeric measurements obtained from a Gleeble simulation. These volume changes can be accounted for in the temperature dependant thermal expansion properties which are specified in the numerical model.

Third, the effect of transformation plasticity was accounted for. Transformation plasticity can be described as plastic deformation that occurs during a phase transformation. It occurs because as the structure of the crystal lattice changes during phase transformation the

material loses strength. This phenomena was accounted for by introducing a dip in the strength verses temperature curve at the transformation temperature which is similar to the approach of Josefson (1985).

In the study conducted by Oddy et al (1990), yield stress hysteresis was found to have no significant effect on the residual stress. However the effect of transformation plasticity and volume change proved to be significant and better agreement with experimental results was achieved in the HAZ and the fusion zone when these effects were included.

2.3.4.2 Axisymmetric Models

Most analyses of residual stress in circumferential welds to date have used 2-D axisymmetric models. These models assume that the entire girth is welded simultaneously. They have the advantage that they are computationally efficient while still providing a useful indication of the residual stress produced. However it has been found by Rybicki and Stonesifer (1979) and Brust et al (1981) that experimental stress measurements often do not agree with results calculated with 2D models. This has been attributed to the effect of start and stop positions of welding. This effect becomes more pronounced with factors such as incomplete root passes, more than one weld being laid at a time and reversing the welding direction for capping passes.

Rybicki et al (1978) produced an elastic-plastic welding simulation involving an analytical thermal model, which served as input to a mechanical model and simulated two welding

passes. Later Rybicki et al (1979) also developed models to simulate seven and thirty pass welds with reasonable computational efficiency. These models however were limited by the use of analytical models to develop a temperature history for the welding process. However this method allowed multiple passes to be modelled which would have not been possible otherwise due to the computational cost of 3D models.

Residual stress measurement and finite element models for the prediction of residual stress in root pass welds have been produced by Suzuki et al (1986). It was found that inside the girth weld of a pipeline, there are residual stresses that nearly equal the yield strength of the pipeline material. The residual stress in a Lehigh slot weld test was found also to have a residual stress close to that of the parent metal. Suzuki et al (1986) decided that this would be a suitable test to determine the susceptibility of line pipe to hydrogen cracking.

An axisymmetric model was produced by Teng et al (1997), which considered a circumferential weld completed in four passes. The results obtained summarize what is known about residual stress patterns in girth welds. These results are well established and demonstrate the ability of axisymmetric models to simulate three dimensional residual stress fields. The results of the study conducted by Teng et al (1997) are given below:

- On the weld line a high tensile residual axial stress occurs on the inner surface and a compressive axial residual stress occurs on the outer surface. Away from the weld centre line a compressive axial residual stress occurs on the inner surface and a tensile axial residual stress occurs on the outer surface.

- Thicker pipes have less axial residual stress and a larger tensile region.
- The inner surface of the weld centre line has a tensile hoop stress and the outer surface has a compressive hoop stress.
- Thinner walled pipes have higher tensile residual hoop stress than thicker walled pipes and large diameter pipes have a larger zone of tensile stresses.

One of the deficiencies of axisymmetric models has always been the inability to simulate welding end effects, however Dong et al (1997) and Edwards et al (1998) used axisymmetric models in order to verify the experimentally measured result from a part-circumference weld repair. It was found that even with only part of the circumference welded, an axisymmetric model could still provide good agreement with experimental results away from the weld start and stop positions.

One other example of an axisymmetric model used to good effect was in a computational model produced by Zhang et al (1998) to predict the residual stresses in a girth weld in a BRW core shroud. The weld used a vee preparation on both the inside and outside wall of the shroud. This left the residual stress on the wall in tension near the surfaces and in compression in the middle of the wall thickness. This demonstrates how useful results can be developed using 2D models.

It could be said that 2D axisymmetric models are quite capable of analysing residual stress fields in circumferential welds. While there are some limitations such as not being able to

simulate weld end effects and an over estimation of the residual stress on the weld centre-line they have been used successfully to research circumferential welds up to the present time. They offer such vastly faster computation times compared with 3D models and for many types of analyses, such as multi-pass welding they are still the only practical means of residual stress calculation.

2.3.4.3 3D Models

Some analyses however do warrant the use of 3D models despite their long solution times. Some examples of residual stress modelling using 3D models are given below.

A fully three dimensional transient residual stress model was compared with an axisymmetric residual stress model by Karlsson (1989). This model considered a single pass girth weld. The three dimensional analysis used a thermal model of the welding process to provide the temperature history for the mechanical model. The calculated hoop stress however did not agree well with the measured data. Karlsson attributed this to the phase transformation that occurred in the welding process, which was not allowed for in his model. Karlsson et al (1990) later produced a model of a single pass girth weld, which did allow for transformation plasticity by reducing the yield strength at the transformation temperature. This did help approximate the residual stress in the hoop direction. The material was also assumed to be perfectly plastic when the yield strength was exceeded. The justification for this assumption was that the plastic strains accumulated before the final solid-state phase transformation to a large extent are relieved during the transformation. In doing this

comparison it was found that the results from the two models were similar and that ignoring the start and end effects of welding, the results were almost rotationally symmetric in the 3D model. It was also found that using a coarse mesh in the mechanical model yielded stress values and shapes with reasonable accuracy when compared to finer meshes.

Two dimensional and three dimensional analyses of residual stress were also compared for welds on flat plates by Mc Dill (1992). The results were compared with experimental results found using X-ray diffraction. It was found that generally the 3D analysis approximated the measured results, however the 2D models exaggerated the magnitude of the longitudinal residual stress in the HAZ due to the plane strain assumption. The 2D models also failed to capture the effect of the phase transformation on the near weld region.

Li et al (1995) made progress towards the production of a three-dimensional multi-pass transient model. The temperature fields were assumed to be axisymmetrically distributed about the girth, which was in good agreement to the experimentally measured results, except at the start and stop positions. The stress results were found to be also axisymmetrically distributed about the girth, however this was not in good agreement with the experimentally determined results found by X-ray diffraction. It was concluded that better experimental results were required to develop this model further.

Dong et al (1997) produced a 3D model using shell elements, which used a transient heat source. The purpose of this research was to demonstrate that using shell elements was a

computationally-effective way to predict global stresses. The analysis was able to predict stress patterns through the thickness of the weld region similar to that which had been previously found using axisymetric models. The problems associated with the weld start / stop positions that cannot be taken into account in axisymmetric analyses were addressed using a shell element model.

Dong et al (2001) compared the method of using 3D shell elements against a 2D axisymmetric model and some experimental results. It was shown in the 3D model that the residual stress is not extremely close to axisymmetric. However 3D models are useful as they can provide prior knowledge of the region under consideration before an axisymmetric model is produced. It was stated that the start and stop positions of the weld were largely responsible for the disagreement in results between experimentally measured results and axisymmetric models.

A full 3D finite element model of a circumferential weld was carried out by Dike et al (1998). The justification behind using such a computationally intensive analysis was that "*three dimensional analysis are required to achieve the correct structural deformations.*" (Dike et al, 1998 pp. 961) Goldak's (1984) heat source was used in the finite element heat conduction analysis using linear eight noded tetrahedral elements. The same mesh was also used in the mechanical analysis. Use of 8 noded tetrahedral elements is acceptable in thermal analysis, however, it is generally accepted that parabolic 20 noded tetrahedral elements should be used when solving non-linear stress analysis problems. 8 noded tetrahedral elements were used

however to enable transfer of the temperature history to the mechanical model without interpolation and to reduce the number of nodes and the solution time. X-ray diffraction was used to validate the models created. While the results from the modelling fell within the experimentally determined results there was a significant scatter within the X-ray diffraction results.

From past research it can be seen that it is now possible to use 3D residual stress models despite the computational cost. It is also clear however that while axisymmetric models have some deficiencies they are still a very useful and efficient method of residual stress modelling. In summary if weld end effects are not important or if the analysis is highly intensive then, axisymmetric models are still worth considering. Another potential path that could be taken is the use of axisymmetric models in conjunction with 3D models as suggested by Dong et al (1997).

2.3.4.4 Multiple Passes

Another benefit in the use of numerical models is the ability to model multiple passes. Generally multiple passes are modelled using axisymmetric analyses due to the computational intensity required. A number of studies have simulated multi-pass welding but they are generally concerned with the modelling techniques themselves.

Work has been carried out in the past on determining the best and most efficient ways of simulating multiple weld passes. For example some researchers such as Ueda and Nakacho

(1982) looked at the mesh density requirements for multi-pass welding simulation and the effect of the number of passes on CPU time.

More recently the development of modelling techniques relating to the simulation of multiple passes using the concept of lumped passes was described by Hong et al (1998). This technique involves lumping all passes in each welding layer in order to reduce the computation time. It appears to be a useful way of simulating multi-pass welds efficiently and with reasonable accuracy.

Zhang et al (1997) used a 3D analysis with shell elements and assumed that they were laminated. This allowed the researchers to consider multi-pass welds by adding filler metal using element birth and death facilities provided in the ABAQUS software. The method proposed was applied to a repair weld, which could not be modelled accurately using an axisymmetric model.

Multi pass welding is generally required in pipeline construction to fill the weld groove. In Radaj (1992) it is explained that the longitudinal residual stress in the first passes is generally reduced by the layers welded over them. This is one reason for the reduction in HACC risk that occurs after the hot pass is laid on top of the root pass. It is stated in Australian Standard, Pipelines - Gas and liquid petroleum AS 2885.2-2002 that if the hot pass is not laid within six minutes of completion of the root pass then the risk of HACC is greatly increased.

Many researchers have created simulations of multiple passes using sophisticated techniques such as element birth and death with 2D axisymmetric models. It would appear from the open literature that 3D simulations of multiple weld passes using a transient heat source with the addition of weld metal is yet to be achieved. While some researchers have been able to create such models with single passes, current computing technology is yet to allow thorough 3D simulation of multiple passes.

2.3.5 Effect of Process Parameters

A significant amount of work on modelling residual stress in circumferential welds has been carried out to date. The pattern of residual stress in a circumferential welds is well understood, however, a complete compilation of results demonstrating how the stress field is altered by changing different process parameters is lacking. Some preliminary work has been conducted and that which is stated in the open literature is given below.

There are some conflicting results published in the literature. For example, the influence of pipe wall thickness and pipe diameter which was investigated firstly by Chrenko (1978) and later by Rybicki et al (1982). Chrenko (1978) compared pipes of varying diameter with a constant wall thickness. It was found that the tensile axial residual stress on the inside wall in the HAZ was lower in the larger diameter pipes. Rybicki et al (1982) however found that the axial tensile residual stress varied very little in thick walled pipes when considering the radius to thickness ratio of pipes.

Other effects such as the influence of yield strength of the material and the heat input have also been examined in the past. Burst and Stonesifer (1981) found that increasing the yield strength resulted in slightly higher values of residual stress. It was also stated after examining the effect of two different weld heat inputs that there was little difference in the residual stress. However the higher heat input resulted in a greater residual stress.

A summary of the residual stress in circumferential welds results which are available in the literature up to 1995 was collated by Mohr (1996). The object of this summary was to create a method of predicting residual stress based on limited information. He found some trends relating to wall thickness and pipe diameter, however the varied process parameters used by different researchers caused variability in results.

Later Michaleris et al (1996) created a limited matrix of residual stress results which covered variation in radius to wall thickness ratios, single and double V bevels and residual stresses before and after hydrotest. Finite element models were used to develop these results. From this work a method of predicting residual stress was developed in Mohr (1997) which was based on what was believed to be the most influential parameters; the number of passes, the wall thickness and the yield strength of the pipe material. This method was developed using empirical relationships from results of finite element models. While this method provides a less conservative way to predict residual stress than the existing guidance provided, it still is a very conservative way of predicting residual stress. This level of conservatism is required

due to the many important process parameters that were ignored and produced the variability of results seen in Mohr (1996).

In a study carried out by Lin and Perng (1997) which considered the effect of welding parameters on residual stress in type 420 martensitic stainless steel it was found that the higher the heat input used when welding the greater the residual stress. They also considered the effect of pre-heat on the residual stress. It was found that using higher pre-heat temperatures could have the effect of increasing the equilibrium temperature and therefore the heat input and cause increased residual stress. This highlights the complexity of considering the effect of welding process parameters on the residual stress.

Because of the complex influence of process parameters trends observed often need to be qualified. It is this reason why investigation of process parameters specifically relating to the pipeline construction process need to be considered.

2.3.6 Methods of Stress Relief

There are many methods available for the relief of welding residual stresses, including pre-welding measures such as joint preparation, to process techniques like backlay welding and post-weld treatments such as annealing. For a detailed description of many techniques for the reduction of residual stress see Radaj (1992). This work is interested specifically in the

reduction of residual stresses in circumferential welds. Examples of studies into such techniques are given below.

Residual stress relief can improve the structural integrity of welded joints. It also can have the effect of reducing the driving force for HACC. Different methods of stress relief have been studied for use in circumferential welds such as pre-heating or post-heating the weld, Last Pass Heat Sink Welding (LPHSW), Induction Heating for Stress Improvement (IHSI) and backlay welding. Similar methods could be developed to reduce the residual stresses experienced during pipeline construction.

Backlay welding is carried out in order to transform the tensile residual stress on the inside surface of the pipe into compressive stress. This is done by laying a series of welds over the girth weld in the axial direction. This has been shown by Brust and Rybicki (1981) to be an effective way to completely eliminate any tensile stress on the inside surface of the pipe. While this could be a useful process it would be impractical for use in pipeline construction due to the additional time required to carry out such a process. Also it is an inefficient use of weld metal.

Josefson (1982) considered the effect of post weld heat treatment (PWHT) on the residual stress in a single pass girth weld. In this analysis a two-dimensional axisymmetric finite element model was used. The effects of stress relaxation creep and phase transformation were included. It was found that the optimal PWHT was when the weld is held at 575-600°C

for 1-2 hours, which would leave a residual stress of 80-110 MPa. It was also found that a longer PWHT did not produce significantly lower stress levels but did cause deterioration in the material properties.

A technique that has been used in the past for relieving residual stress in girth welds is known as Induction Heating for Stress Improvement (IHSI). This method involves creating a temperature differential across the cylinder wall by using an induction heating coil around the girth while cooling the inner surface with water. A redistribution of the residual stress field results in reduced tensile stresses on the inside wall. This technique has been described and investigated using numerical models by Rybicki et al (1980).

A similar method known as cooling stress improvement (CSI) was described by Li et al (1993). The theory behind CSI is that after girth welding the weld can be treated by keeping the temperature at the inside of the pipe cool and heating the outside to reduce the residual stress gradient in the pipe in the through thickness direction. The concept was proposed as it is known that the residual stress in girth welds generally are left with the inside surface in tension and the outside surface in compression. While this method would be impractical during pipeline construction due to the increased time required to complete the joint, it demonstrates the type of methods available for residual stress relief.

Another similar method was modelled by Enzinger and Cerjak (1998) called Last Pass Heat Sink Welding (LPHSW). This technique uses water flowing through the pipe as a high heat

input final pass is laid to provide heating of the outside wall of the pipe. Cerjak and Enzinger (1998) used a finite element model of LPIISW to consider its effect on the development of residual stress.

It can be seen from the above examples of residual stress reduction strategies, that currently available methods are unlikely to be used in the pipeline construction process. However modification of the pipeline construction procedure could influence the residual stress induced in the girth weld. There are a large number of process parameters and investigating their influence may reveal how the residual stress can be minimised. By understanding the influence of process parameters it is possible that residual stress reduction strategies could be developed for the pipeline construction process.

2.4 HYDROGEN DIFFUSION MODELLING

Numerical analysis has been shown to be the most useful method of calculating hydrogen concentration due to the rapid rates of hydrogen diffusion and the complex geometries of the welding process. Numerical analysis is deemed useful due to its ability to calculate hydrogen concentrations in crack susceptible regions. Experiments have shown (Bailey et al 1993) that the diffusion of hydrogen through metals follows Fick's Second Law of Diffusion which, is given below:

$$\frac{\partial C}{\partial t} = d\nabla^2 C \qquad (2.7)$$

where

C = Concentration of hydrogen

∇^2 = Spatial distribution

t = Time

d = Diffusivity

When modelling hydrogen diffusion the approach that has been taken by a number of researchers such as Chew et al (1975) and Anderson (1980) is to model the hydrogen diffusion using Fick's Second Law. While this has allowed a quantitative view of hydrogen diffusion through weldments it was recognised by McNabb et al (1963) that there are

hydrogen-trapping sites, which exist in the material. McNabb treated these trapping sites as uniformly distributed potential wells of significantly greater depth than those in regular regions of the crystal lattice. Chew et al (1975) also developed a similar model, named a 'void model' to account for the effect of hydrogen trapping.

Goldak and Zhang (1991) used a numerical method of calculation that uses the chemical potential of hydrogen as the driving force for diffusion. More complex models have been developed such as that of Anderson (1980), which include the trapping effects modelled by McNabb and stress assisted diffusion. There is however a lack of consistent values in the literature regarding the quantity of diffusion retarding traps or the density of diffusion accelerating dislocations in weld metal. Because of this it has been suggested by Boellinghaus et al (1995) that for a quantitative analysis of hydrogen concentration models simply based on Fick's second Law are advisory.

Some progress has also been made toward modelling the effect of the hydrogen content on the propagation of a crack. A simple hydrogen assisted cracking model has been developed by Boellinghaus et al (2000) which considers only the local hydrogen content, local mechanical load and local microstructure. The scheme developed appears to be a reasonable approach to model HACC, however it requires further development to become a useful tool for prediction purposes.

2.5 GAPS IN CURRENT KNOWLEDGE

From the literature surveyed it is apparent that there has been a large amount of work carried out on welding residual stress including residual stress in circumferential welds. The majority of numerical work in this area has been carried out using two-dimensional axisymmetric models. These models have been shown to produce results of reasonable accuracy however they are unable to consider the welding start and stop positions.

Some numerical 3D circumferential residual welding stress literature has been published however this has served more to point out the capabilities and deficiencies of the axisymmetric models, which have been used in the past. There is now opportunity to apply these techniques to increase the knowledge of stress evolution during the pipeline construction process.

The effect of the lift height has been recognised in relation to residual stress by Higdon et al (1980). They considered it with the use of a combination of analytical and 2D-axisymmetric numerical models. The numerical models that were used however were not thermo-elastic plastic models but a simplified residual stress model where a 2D longitudinal residual stress field in a flat plate was wrapped into a cylinder and allowed to deform. This ignores the 3D effects, phase transformation, elevated temperature of the material and the transient stress during construction. It also makes the assumption that lifting has no effect on the final state of residual stress. There is opportunity to consider the effect of a number of process

parameters on the residual stress. For example the timing of the lifting process during construction.

There has now been much research done on modelling of hydrogen diffusion due to the welding process. This has advanced from models simply based on Fick's second Law of diffusion with an initial hydrogen concentration, to models based on the mass transfer equation coupled with heat transfer models and thermo-elastic-plastic models with hydrogen traps.

There is an opportunity to now consider the transient temperature, stress and hydrogen concentration during pipeline construction. A transient view of stress, temperature and hydrogen concentration would allow an understanding of the transient risk of HACC which until now has been reported but not explained.

2.6 RESEARCH PROBLEM

The overall objective of this research is to produce a transient numerical simulation of pipeline fabrication using finite element modelling techniques. To relate the knowledge gained by modelling pipeline construction to reduce the possibility of HACC. To simulate the construction process, the stresses due to lifting of the front end, the temperature cycle and the thermal welding stresses and the transient hydrogen concentration needed to be considered.

The key features required are:

- To model the stress induced in the root pass of a girth weld due to lifting and lowering. These stresses are dependent on the height of lift, the geometry of the root pass and the temperature field within the root pass.
- To undertake a transient heat transfer analysis of the near weld region which will produce temperature history for the material during the construction process. This is important, as the material properties of steel (such as strength and thermal conductivity) are temperature dependent.
- To produce a transient thermal stress model using the temperature history previously derived in the heat transfer analysis.
- To efficiently combine the transient thermal stress and lifting models to simulate the complete construction process.

- To experimentally verify the residual stress model developed and to indicate the level of accuracy that can be expected.
- To vary the process parameters (such as the timing of the process, welding speed, percentage completion of root pass before lifting etc) to:

  -demonstrate how a residual stress in the root pass can be minimised. This will have the effect of reducing the likelihood of HACC.

  -increase the forward pace of construction which is the limiting factor in reducing the cost of pipeline construction.
- Create a transient hydrogen diffusion model of the welding process.
- Combine the knowledge of the evolution of stress, temperature and hydrogen concentration to explain the transient risk of HACC which can be used when designing construction procedures.

2.7 JUSTIFICATION OF WORK

While it has been recognised by some researchers that lifting of the pipeline front end (Higdon et al, 1980) and other process variables have implications for the residual stress experienced in girth welds, it has not been possible until now to consider their effect in a transient manner. The timing of events has a significant effect on the stress and hydrogen concentration. For example, if a number of forces are applied to an object simultaneously it could result in plastic deformation, while if these forces were applied one at a time the object would only be elastically deformed.

Consider the analogy of a bridge which has a capacity to support ten people. If fifteen people walk across the bridge simultaneously the bridge may collapse. However if they walk across one at a time the bridge will not fail. Therefore in order to know whether the bridge will collapse when fifteen people try to cross, the timing of each person crossing needs to be known.

With the current push toward thinner walled higher strength pipe to reduce construction costs, avoidance of HACC is of increased importance. If it is possible to safely use X80 or X100 pipe there is a significant material reduction in the pipe tonnage required per unit length of pipeline. The use of higher strength pipe may increase its susceptibility to HACC making the pipeline more vulnerable to the existence of hydrogen cracks.

The major determinant of pipeline construction cost is the speed of front end construction. There have been various methods proposed by other researchers in the past which could be used to improve the efficiency of the process, however these methods generally place the pipeline at greater risk of HACC. Further investigation is required in order to determine what improvements can be safely made.

The cost of shutting down a pipeline which supplies gas to a city to repair weld defects could run into millions of dollars. There is also the risk of loss of life in the event of an accident. Due to the high cost of failure it is extremely important to have a good understanding of the potential for HACC. This thesis aims to address these issues.

Chapter 3

CONSTRUCTION MODELLING

This work seeks to determine the effect of process variables on the development of residual stress in the region of a girth weld during pipeline construction. It is intended that by minimising the welding residual stress, the possibility of HACC is reduced. The method undertaken to carry out this research has been to create numerical models to map the thermal and stress cycle of the near weld region. The models described in this chapter are compared and verified against experimental results in Chapter 4. The experimental results described in Chapter 4 indicate the accuracy that should be expected from residual stress measurement. The experimental work conducted as part of this research gave confidence that the numerical models have the ability to predict residual stress trends due to certain combinations of process parameters.

While studies of thermal stresses induced in the near weld region of circumferential welds have been carried out by a number of researchers before such as Karlson (1989), the studies have always been on models of only the near weld region. This has been an acceptable approach as it is well known that the residual stresses induced in the near weld region fall away to zero only a short distance from the weld centre line. With pipeline construction

however the front end of the pipe is lifted a long way from the weld which induces a stress on the weld. In order to incorporate both these effects into the one thermo-elastic-plastic model to avoid inaccurate assumptions such as made by Weickert (1984) would require a mesh of such proportions that computation would be prohibitive. For example Weickert (1984) assumed that the lifting and lowering process had no influence on the final state of residual stress. In this thesis a sub-modelling technique has been developed to simulate the influence of the lifting process onto a model of only the near weld region. This enabled the efficient use of computing resources while avoiding inaccurate assumptions such as superposition.

The process used to model pipeline construction in this thesis is as follows. Firstly a 'Lifting Model' was created which calculated the stress induced in the root pass due to the lifting and lowering process without considering the effect of the thermal cycle. Then a 'Thermal Model', based on Goldak's double ellipsoidal heat source was created to calculate the temperature history of the near weld region. This temperature history was used to calculate the transient stress due to the welding thermal cycle. A model of the clamping process was created to examine the effect of the internal line-up clamps. The effect of the lifting process was simulated onto a model of the near weld region using the sub-modelling technique developed and the results were compared with those of the full pipe model. These external mechanical loads were applied to the thermal stress model of the near weld region to simulate the complete construction process. A schematic of this calculation scheme is shown in Figure 3.1.

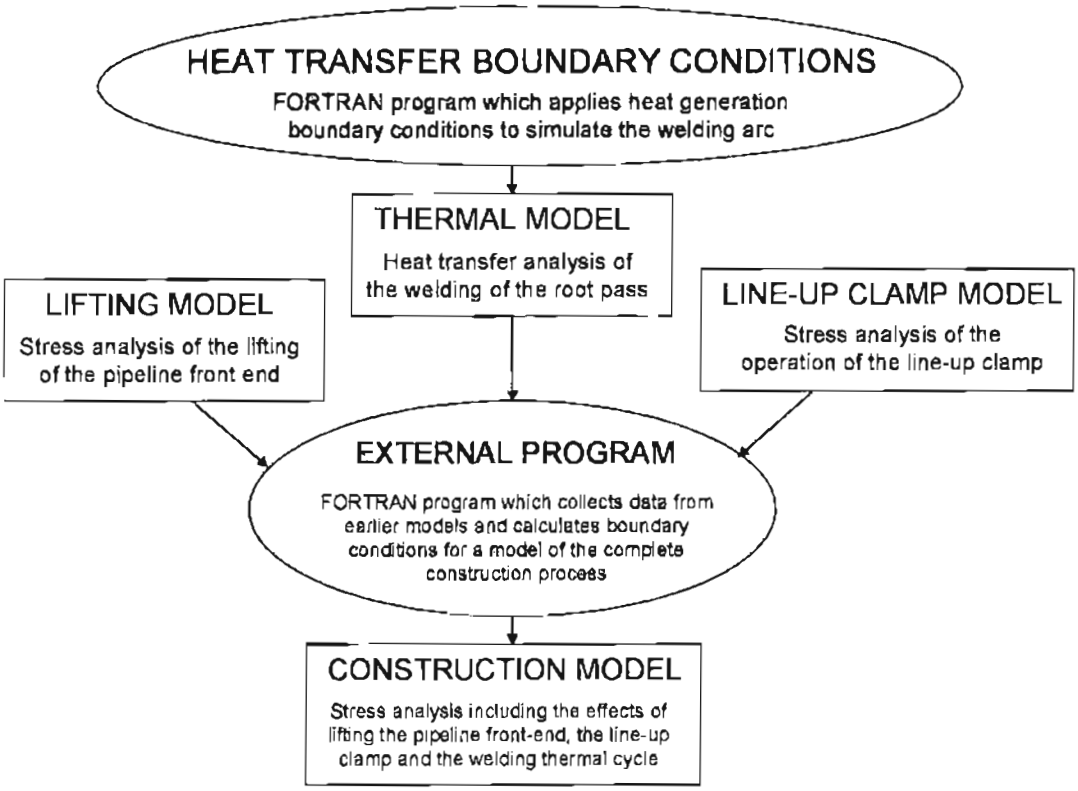

Figure 3.1: Schematic diagram of modelling procedure.

3.1 LIFTING MODELS

To analyse the stress in the root pass of a girth weld due to the lifting and lowering operation, stress models of three pipe lengths with a refined mesh in the region of the root pass were produced. While these models gave an indication of the stress induced in the root pass due to the lifting and lowering process, they ignore the effect of the thermal cycle on the evolution of stress in the weld. For this reason a modelling strategy has been developed which allows the efficient and effective modelling of the lifting and lowering process.

Non-linear stress models were created and results were produced with relative computational ease considering a mesh of three pipe lengths with 25000 nodes was used. The solution time was reasonably quick due to the relatively few time steps that are required when the thermal cycle is considered not to change. The temperature cycle is assumed not to change as the lifting and lowering process occurs within a few seconds so the change in temperature during this time interval is insignificant. The temperature field in the near weld region at the time of lift was included as it influences the strength of the material.

In the past Higdon et al (1980) and North et al (1981) calculated the bending stresses due to lifting the pipeline front end. They assumed that the pipeline lay on a solid foundation, ignoring the existence of the support skids placed at the end of each pipe segment. This allowed calculation of the bending stresses using simple analytical techniques.

In this study pipe lifting was modelled so that the pipe was able to contact and break contact with the support skids when the front end is lifted and lowered off. This approach allows calculation of the pipe bending stress with height which cannot be taken into account using analytical techniques.

3.1.1 Nominal Dimensions

For the purpose of setting up the modelling procedure a generic pipe size was selected. The lengths of the pipe segments were assumed to be 12m in length, 300mm in diameter and have a wall thickness of 6mm. The joint preparation that was used for the root pass was a 60^{o} included angle with a 1.6mm root face and a 1.6mm root gap. The height of the root pass was taken to be 4mm. These nominal dimensions were used to set up the modelling procedure but dimensions and other process parameters were varied during the investigation described in Chapter 5.

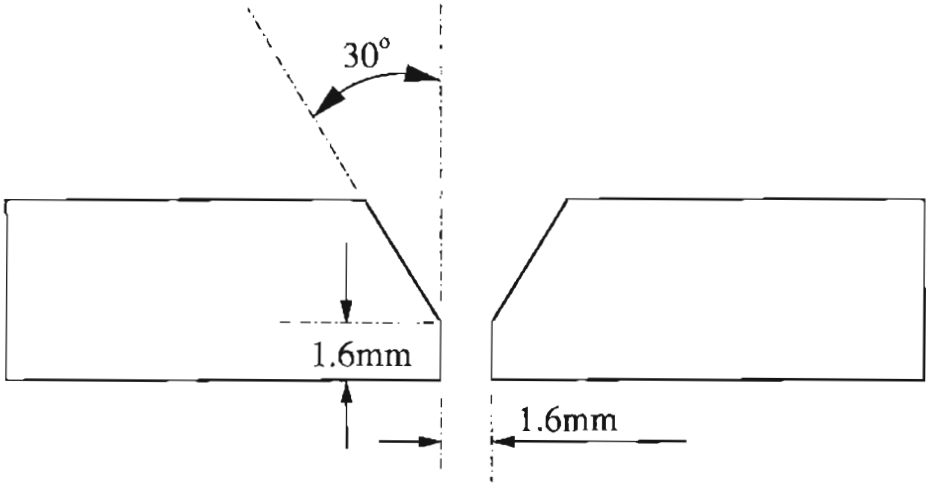

Figure 3.2: Nominal dimensions used for the joint preparation.

3.1.2 Simulation of Support Skids

In finite element methods, when simulating objects which contact or break contact during deformation, measures need to be taken to communicate their positions otherwise meshed bodies will effectively glide through one another. One method is to use special elements to bridge the gap, often known as contact elements. Contact elements effectively operate as a non-linear progressive spring between two nodes on each side of the potential contact zone.

When modelling the lifting of the pipeline front end, contact between the pipe body and the skids need to be simulated. However during lifting, the gaps between the pipe and the skid that require bridging are large and this can produce solution convergence problems. Therefore an alternate methodology was developed.

Initially a model was run which excluded the skids. This allowed the free displacement of nodes in the location of the skids to be determined. With the introduction of the skids this free displacement is constrained. This constrained motion can then be calculated and forced as a displacement verses time boundary condition. A boundary condition was created, which mimicked the displacement of the pipe in the region above the skid but did not allow it to be displaced below the level of the support skid before and after the lift. This technique required that the solution was re-run as each skid was simulated by the displacement boundary condition until all skids were simulated up to the front end. The maximum number of skids the pipe is lifted off, is two, which occurs during an extreme lift case. Therefore simply restraining the pipe where the third support skid was placed simulated all other skid contact further away from the pipeline front end.

In Figure 3.3 the deformed shape of the pipeline front end during lifting and lowering is shown for two scenarios. The first is where the skid closest to the front end is both present and absent and the second where the skid closest to the front end is there to support the pipeline when it is lowered.

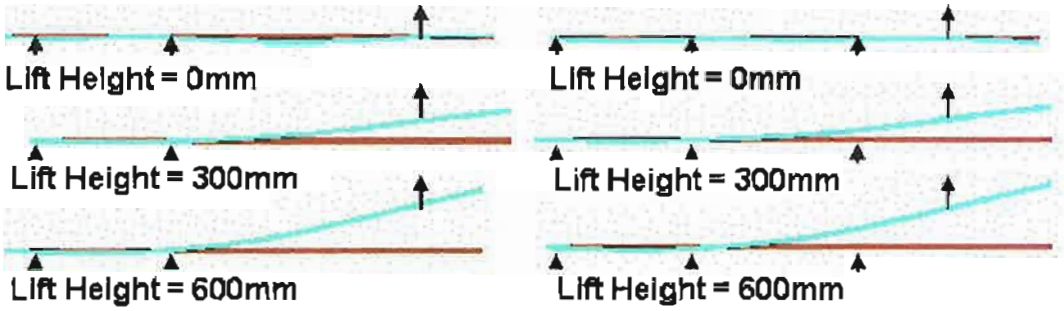

Figure 3.3: The undeformed pipe is shown in red and the deformed pipe is shown in blue. On the left side, the lifting process has been modelled without the skid closest to the front end and on the right the lifting process has been modelled with the skid closest to the front end. The distortion of the pipe has been increased by a factor of 5.

In Figure 3.4 the pipe body stress for a given lift height at the 6 o'clock position on the inside wall at the joint closest to the pipeline front end is shown. The result published by Higdon et al (1980) which assumed the pipe lay on a solid foundation and the result found in this study by including the support skids in the analysis is given. It can be seen that when the pipe is lifted off the second support skid the stress rises rapidly. This would suggest that when specifying a maximum lift height in a construction procedure, the number of support skids the pipe is lifted off should also be specified.

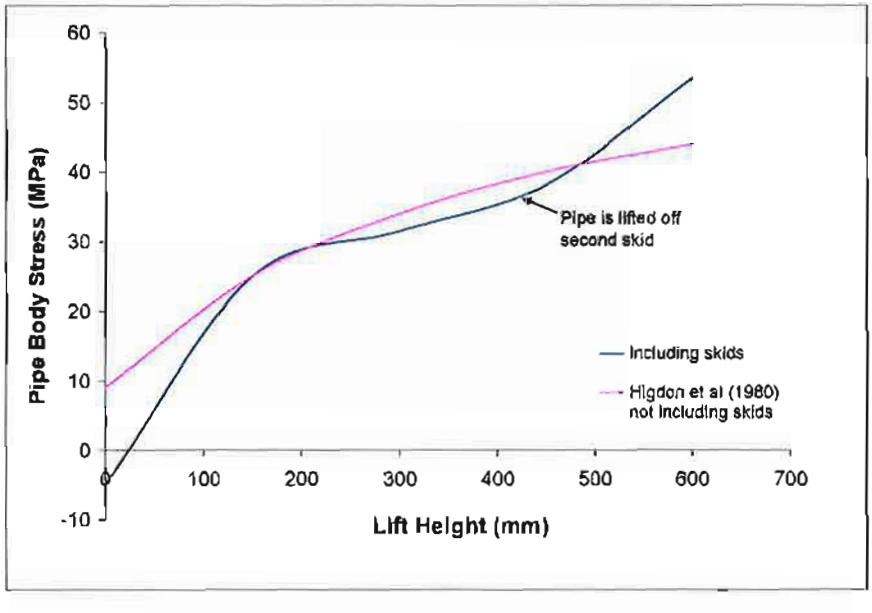

Figure 3.4: Graph of axial pipe body stress verses lift height for the 6 o'clock position on the inside wall at the joint closest to the pipeline front end.

While this analysis is useful for determining the pipe body stresses that are experienced due to lifting the pipeline front end, examining the resultant stress in the near weld region would give an incorrect interpretation of the stresses. This is because the stress due to the welding thermal cycle are not taken into account. It is for this reason that a sub-modelling technique was developed.

3.1.3 Sub-modelling the Lifting Process

To accurately model the construction process the effect of the welding thermal cycle also needs to be considered. The thermal and stress models required to simulate this process are

time dependent and require that short time steps be used in order to achieve convergence. Due to the computational intensity required it is almost impossible because of excessive computation time to consider a full pipe mesh for these models. To overcome this dilemma a sub-modelling technique was developed in which the stress due to lifting was applied onto a mesh of only the near weld region. The bending loads induced in the pipe during lifting and lowering is simulated onto a sub-model as shown in Figure 3.5. The forces used in the sub-model were calculated from the pipe body stresses in the previously generated pipe lifting model.

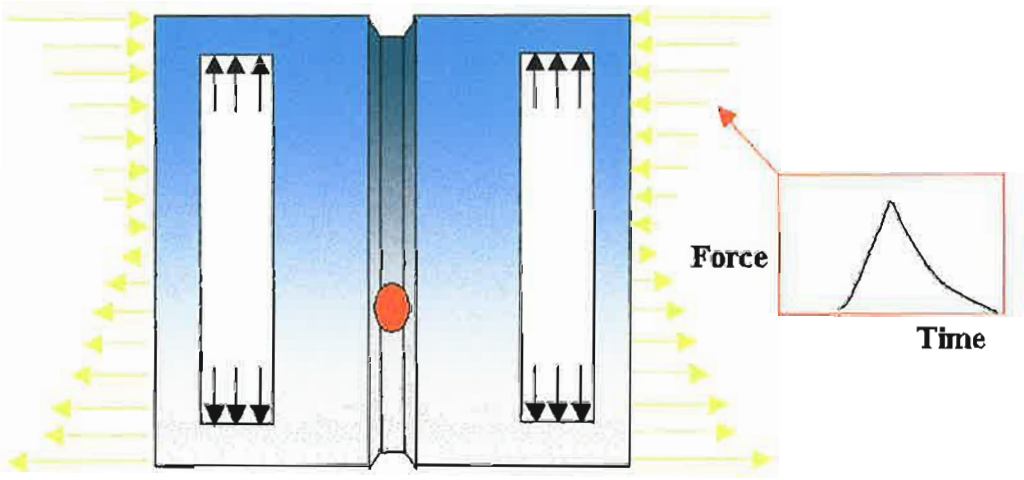

Figure 3.5: Forces applied to sub-model to simulate stress in the root pass due to lifting the pipeline front end.

The sub-model produced uses the same mesh geometry in the near weld region as the full pipe model. The stress results at the nodes in the full pipe model where the forces are to be

applied were resolved into the longitudinal direction and the forces were calculated. To test and validate this approach it was verified that these forces produced very similar stress results on the sub-model as was produced on the near weld region using a full pipe model as demonstrated later in Section 3.1.5.

3.1.4 Calculation of Forces to Simulate Lifting

The stress at each node on the boundary of the sub-model was transformed into a force using an external computer program (Fortran program separate from the FEA software) that was written to calculate and apply forces to simulate bending due to the lifting and lowering process. The program strategy was as follows:

- The coordinate positions, coordinate identification numbers and component stresses are read into the program from the output file of the full pipe lifting model.
- The coordinate positions and node identification numbers are read in to the program from a file containing the mesh geometry data to be used in the sub-model.
- The nodes in the full pipe model are then scanned through to find which ones share the same coordinate position with those in the sub-model. These nodes are then placed into an array.
- The stresses on these nodes in the longitudinal direction are then used to calculate the forces to be applied in the sub-model.

- These forces and their corresponding node ID numbers are then written out into an external file.
- This external file is then read into the sub-model as boundary conditions.

The nodes in the cross section are evenly spaced and each node on the inside diameter represents the same amount of area as every other node on the inside diameter. Similarly the nodes on the outside diameter represent the same amount of area as every other node on the outside diameter. In the cross-section where the forces were applied the nodes were spaced regularly around the girth as shown in Figure 3.6. The nodes on the outside diameter cover a greater area than those on the inside. Therefore the nodes on the outside require proportionally larger forces to produce the intended pressure. A multiplication factor was produced to allow for this difference in area between the inside and outside nodes.

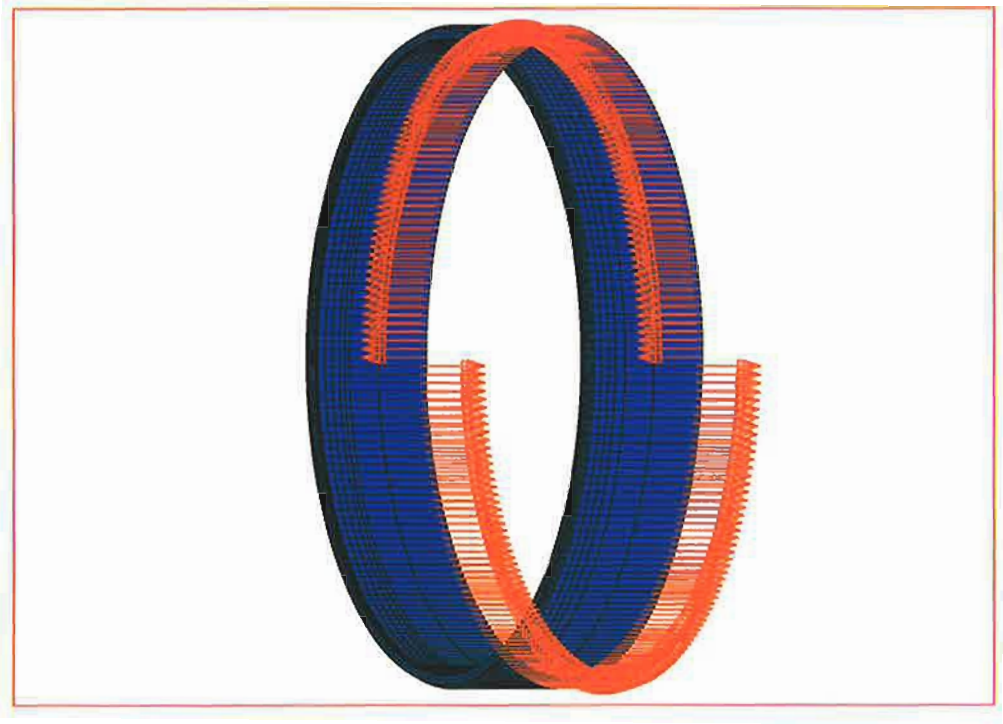

Figure 3.6: The nodes in the pipe cross section where the forces are applied were evenly spaced.

The multiplication factors used to proportion the forces applied to the nodes on the inside and outside surfaces of the pipe were calculated using the following equations.

$$MF_{inside} = 2 \times \left(\frac{A_i}{A_i + A_o} \right) \tag{3.1}$$

$$MF_{outside} = 2 \times \left(\frac{A_o}{A_i + A_o} \right) \tag{3.2}$$

where

MF = Multiplication Factor

A_i = Inside area

A_o = Outside Area

The areas were assigned to the inside and outside nodes as follows.

$$A_i = \pi(R_m^2 - R_i^2) \tag{3.3}$$

$$A_o = \pi(R_o^2 - R_m^2) \tag{3.4}$$

where

R_i Inside radius of pipe

R_m Mean radius of pipe

R_o Outside radius of pipe

The force applied to nodes to simulate bending was then calculated using Equation 3.5.

$$F_n = MF\left(\frac{\sigma_n \times A}{n}\right) \tag{3.5}$$

where

F_n Force on node

σ_n Stress on node

A Cross-sectional area of pipe

n Number of nodes in cross-section

3.1.5 Verification of Sub-modelling Technique

In order to verify this sub-modelling technique the calculated bending stresses induced by lifting on the near weld region from a sub-model and the full pipe model were compared. It can be seen by comparing the stress fields for the full pipe model in Figure 3.7 and the submodel in Figure 3.8 the two models are not identical. This variation is due to the forces which are applied in the sub-model to simulate a pressure. This variation is caused by induced stress concentrations which occur in the sub-model at the loaded nodes.

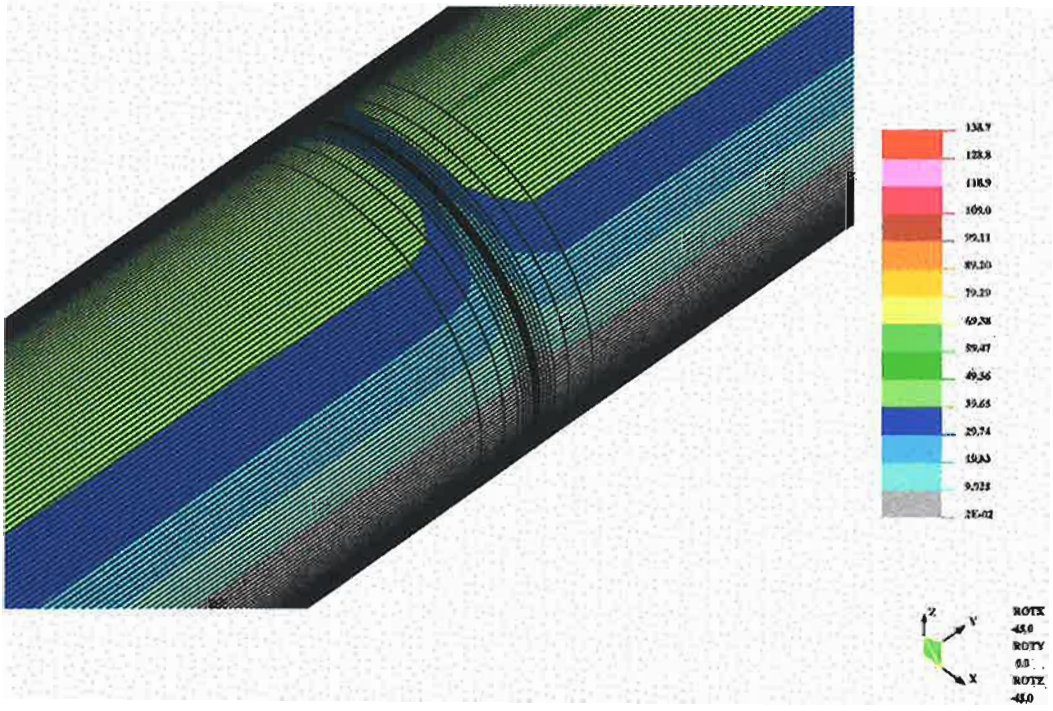

Figure 3.7: Von-Mises stress (MPa) field results from full pipe lifting model during a maximum lift of 600mm.

Figure 3.8: Von-Mises stress (MPa) field results from a sub-model of the lifting pipe model during a maximum lift of 600mm.

The effect of these stress concentrations can be seen by considering a larger submodel. The forces, which were being used in order to simulate bending were applied on nodes so a fairly uneven pressure was applied to the sides of the sub-model. This pressure starts to become more evenly spread away from where the forces are applied. This follows Saint Venant's principle, which states that for the purpose of computing the stresses in a structural member it is possible to replace a given loading for a simpler one. This is provided that:

- The actual loading and the loading used to compute the stresses must be statically equivalent.

- Stresses cannot be computed in this manner in the region where the loads are applied.

Therefore by creating a larger sub-model the simulated pressure becomes more uniform in the near weld region as it is further away from where the forces are applied. The result of this is shown in Figure 3.9.

Figure 3.9: The Von-Mises stress (MPa) in the near weld region produced by a larger linear elastic sub-model.

In Figure 3.10 the Von-Mises stress vs distance from the weld centre line at the 6 o'clock position on the inside wall is plotted for the small sub-model, the large sub-model and the full pipe model. In the region close to the weld centre line (the area of interest) the stress

results agree closely however in the region where the forces are applied the results vary significantly. The difference in the results shown in Figure 3.10 is due to a phenomenon known as St Venant's Principal (see page 92).

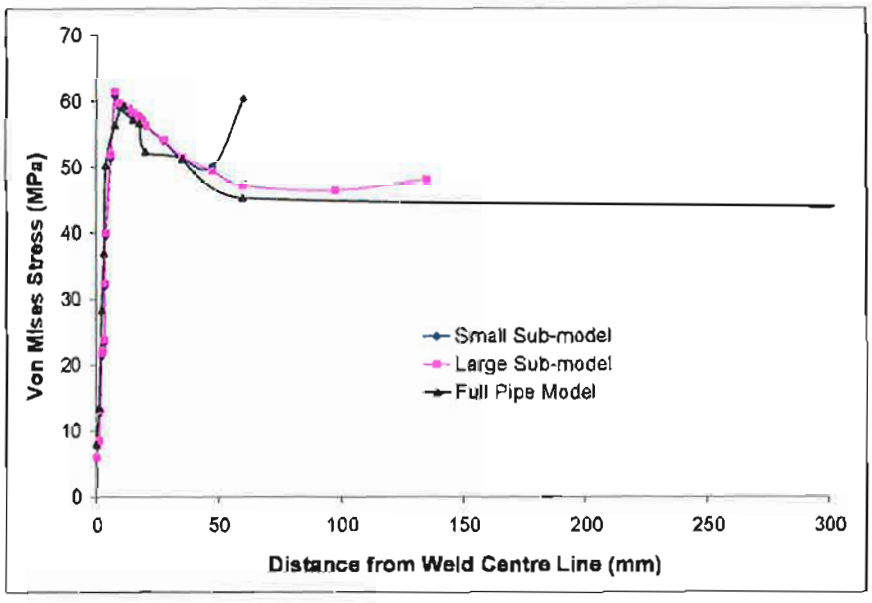

Figure 3.10: The Von-Mises stress vs distance from the weld centre line at the 6 o'clock position on the inside wall for the small submodel, the large sub-model and the full pipe lifting model.

Using a larger sub-model did help to move the stress concentrations that occur where the forces are applied further away from the near weld region. These stress concentrations however only produce an anomaly in the region where the forces are applied and not in the root pass which is the area of interest.

The lift height of the pipe is a fairly approximate measure as it varies with each lift depending on the terrain and other factors. For this reason it is not necessary to model the magnitude of the lifting stress exactly so long as the shape of the stress field is reasonably approximated, which it is. It was concluded therefore that the sub-modelling technique approximates the lifting and lowering process adequately on a sub-model of only 60mm in pipe length.

3.1.6 Lifting Model Summary

The models created to simulate lifting and lowering of the pipeline front end were three dimensional. It is possible to create axisymmetric models of the lifting process by using non-axisymmetric loads provided linear elastic analysis is used. The FEA solver 'NISA' does not allow non-axisymmetric loads to be applied to axisymmetric models when using a non-linear solution (as is required for thermo-elastic-plastic analysis). For this reason an attempt was made to simulate lifting at the bottom dead centre of the pipe due to the bending of the pipe by applying a tensile pressure of the order of the pipe body stress during lifting thereby placing the cylinder under tension. The stress field created over estimated the stress induced in the near weld region, so it was evident that lifting could not be accurately simulated onto axisymmetric models of the complete construction process.

In order to model the complete construction process the mechanical handling loads due to the lifting and lowering of the pipeline front end need to be considered in conjunction with the thermal loading induced by welding. While it has been demonstrated in the past that

reasonable thermal stress prediction is achievable using axisymmetric models, the effect of lifting and lowering cannot be accurately simulated with them. This is made even more difficult when combined with incomplete root passes as is commonly the case during pipeline construction.

It has now been shown that the sub-modelling concept is capable of simulating the bending force due to lifting on the root pass with reasonable accuracy. This provides great benefits in terms of computational efficiency, which is essential in order to produce a complete 3D simulation of the construction process.

Previous work done by Higdon et al (1980) produced a 2D axisymmetric linear elastic lifting model and superimposed the results onto a residual stress field calculated using analytical techniques. That approach assumes the pipe is at ambient temperature and the residual stress is fully developed before lifting. It is known that often this is not the case since the pipeline front end is lifted immediately after welding to maximise the pipeline front end speed, so lifting occurs before the weld is completely cooled and before the residual stress field is fully established. It also assumes that no plastic deformation or changes to the final stress state occur due to the lifting and lowering process.

3.2 THERMAL MODELS

Welding residual stresses, which occur due to the non-uniform expansion and contraction of weld metal during the welding process need to be considered in order to accurately model the stress cycle of the root pass during construction. To calculate these transient stresses a temperature history is required. This temperature history was developed using a transient heat transfer analysis. Both three dimensional and axisymmetric models were created and compared. While 2D models are not appropriate for consideration of the lifting process they are extremely useful for looking at factors such as welding heat input and varied pipe geometry due to the computational speed they offer.

3.2.1 Transient Solution

The quasi-steady state assumption considers the weld piece a fluid of high viscosity, which flows below a stationary arc at the welding velocity. The viscosity of the weld piece is taken as an arbitrarily high value so that it is effectively a solid. This means if the weld piece is infinitely long a steady state condition occurs so that any point in a constant position relative to the arc remains at a constant temperature. Any point relative to the weld piece however does not remain at a constant temperature so it cannot be described as steady state hence the term 'quasi-steady state'. The quasi-steady state assumption in thermal modelling has the advantage that a solution can be obtained far more quickly than in a transient model.

Because the welding arc (the heat source) does not move relative to the mesh the 'quasi-steady state' assumption also has the advantage that mesh refinement is only required in the region about the arc itself. In transient models however the arc does move relative to the mesh so mesh refinement is required for the entire length of the weld. The additional nodes and time steps required to achieve this result in a major increase in computation time for a transient analysis.

Quasi-steady state models can be used to provide a temperature history, as the welding velocity and the location of the nodes relative to the arc are known. There are cases however when quasi-steady state models cannot produce adequate results. One such case is where a temperature history is required for the weld start and stop positions.

In the modelling of the front-end construction of pipelines generally incomplete root passes are laid in order to maximise the forward pace. For this reason modelling the welding start and stop positions is important. Hence transient thermal models are used.

3.2.2 Boundary Conditions

A transient heat transfer analysis is used where the arc is modelled using a heat source applied to the region where molten metal exists. The details of the heat source used are discussed later in Section 3.2.4. Heat is lost from the weld piece via both radiation and convection. The emissivity of the material is assumed to be 0.9 as recommended for hot

rolled steel by Goldak et al (1985). The Stefan Boltzman Constant is 5.67e-14 W/mm^2K^4. The convective heat transfer coefficient on all surfaces except in the vicinity of the arc was assumed to be 1.2e-5 W/mm^2K^4. The area below the arc has no heat losses, this is accommodated via a welding arc efficiency of 80% as suggested by Easterling (1992) for the MMAW process.

3.2.3 Material Properties

Temperature dependant material properties are used in the thermal model for density, thermal conductivity and specific heat. The effect of latent heat during phase change can be approximated as a variation in specific heat. Figure 3.11 shows the specific heat and enthalpy data used. In such a technique at the melting point there is a sudden spike in specific heat, which creates convergence problems so the spike was broadened over a larger temperature interval to aid convergence. The thermal conductivity data has a step change at the melting point as can be seen in Figure 3.12. This step change was broadened over 20 Kelvin, which, also enables convergence. This is an approximate method of allowing for increased convective heat exchange within the molten weld pool.

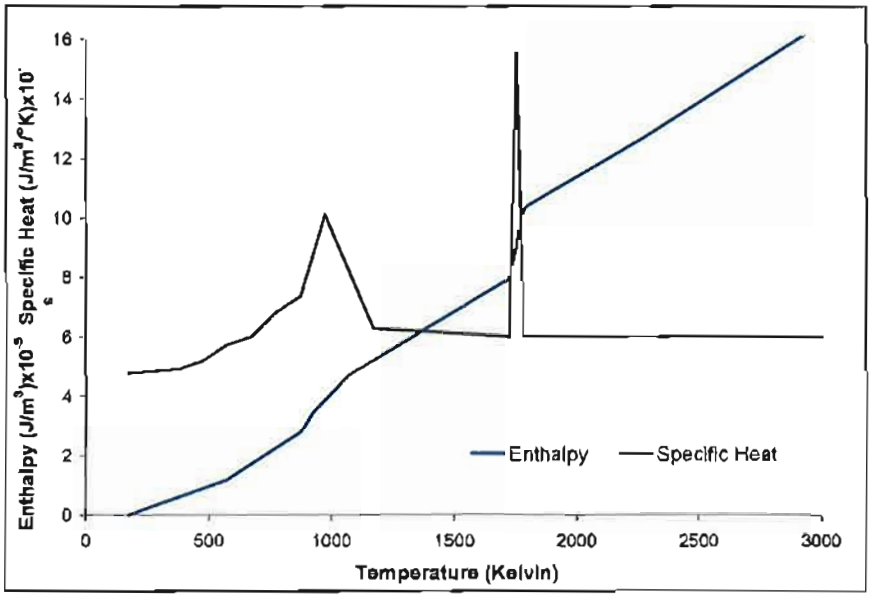

Figure 3.11: Temperature dependent material properties which where used in heat transfer analysis.

Since this spike in specific heat can create convergence and solution problems, these can be avoided by specifying temperature dependent enthalpy data, since enthalpy is related to specific heat as shown in Equation (3.6). Shown in Figure 3.11 is the enthalpy data used to help approximate phase change.

$$\Delta H(T) = \int_0^T c_p(T)dT \tag{3.6}$$

where

ΔH = Change in enthalpy

c_p = Specific heat at constant pressure

T = Temperature

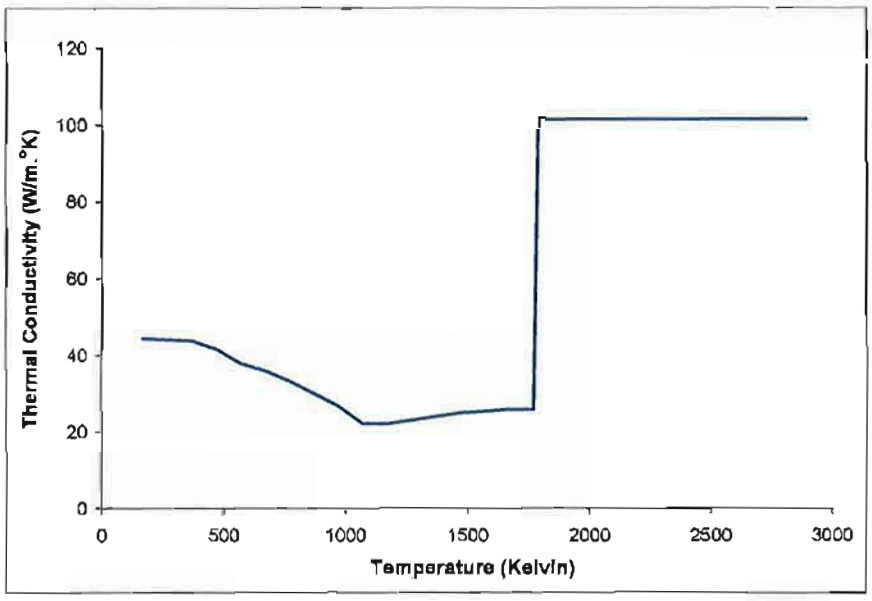

Figure 3.12: Temperature dependent thermal conductivity data, which was used in the heat transfer analysis.

3.2.4 Heat Source

The models used in this present work to simulate pipeline construction follow Goldak et al (1984) who proposed a mathematical model for the geometry of a heat source. This heat source uses a double ellipsoidal geometry with a Gaussian distribution of the heat flux. For further details on this type of heat source please refer to Chapter 2. A Gaussian distribution is used since it:

- approximates the current distribution across the welding arc,

- simulates the decay of molten pool velocity and the reduction in convective heat distribution at the edge of the weld pool.

The dimensions used for the heat source were approximated to the size and shape of a typical root pass. For further information on the parameters which define Goldak's double ellipsoidal heat source see Goldak (1984). The defining parameters for the double ellipsoidal heat source used in this study are as follows:

a_f = 2.25mm (length of front portion of the heat source)

a_b = 8mm (length of rear portion of the heat source)

b = 2.25mm (width of heat source)

c = 4mm (depth of heat source)

f_f = 0.6 (proportion of heat allocated to the front section of the heat source)

f_b = 1.4 (proportion of heat allocated to the rear section of the heat source)

These parameters are tuneable and allow the size and shape of the weld pool to be adjusted to approximate reality as closely as possible. They are required as conductive heat sources ignore the stirring effect that occurs within the weld pool. In this work the important factor was considered to be that the size of the molten zone was close to that of the root pass. While it was endeavoured to create the most accurate temperature field possible, it is known that the accuracy of the temperature in the molten zone has little effect on thermal stress as reported by Easterling (1992). The reason for this is that the melting point for steel is 1773K but steel has virtually zero strength above 1200K.

The heat source used in the preliminary models was assumed to have a welding speed of 5mm/s, with a current of 100 amps and a voltage of 25 volts. This gave a heat input of 0.5kJ/mm and an efficiency of 80% was assumed as taken from Easterling (1992). This heat input was used to set up the modelling procedure, however various other heat inputs are considered later in Chapter 5.

3.2.5 Correction Factors

The mesh used does not represent the geometry of the heat source exactly as hexagonal shaped elements were used. This means that a correction factor needed to be introduced to prevent a discrepancy between the heat load required and the actual heat load applied to the nodes within the double ellipsoid.

The correction factor was determined by finding the ratio between the summation of the heat loads placed on each node within the heat source, Q_{de}, and the required welding heat load, Q_{total}. The heat loads applied to the nodes within the double ellipsoidal heat source, q_{de}, are summed as shown in Equation 3.7.

$$Q_{de} = \sum q_{de} \tag{3.7}$$

The required heat load is determined by the welding heat input and arc efficiency as shown in Equation 3.8.

$$Q_{total} = \eta VI \tag{3.8}$$

The heat load applied to each node within the heat source, q_{nodal}, is then corrected as shown in Equation 3.9.

$$q_{nodal} = \frac{Qtotal}{Qde} \times q_{de} \tag{3.9}$$

3.2.6 Axisymmetric Models

Axisymmetric models assume that the object being modelled is axially symmetric in a 2D revolution about an axis of rotation. As mentioned previously, in the literature there has been much work published on residual stress in circumferential welds using axisymmetric models. If the thermal loading is axisymmetric, the weld being modelled is assumed to be welded 360° around the circumference simultaneously.

An axisymmetric model was created for comparison with the 3D model and for use when factors not concerned with welding start / stop positions or the lifting process are being considered. The geometry of the heat source at each time interval was found by considering a double ellipsoid passing through a 2D plane at the welding speed.

3.2.7 Results of Heat Transfer Analysis

The thermal models assumed symmetry along the weld centre line. In the 3D model only half of the pipe is modelled. This is done because during pipeline construction generally two welders weld the girth simultaneously. The two welders generally work on opposite sides of

the pipe so the welding arc and related thermal fields are sufficiently far apart so they do not influence one another. Therefore modelling only one weld is necessary as the temperature results can be then copied onto the other side of the pipe to simulate two welds in the residual stress models. The weld begins 45° before top dead centre (BTDC) and finishes 45° after top dead centre (ATDC). Figure 3.13 shows a contour plot of the transient temperature field after 24 seconds that resulted from this analysis.

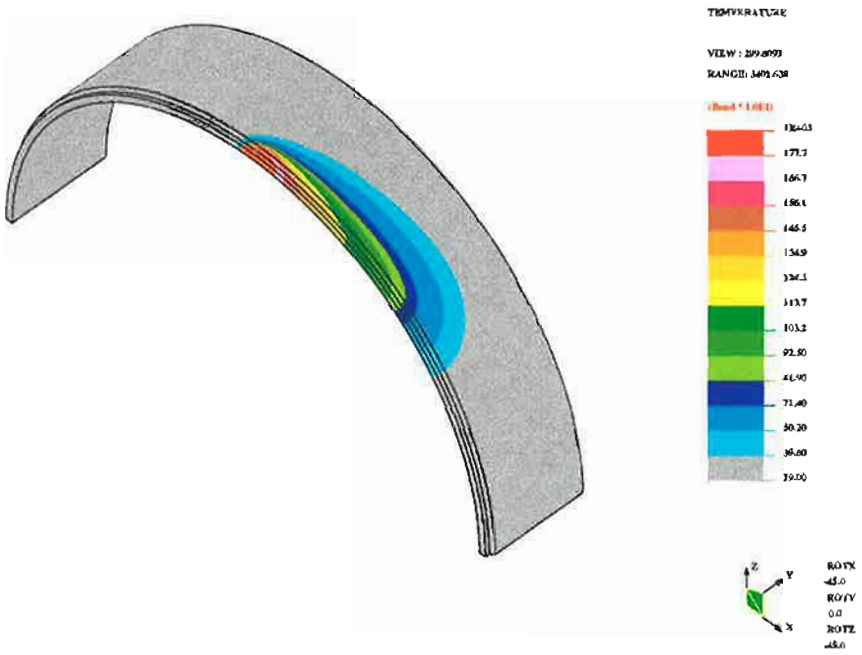

Figure 3.13: The transient heat transfer model results after 24 seconds of welding.

3.2.8 Comparison of Axisymmetric and 3D Results

By using the same geometry, boundary conditions and heat input, axisymmetric and 3D transient heat transfer models where created. Although the boundary conditions that were used were the same there still are some inherent differences. The axisymmetric model assumes the entire girth is welded simultaneously and that there is no conduction in front of the arc during welding and it is therefore expected that the 3D model would provide more accurate results. Therefore it is not surprising that the results from the two models differ slightly.

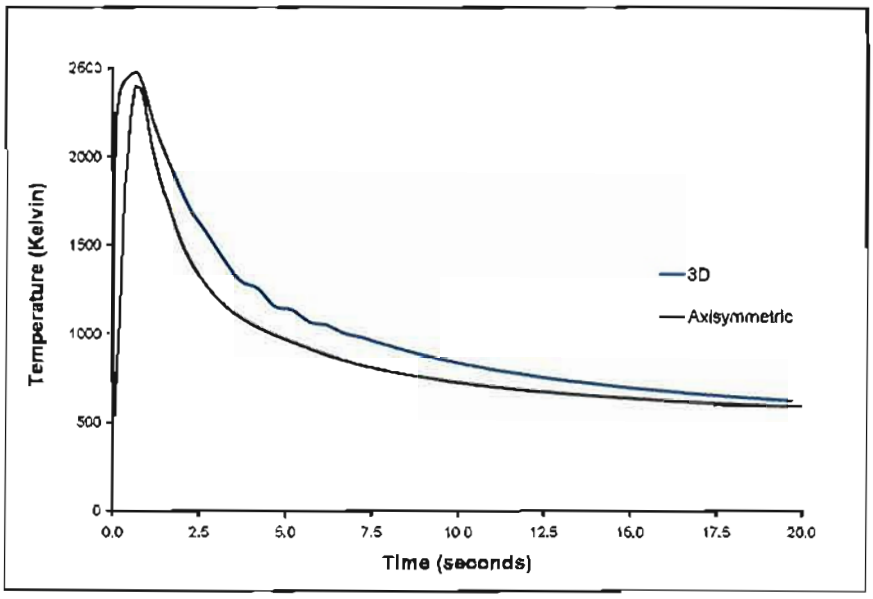

Figure 3.14: Cooling curve produced by the axisymmetric model as the arc passes over a segment of the girth.

In Figure 3.14 it can be seen that from both models a similar peak temperature is calculated. In the 3D model results, the temperature increased before that of the axisymmetric model and the cooling rate in the axisymmetric model is faster, primarily due to the conduction of heat in front of the arc in the 3D model which does not occur in the axisymmetric model.

3.3 RESIDUAL STRESS

The majority of the numerical research undertaken to calculate residual stress in girth welds by researchers in the past, has been done using axisymmetric approximations. The advantage of this is that it vastly reduces the computation time when compared with 3D modelling. It has been suggested that this approximation can produce reasonable results so long as the area of interest is not near the start / stop welding positions (Dong et al, 2001). This modelling technique is also limited in its use for residual stress prediction when isolated repair welds are being considered such as in pressure vessels used in the nuclear power industry or in partial welds used in the construction of pipelines. In pipeline construction full 3D transient stress models are required to consider the effect of the lifting process on the residual stress and stress concentrations that occur at the welding start / stop positions.

The number of nodes in the axisymmetric model is far less than in the 3D model and so it is far more efficient. Although obviously a great burden it was decided that 3D models were required for the following reasons:

- The lifting and lowering of the pipeline front-end can only be simulated using a 3D model,
- The root pass is generally incomplete before lifting and the weld has end effects which cannot be accounted for in 2D,
- The start and stop positions often have stress concentrations, which can only be considered by a 3D model, and

- The root pass is not symmetric in the plane of the lifting process.

3.3.1 Formulation of Residual Stress Models

In this work the models produced consider a completion of 50% of the root pass laid down by two welders working on opposite sides of the pipe at the same time as suggested by Henderson et al (1996). A full circumferential girth weld was meshed and the unwelded portion was assigned a low elastic modulus so it would have little effect on the results. The benefit of having the elements there is that in the complete construction models produced later there is the risk that the two pipe segments may come in contact in the unwelded region during lifting. Including 'soft' elements within this unwelded part of the joint is an approximate way of simulating a gap, which may close. Another benefit is that it allows variation of the amount and location of the root pass to be done using the same mesh.

The approach that is generally taken when producing residual stress models is to use the same mesh geometry in both the thermal and stress model. This is done to transfer the temperature history to the stress model easily. This method however is not ideal, as thermal models require a greater mesh density than the stress models in order to model the geometry of the heat input accurately and due to the high temperature gradients that occur in the thermal model. If the same mesh is used in the two models either the stress model will be too computationally intensive or there will be errors introduced into the thermal model, as the mesh is too coarse.

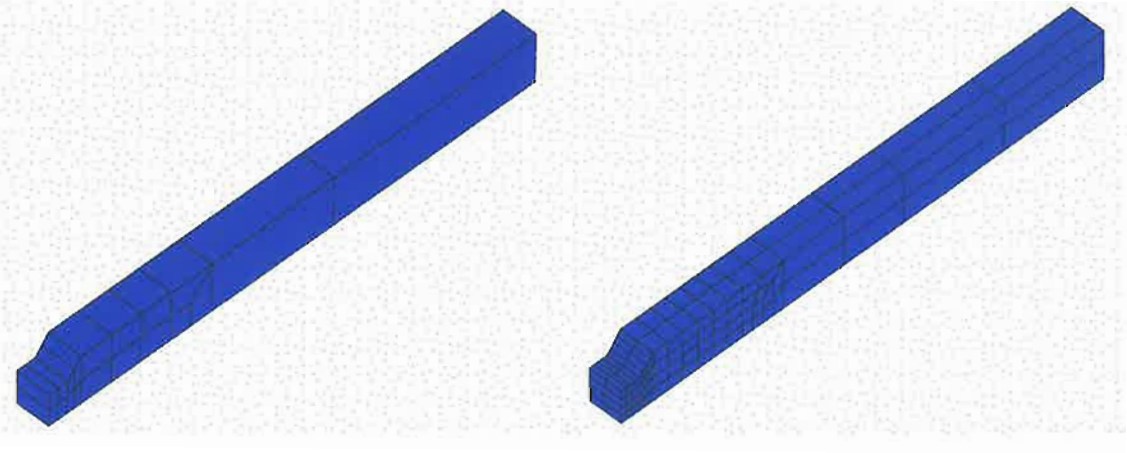

Figure 3.15: The fine mesh used in the thermal model (right) has eight elements for each element used in the stress model (left).

An external program was written to combat this problem by transferring the temperature results from a fine mesh to a coarse mesh. A portion of these meshes are shown in Figure 3.15. It can be seen that there are eight elements in the thermal model inside each element in the stress model. This allowed the transfer of temperature results derived from first order elements onto the nodes of the coarse second order mesh without any interpolation. The element size used in the root pass of the thermal model was 1mm x 2mm x 1.25mm and the element size used in the root pass of the stress model was 2mm x 4mm x 2.5mm. This mesh density was deemed adequate following the finding of Karlsson (1989) who investigated the mesh density requirements of thermal stress modelling of the welding process.

This also had the benefit that the mesh in the thermal models could be refined enough so that the heat input could be placed as element heat generation rather than nodal heat generation.

This is beneficial as the NISA software has a fundamental limit on the number of boundary conditions that can use a 'time-amplitude' condition, which would be exceeded using nodal heat generation. The 'time-amplitude' function in the NISA software is used to vary the amplitude of a boundary condition with time as specified within a table. To achieve further mesh refinement linear elements were used which is an acceptable approach in thermal models.

It is generally considered that in order to produce stress analysis results of a reasonable accuracy, second order elements are required. This was achievable due the coarser mesh used in the stress analysis model.

3.3.2 Material Properties

The material properties that were used were taken from Goldak et al (1986). The accuracy achieved in these models is limited by the availability of accurate material property data. The software used in this present work has the ability to alter material properties depending on temperature but not temperature history. Because of this software restriction limited approximations of transformation plasticity were included within the numerical procedure.

The commercial finite element analysis software used (NISA) requires that the temperature dependant material property data is defined using only five data points. Although this does

restrict how accurately the material properties can be defined, the pertinent material properties for steel can still be described reasonably well as shown in Figure 3.16.

In the models created in this study the effect of yield stress hysteresis is ignored following the finding by Oddy et al (1990). The effect of volume change is allowed for in the definition of the thermal expansion properties and transformation plasticity is approximated with a reduction in material strength at the transformation temperature as described in Josefson (1985). An elastic-perfectly plastic, yield criterion was used as it is assumed that during the phase transformation there would be little strain hardening.

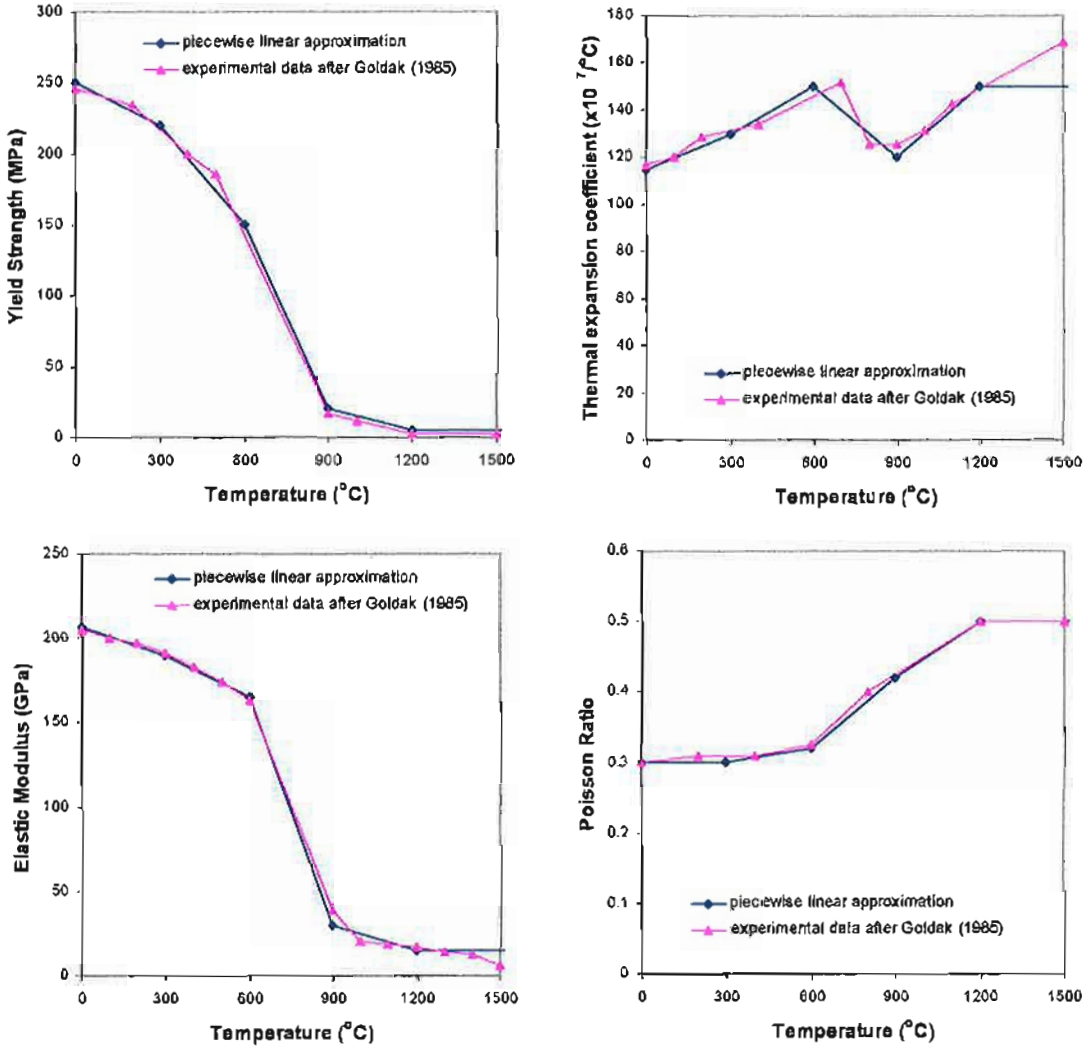

Figure 3.16: Temperature dependant material property data and the manner in which it was approximated with five data points as required in the NISA software.

3.3.3 Results of Transient Stress Analysis

The instantaneous thermal stress in the material after 24 seconds of welding can be seen in Figure 3.17. The Von-Mises Stress is shown as this allows a view of the stress intensity in the material independent of stress direction.

In Figure 3.18 the residual Von-Mises Stress in the girth weld after the material has cooled to ambient temperature is shown. Only the half the girth weld was modelled as two welders usually weld simultaneously, so symmetry was assumed. An incomplete root pass was made 90^{o} around the girth so that the weld start and stop positions could be observed. It can be seen (Figure 3.18) that there are stress raisers at the weld start and stop positions but that away from these positions the residual stress field appears to be uniform around the girth. By observing this phenomena demonstrates how the use of axisymmetric models have been found to produce accurate results away from the weld ends.

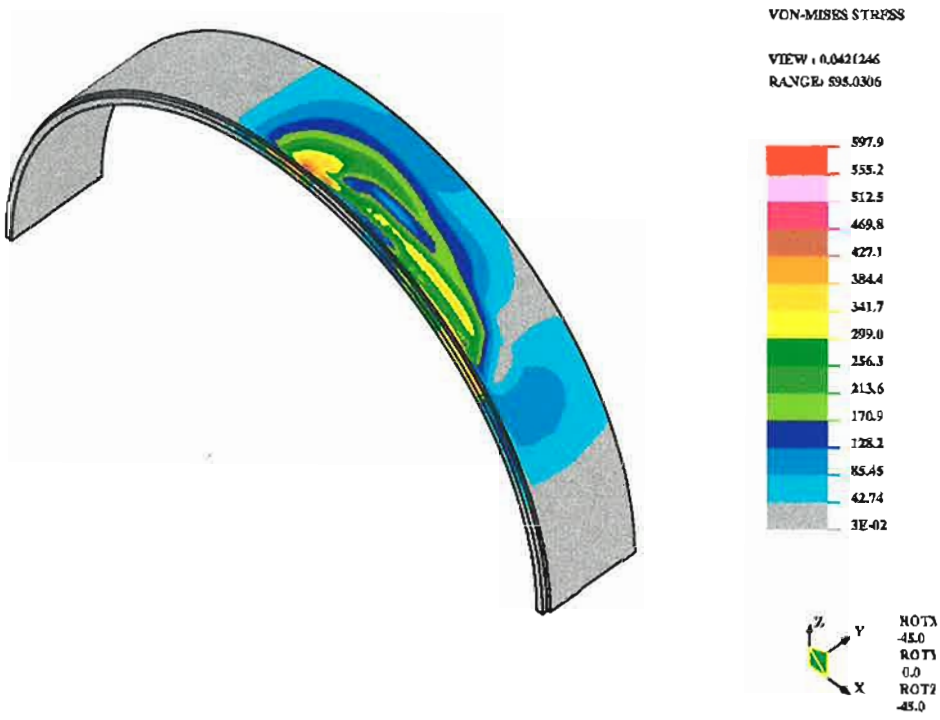

Figure 3.17: Transient Von-Mises stress (MPa) after 24 seconds of welding in the anti-clockwise direction.

Figure 3.18: Residual stress field after an incomplete root pass was laid.

The results from the model developed in this study as shown in Figure 3.19 demonstrate that a tensile residual stress develops at the root of the weld and a compressive residual stress develops at the top of the weld. This result is supported by Teng et al (1997) who described the pattern of residual stress that occurs in a typical girth weld. The accuracy of the modelling scheme developed here is experimentally verified in Chapter 4.

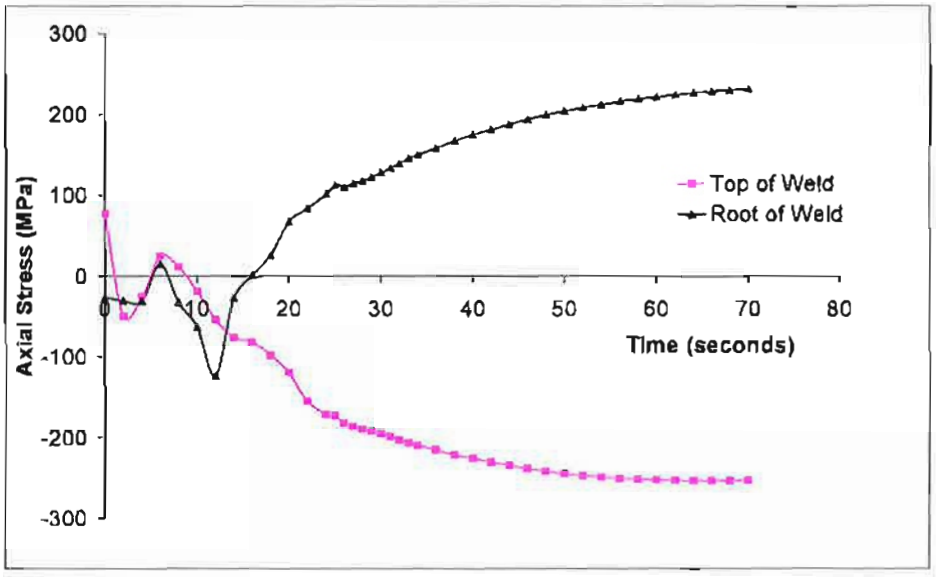

Figure 3.19: The evolution of axial stress in the root pass during welding and cooling at the top and the root of the weld.

The three dimensional residual stress models, while producing results which were expected from the literature, are computationally intensive making it difficult to consider many process variables. For this reason it was decided to investigate the possibility of using axisymmetric models where possible, if their results proved acceptable. The same joint and pipe geometry, welding speed, heat input and other boundary conditions where used in both the 3D and axisymmetric models.

HACC requires a tensile stress as the driving force. In circumferential welds a tensile residual stress develops on the inside wall of the cylinder. The inside wall is therefore the area of interest and is the area that is considered primarily in this study.

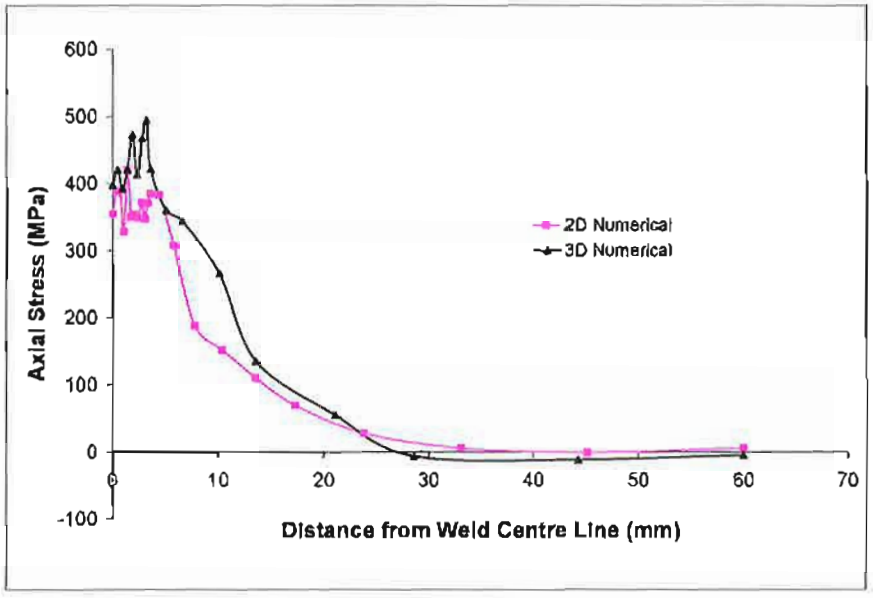

Figure 3.20: Comparison of axial residual stress results along the inside surface of the pipe which were produced by an axisymmetric model and a 3D model.

In the central region of the girth weld, well away from the weld ends, the residual stress and transient stress is compared for the axisymmetric and 3D models. In Figure 3.20 the axial stress verses transverse distance from the weld centre line is shown. The transient axial stress at the root of the weld for the first 60 seconds after the weld is laid is shown in Figure 3.21. On the weld centre line, the axisymmetric model has calculated a slightly lower residual stress. However it can be seen that the two models follow the same trend.

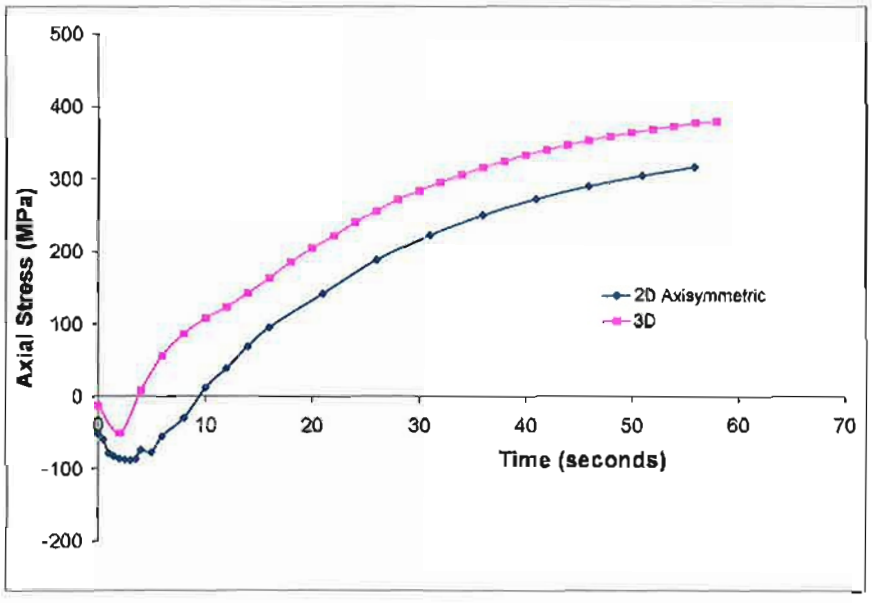

Figure 3.21: Comparison of transient axial stress at the root of the root-pass results from 3D and axisymmetric models.

3.3.4 Experimental Validation

When using numerical models it is always advisable to verify the results obtained experimentally. However measurement of transient stress during the welding thermal cycle is a difficult task. Strain gauges cannot simply be placed on the HAZ during welding due to the high temperatures they would need to endure. Therefore residual stress measurement techniques usually involve placing strain gauges on the material after welding and relieving the stress by removing material around or in the vicinity of the strain gauges. There are other methods also available as described in Chapter 4. All methods seek to determine the residual stress so the transient stress history remains unknown and many methods have significant

restrictions. The numerical results achieved here appear to agree with observations made in the literature (Teng et al, 1997), however in order to gain enough confidence in these models to conduct a study of pipeline construction some experimental verification is required. This has been carried out using the 'Blind Hole Drilling' technique of residual stress measurement and is described in Chapter 4.

3.4 CONSTRUCTION MODELS

The construction process is simulated with the use of a thermo-elastic-plastic model to account for the non-linearity of the material properties. To do this boundary conditions were placed on the previously developed thermal stress model to simulate the lifting and lowering of the pipe and the clamping force of the line-up clamp. The development and application of the lifting and lowering boundary conditions are outlined in Section 3.1.3.

Previous research undertaken by Higdon et al (1980) on the residual stress due to the construction process used an axisymmetric lifting models and superimposed the results onto a residual stress field calculated using analytical techniques. Rather than take the approach taken by Higdon et al (1980), in this thesis, the entire process has been incorporated into the one model. The reason for this is due to the plastic deformation that occurs during construction, which is directly related to the timing of the lifting and lowering process. A thermo-elastic-plastic analysis is required to determine whether the mechanical handling loads alter the final state of residual stress. This has been numerically investigated for the first time in this work.

3.4.1 Simulation of Lifting During Construction

Lifting of the pipeline front end occurs shortly after completion of the root pass. In the model created in this study an extreme lift of 600mm and an even higher 1200mm lift was simulated. The lifting and lowering had the effect of altering the residual stress in the root

pass. In order to demonstrate the effect of lifting and lowering on the residual stress in the root pass, the transient stress with and without lifting and lowering are compared in Figure 3.22. Of greatest concern is the way in which the inside pipe wall, which experiences a tensile residual stress, is affected. Tensile stress exists in this area and it is where cracking is most likely to occur.

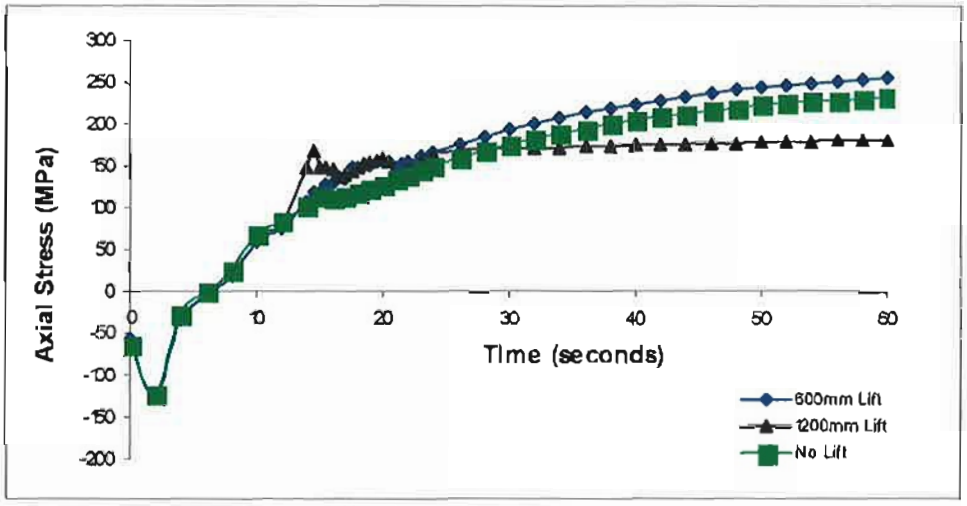

Figure 3.22: Transient stress with and without lifting at the root of the weld at BDC.

When the transient stress results with and without lifting are compared it can be seen that as a result of lifting, the root pass can become increasingly stressed as in the case of the 600mm lift and can be stress relieved as in the case of the 1200mm lift. It can be seen that the resultant stress due to the addition of lifting had some unexpected results that could not have been predicted using superposition.

This is because the lifting and lowering process influences the plastic deformation that occurs as the residual stress develops. Therefore placing the root pass under a tensile stress thereby producing plastic deformation, can have the effect of relieving some of the tensile residual stresses.

A residual stress field is a balance of tensile and compressive stresses all in equilibrium. Therefore by plastically deforming some areas within the structure, a redistribution of the residual stress field will occur. A pipeline weld is a complicated 3D structure so the redistribution cannot always be explained with the use of simple one dimensional analogies such as used in Chapter 2 for the explanation of the concept of residual stress. It is for this reason that the use of finite element models are so useful when investigating 3D residual stress fields.

3.4.2 Simulation of Line-up Clamp

The clamps that are used to line-up the pipes before welding place an additional load on the pipe. Line-up clamps produce an internal pressure approximately 20mm from the weld centre line during welding. The internal line-up clamp that is used during the construction process, rounds the ends of two pipe segments during welding and prevents any weld mismatch. The stress that is induced in the pipe segment ends may have an effect on the residual stress in the root pass. In Figure 3.23 a photograph of a typical line-up clamp is shown.

Figure 3.23: Photograph of a line-up clamp used to round and align pipe segments during pipeline construction.

In order to simulate the effect of the line up clamp an internal pressure of 3.8MPa was applied to the inside of the pipe in the region where the line up clamp was actuated. The method of calculation of this internal pressure is given in Appendix A. The line up clamp was assumed to be actuated during the welding of the root pass and then released. As can be seen in Figure 3.24 the line up clamp had virtually no effect on the transient and residual stress. While this investigation was only undertaken for only one pipe diameter and wall thickness the effect is unlikely to be more significant with other pipe grades and sizes as a low strength steel with a relatively thin wall was used in this experiment.

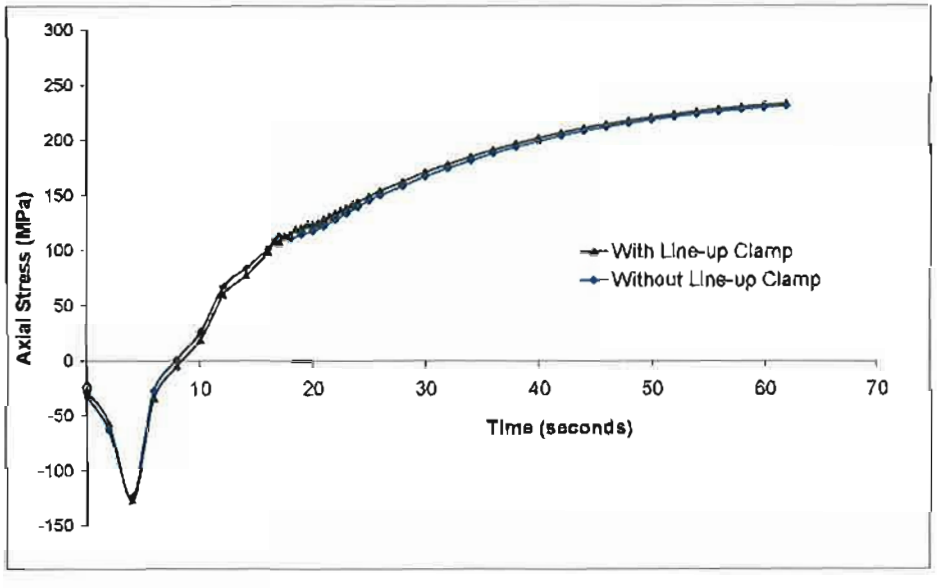

Figure 3.24: The transient stress with and without the use of the line up clamp at the root of the weld at BDC. X42 pipe with a diameter of 300mm with a wall thickness of 6mm was used.

The pipeline construction industry is particularly interested in how timing of the line-up clamp release influences the residual stress induced in the root pass. This interest is due to the potential increase in the forward pace of construction by early release of the line-up clamp. Currently there is a requirement in most construction procedures that the line-up clamp should not be released until after lifting of the pipeline front end. In the Australian Standard AS-2885.2-2002 under items for qualified procedures it is stated that:

- greater than 50% of the root pass must be completed before line up clamp removal,
- when the proportion of the root pass completion is less than 100%, then greater than 80% of the top and bottom quadrants must be completed.

From the result obtained in this study it would suggest that these requirements are acceptable and perhaps even conservative. It would seem that provided any weld mismatch was avoided the line up clamp has no influence on HACC.

Chapter 4

EXPERIMENTAL VERIFICATION

Whilst numerical methods for calculating transient stress obviously avoid the difficulties of experimental determination, it is necessary to verify the accuracy of such numerical procedures. By making experimental measurements of residual stress, confidence in the numerical modelling scheme developed can be gained and an indication of the level of accuracy that can be expected when using the numerical models can be established. In this work the experimental measurement of residual stress in a test circumferential girth weld is directly compared with the results of a numerical model.

4.1 METHODS AVAILABLE FOR EXPERIMENTAL VERIFICATION

Measurement of transient or residual stress formed during welding is difficult as strain gauges or extensiometers cannot be used to measure the stress history endured by a material in the near weld region. There are however a number of ways in which measurements of welding residual stress can be undertaken. Most methods are destructive, whereby a change in strain is measured whilst relieving some of the residual stresses and this information is used to determine the original stress. The destructive methods of relieving residual stress include cutting and sectioning the part, removing successive layers and trepanning and coring. There are also non-destructive methods of residual stress measurement such as X-ray diffraction, neutron diffraction, ultrasonic and electromagnetic strain measurement which broadly seek the current state of stress by measuring the elastic distortion within the structure.

4.1.1 Non-Destructive Methods

Examples of non-destructive methods include X-ray diffraction, neutron diffraction and ultrasonic techniques. Neutron diffraction and ultrasonic techniques are limited by bulky and complex equipment whereas X-ray diffraction equipment is portable and commercially available. X-ray diffraction is only capable of considering stresses at the surface however it is the most commonly used non-destructive method currently available.

X-ray diffraction and neutron diffraction are known to produce some excellent results when conducted by a skilled operator however there are difficulties when using them in welding applications. The unstressed crystal lattice spacing must firstly be measured for comparison with the stressed crystal lattice spacing. When the weld metal is different to the parent metal the unstressed lattice spacing is also different. As long as the unstressed lattice spacing at a given locations is always known satisfactory results can be obtained. However there is usually mixing of the weld and parent metals during welding so the unstressed lattice spacing is not known at these locations. Also depending on the cooling rate the microstructure of the material in different locations differs. Therefore the unstressed lattice spacing once again is difficult to ascertain.

4.1.2 Destructive Methods

Destructive methods of residual stress measurement include hole drilling, sectioning and saw cutting. These methods are also known to produce reasonable results in the hands of skilled operators.

The 'sectioning method' uses strain gauges placed at different locations on the inside and outside of the pipe wall away from the weld centre line and then strips are parted away from the surface parallel to the longitudinal axis while strain measurements are recorded. In another method, strains are recorded on the inside and outside pipe wall as the pipe is cut perpendicular to the longitudinal axis. This method however limits the measurements to

axisymmetric ones. Figure 4.1 shows how the pipe segment is sectioned while recording the strain changes. The cuts are made using an electrical discharge machine (EDM).

The 'sectioning method' has been used in the past by Ellingson et al (1979). Bulk displacement measurements were made at different locations around the girth as layers parallel to the longitudinal axis were parted away. This experimental procedure was undertaken to verify the numerical results obtained by Rybicki et al (1977).

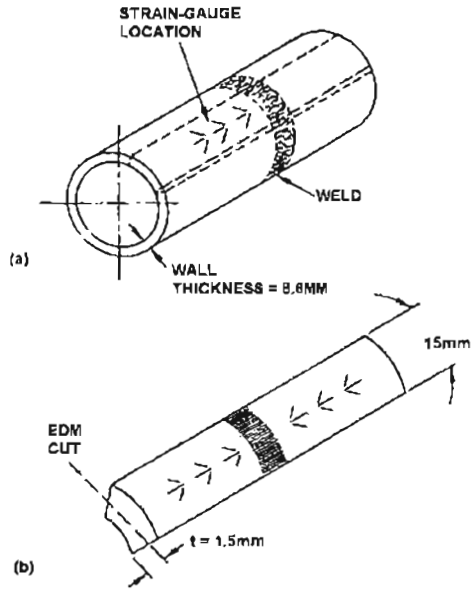

Figure 4.1: Layer removal technique for bulk residual stress measurements. (a) Isometric sketch of a typical section to be instrumented and removed; (b) division of the removed section into two pieces by EDM technique. (Ellingson and Shack,1979)

Cheng et al (1985) produced a variation of the 'sectioning method' that was termed the 'compliance method'. This method involves recording strains on the outside wall of a circumferential weld as a slit around the complete girth is cut to increasing depths. The experimental results achieved reasonable agreement with the predicted results, however this method is somewhat unquantified and is used little these days.

The most common method of residual stress measurement is the 'Blind Hole Drilling' method. This method involves drilling a hole in the centre of a three strain gauge rosette which has been attached to the surface of a specimen containing a residual stress. The hole relieves the local strain which is measured by the strain gauges and this allows calculation of residual stress magnitude and direction. The 'Blind Hole Drilling' method has achieved wide acceptance as a standardised test method. This method however is limited to depths of only one third the wall thickness. This technique is illustrated in Figure 4.2.

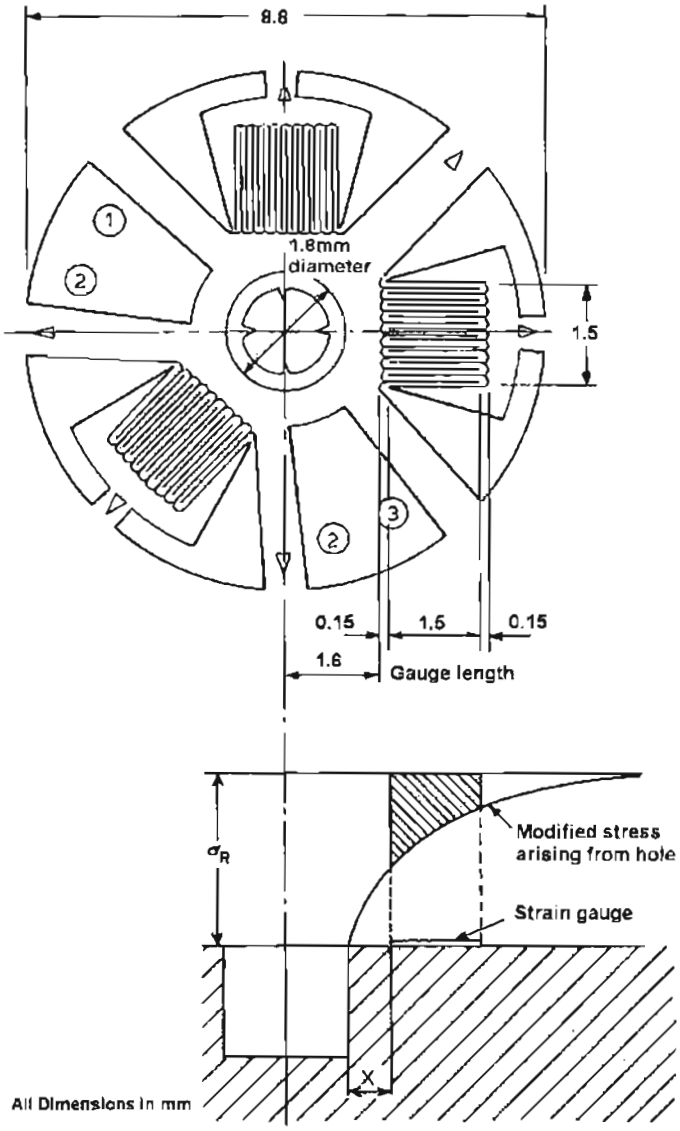

Figure 4.2: Schematic layout of the hole drilling technique in which the change in residual strain due to drilling a hole is measured by the strain gauge rosette. Easterling (1992)

The maximum and minimum residual stresses can be calculated from the strain relief measured by the rosette. This is done using the relation given in Equation 4.1.

$$\frac{\sigma_{max}}{\sigma_{min}} = -\frac{1}{K_1} \times \frac{E}{2} \times \left\{ \frac{\varepsilon_1 + \varepsilon_2}{1 - \nu K_2/K_1} \pm \frac{[(\varepsilon_1 - \varepsilon_3)^2 + 2\varepsilon_2 - (\varepsilon_1 + \varepsilon_3)^2]^{0.5}}{1 - \nu K_2/K_1} \right\} \quad (4.1)$$

where

E = Young's modulus

σ_{max} = Maximum principal stress

σ_{min} = Minimum principal stress

$\varepsilon_1, \varepsilon_2, \varepsilon_3$ = Strain gauge numbers 1, 2 and 3

ν = Poisson's ratio

Variables K_1 and K_2 are calibration constants which are dependant on the dimensions of the rosette and the diameter of the hole drilled. For each available rosette, a range of calibration coefficients are given for a range of hole sizes. The direction of the principal stress directions can be calculated using Equation 4.2.

$$\beta = 0.5 \operatorname{atan}\left(\frac{\varepsilon_1 - 2\varepsilon_2 + \varepsilon_3}{\varepsilon_1 - \varepsilon_3}\right) \quad (4.2)$$

where

β = Angle between gauge one and principle stress

Makhenko et al (1970) were the first to consider residual stress experimentally in the circumferential configuration however their experimental work was limited and showed

significant differences from finite difference solutions developed. A more successful result was achieved in an experimental study undertaken by Vaidyanathan et al (1973). In that study two hemispherical shells 0.080 inches thick with a radius of 4 inches of 5083-0 Aluminium were joined using electron beam welding. It was decided that spherical shells would be used as the residual stress in a cylinder sharply declines a short distance away from the weld centre line making measurement difficult. After the welding was completed, strain gauges were placed in the axial and hoop directions in the region of the weld and the 'Hole Drilling Method' of residual stress measurement was carried out. In order to validate this method of residual stress measurement, the same technique was applied to a butt-welded flat plate of the same material and the results were compared against an approximate analytic solution for residual stress. Although it was only possible to obtain a few data points using the experimental technique, there appeared to be reasonable agreement between the two sets of results.

While the 'Blind Hole Drilling' technique has been shown to be a very practical and useful technique it does have the following potential deficiencies when used in welding applications.

- When stress exceeds 50% of the yield strength of the material, localised plasticity effects cause measurements to be exaggerated.
- Welds are expected to generate residual stress fields that vary through the thickness whereas 'Blind Hole Drilling' is best suited to stress fields that do not vary with depth.

It was demonstrated by Weng and Lo (1992) that this method only produces accurate results where the residual stress is less than 50% of the yield strength of the material. If the residual stress is greater than 50% of the yield strength localised plasticity occurs around the hole introduced into the material causing the residual stress to be overestimated. This has been recognised by a number of researchers and methods to correct for localised plasticity have been suggested.

Weng and Lo (1992) carried out calibration tests and calculated new calibration coefficients that could be used in regions of high residual stress such as occurs in the vicinity of weldments. These calibration coefficients are not made available in ASTM E837, (Standard Test Method for Determining Residual Stresses by the Hole Drilling Strain-Gauge Method).

Beghini et al (1994) recognised that the calibration coefficients were dependant on the biaxiality ratio (the ratio between the maximum and minimum residual stress), the orientation of the rosette, the yield strength and strain hardening parameters, when the residual stress exceeded 50% of the yield strength. They conducted a study using through hole analysis (for which analytical solutions are possible). They suggested the use of a four gauge rosette to remove inaccuracies caused by orientation. Latter in Beghini et al (1998) a review of the work conducted in this area was published and a procedure for allowing for localised plasticity was given. This procedure is limited in its accuracy if the principal stress directions are not known prior to measurement.

Zhao et al (1996) proposed a far simpler method for correcting the effect of localised plasticity. Their method is based on a distortion energy parameter. The technique is relatively simple and is practical for use in engineering applications, however this method also required that the principal stress directions be known prior to drilling to avoid inaccuracies.

Later Vangi and Ermini (2000) also demonstrated that when the residual stress exceeded 50% of the yield stress the calibration coefficients were dependant on the biaxiality ratio (ratio of maximum and minimum residual stress) and the angle of the principle stress in relation to the position of the rosette. This work however does not appear to offer anything not previously known or provide alternate methods of plasticity correction.

Another problem, which is recognised in the 'Measurements Group Tech Note TN-503-3', is that the 'Blind Hole Drilling' technique of residual stress measurement is best applied to stress fields that are uniform with depth or inaccuracies are introduced. This can be problematic when studying weldment stress as it is well known to vary with depth. However there are calibration coefficients available that vary with depth so this criteria can be considered.

4.1.3 Summary

When using numerical modelling, validation of the numerical scheme developed is required. One method of validation available is by experiment. The validation experiment proposed is

to compare the calculated residual stress in the region of a pipe girth weld with an experimental determination using the 'Blind Hole Drilling' technique.

The 'Blind Hole Drilling' technique is widely accepted and standardised. It enables model verification to be conducted economically. A large number of measurements are not required for model verification and the residual stress through the pipe wall is not needed as the area of interest is the inside surface of the pipe. There are some limitations with this technique and they are generally well understood, however before applying this method to weldments, a bench mark test will be carried out. This will be conducted to determine the accuracy that can be expected from the 'Blind Hole Drilling' method in a residual stress field that does not vary with depth and to determine whether increased accuracy can be acquired by developing new calibration constants.

4.2 BENCHMARK TEST

A mild steel bar was loaded to a known uniaxial stress to simulate a residual stress and then the 'Blind Hole Drilling' method was applied. This allowed comparison of the actual stress in the steel bar with the results of the 'Blind Hole Drilling' method. A finite element model of the bench mark test was also created which allowed consideration of the accuracy of the calibration constants used in the analysis.

4.2.1 Experimental Equipment

The equipment used for the benchmark test is listed below and the test rig is shown in Figure 4.3 and Figure 4.4.

- A mild steel bar with a cross sectional area of 32.43mm x 5.06mm.
- A Hounsfield Tensometer was used to load the mild steel bar to simulate a residual stress.
- A 20kN load cell was used to measure the load applied to simulate residual stress in the test piece.
- Strain gauge rosettes were applied to the bar to used to make residual stress measurements using the 'Blind Hole Drilling' technique.
- The Model RS-200 Milling equipment was used for analysing residual stresses by the 'Blind Hole Drilling' technique.
- Strain gauge bridges were used to measure changes in resistance of the strain gauges during operation.

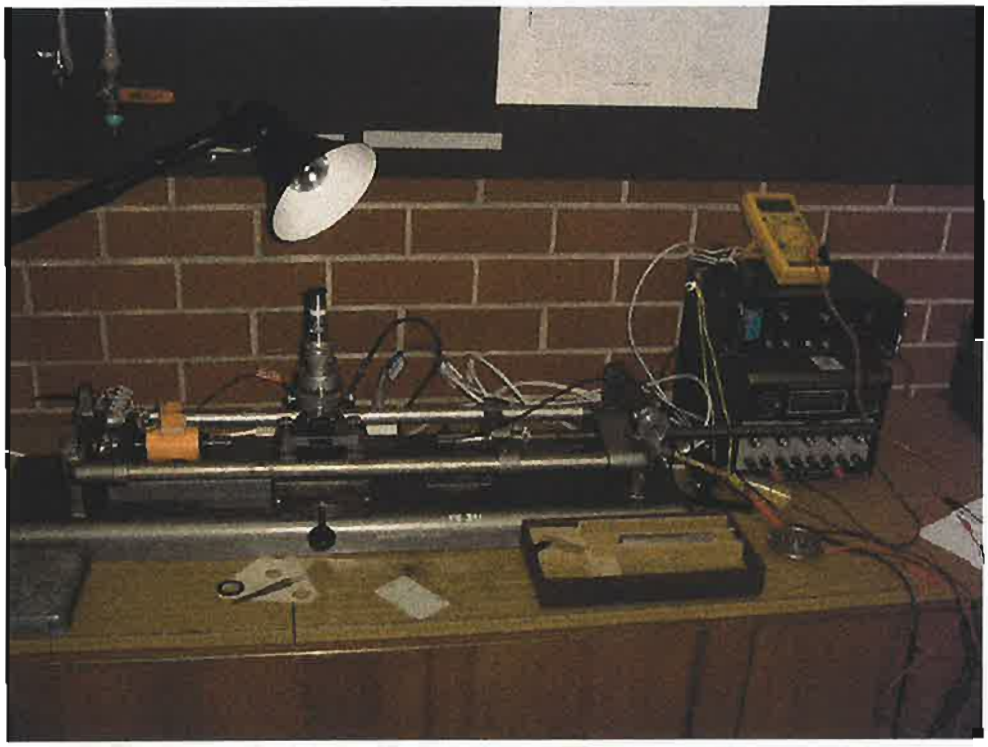

Figure 4.3: Experimental set up used for benchmark test.

Figure 4.4: The tensile sample used in the benchmark test is held in a Hounsfield Tensometer which is connected to a load cell.

4.2.1.1 TYPES OF STRAIN GAUGE ROSETTES

The EA-XX-062RE-120 design of strain gauge rosette (see Figure 4.5) is the most commonly used and is available in a range of sizes to conform with different hole sizes and depths. The TEA-XX-062RK rosette has an identical geometry to that of the EA-XX-062RE-120 but offers an encapsulated design with heavy copper solder terminals for ease of soldering. The CEA-XX-062UM-120 also offers an encapsulated design with heavy copper solder terminals for ease of soldering but has a different grid geometry. This grid geometry

enables measurements to be taken more closely to welds or other irregularities. For this reason the CEA-XX-062UM-120 rosette was chosen.

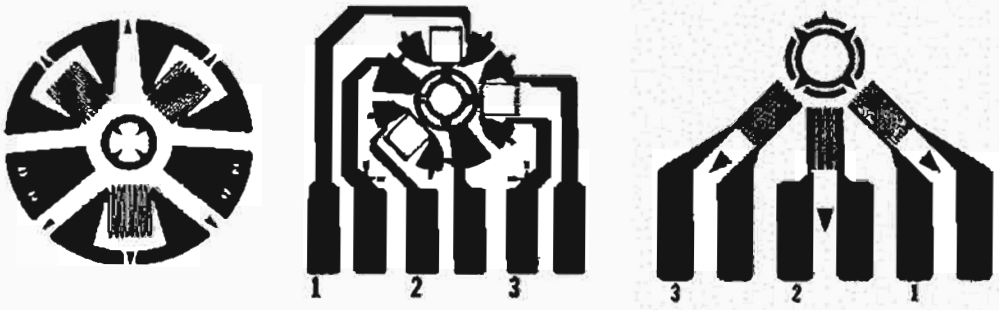

EA-XX-062RE-120 TEA-XX-062RK-120 CEA-XX-062UM-120

Figure 4.5: Residual stress strain gauge rosettes. (ASTM Standard E837)

4.2.2 Experimental Procedure

The mild steel bar used in the test was firstly stress relieved to remove any pre-existing residual stresses in the bar. The bar was heated to 600°C and held at that temperature for two hours before allowing it to cool to 300°C and removing it from the furnace. This procedure for stress relief was taken from the Materials Handbook (Brady et al, 2002).

The steel composition was determined and is given in Table 4.1. The microstructure after heat treatment was compared with the non-heat-treated steel to ensure no significant change in material properties occurred as a result of the heat treatment. As can be seen in Figure 4.6 no significant change in grain size occurred as a result of stress relieving.

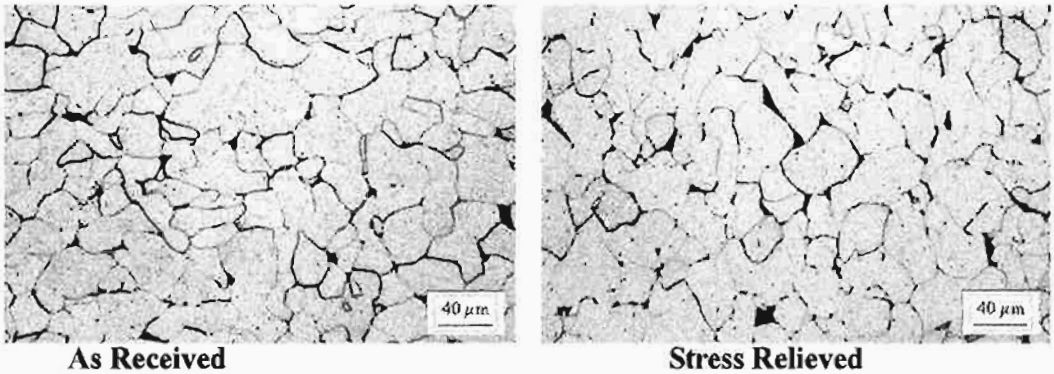

Figure 4.6: Microstructure of material used in benchmark test, before and after stress relieving.

Element	C	Si	Mn	P	S	Cr	Mo	Ni
%	0.035	0.009	0.297	0.018	0.009	0.015	<0.002	0.02
Element	**Ni**	**Al**	**Co**	**Cu**	**Nb**	**V**	**W**	**Pb**
%	0.02	0.039	0.003	0.012	0.001	0.002	0.011	<0.003
Element	**Sn**	**As**	**Zr**	**Ce**	**Ta**	**B**	**Zn**	**La**
%	<0.001	0.005	0.002	<0.004	0.007	0.001	0.003	<0.001

Table 4.1: Composition of steel bar used in benchmark test.

A strain gauge rosette was installed on the test piece as described in the Vishay Measurement Group Instruction Bulletin B-129, 'Surface Preparation for Strain Gauge Bonding.' The strain gauge rosette used was of the 062UM variety (see Figure 4.5). The rosette was positioned with gauge 1 aligned in the direction of the induced stress.

The specimen was loaded in the Hounsfield Tensometer with the load cell to a tension of 11.49kN which induced a stress in the bar of 70MPa. While the bar was held under this

simulated residual stress the strain gauge bridge was calibrated and zeroed. 'The Standard Test Method for Determining Residual Stresses by the Hole-Drilling Strain-Gage Method', ASTM Standard E837-95 was then used.

4.2.3 Results From Benchmark Test

The expected residual stress results were a maximum stress of 70MPa, a minimum stress of 0MPa and the maximum stress aligned zero degrees from strain gauge 1. As shown in Table 4.2 the agreement between measured stress and the applied value was very good.

Table 4.2: Benchmark test results

	ε_1	ε_2	ε_3	**Residual Stress Max. (MPa)**	**Residual Stress Min. (MPa)**	α **(Radians)**
Experimental	-17	-65	-26	65	4	-0.05

It can be seen from this result that a reasonable calculation of residual stress was made since this measurement technique is only expected to yield results within ±10%. However one possible source of error that is not related to the experimental technique is inaccuracy of the data reduction coefficients. In order to test the accuracy of the data reduction coefficients it was decided that a numerical model of the benchmark test would be created which simulated the change in strain that occurs when a hole is introduced into the material. A numerical model is best technique for this test as the data reduction coefficients cannot be calculated analytically.

4.2.4 Finite Element Model of Benchmark Test

Linear elastic models of the specimen under tension were produced with and without a hole introduced into specimen. In total eight separate models were created all with varying hole depths. This was done to simulate the hole being drilled incrementally and allowed calculation of data reduction coefficients for varying hole depths as explained later in Section 4.2.5.

The geometry of the hole simulated was the same as that of the benchmark test which was 0.074 inches in diameter and was drilled in incremental depths of 0.0101 inches to a maximum depth of 0.0808 inches. Imperial units were used as this made calculations simpler. The maximum mesh density used was around the hole. First order eight noded hexagonal elements were used, which typically provide good results when only elastic deformation is simulated. The smallest of these elements were approximately 0.243mm x 1.146mm x 0.257mm. A pressure of 70MPa was applied to one end of the specimen and the other end was restrained to simulate the induced stress.

The difference in strain between the models with and without a hole was assumed to be the amount of strain relieved by drilling the hole. Figure 4.7 shows the calculated Von-Mises stress for the model of the specimen with a hole drilled into the material to a depth of 0.0808 inches.

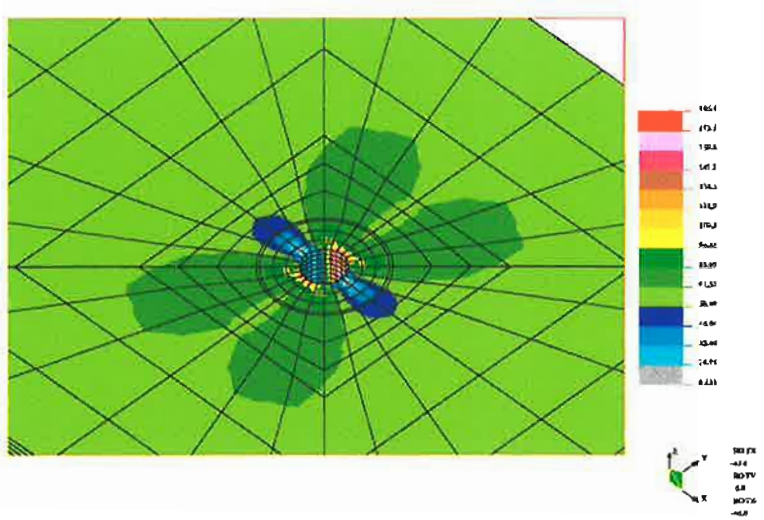

Figure 4.7: The Von-Mises stress (MPa) field calculated using finite element model of 'Blind Hole Drilling' technique.

The change in strain calculations for a full depth hole were used to calculate the residual stress. A comparison with the experimental results as shown in Table 4.3. It can be seen that the numerical results were quite accurate however they too underestimated the residual stress. For this reason the numerical model was used to calculate new data reduction coefficients.

Table 4.3: Experimental and numerical results from the benchmark test.

	ε_1	ε_2	ε_3	**Residual Stress Max. (MPa)**	**Residual Stress Min. (MPa)**	α **(Radians)**
Experimental	-17	-65	-26	65	4	-0.05
Numerical	-120	-33	44	69.2	-1.5	0.02

4.2.5 Calibration of Data Reduction Coefficients

The experimental and numerical results show good agreement with each other, however both methods underestimated the actual residual stress. This led to a decision being made to calculate a new set of data reduction coefficients which would more accurately calculate the residual stress. Data reduction coefficients are used with the 'Blind Hole Drilling' technique to calculate the residual stress.

The variation of residual stress with depth is also an important consideration when making residual stress measurements. These coefficients vary with the depth of hole drilled and cannot be found analytically as in 'Through Hole' analysis. Instead in the past they have been calculated using experimental measurements such as was done by Pang (1989) or by numerical simulation such as by Schajer (1981).

The strain gauge rosettes that were used are of the CEA-XX-062UM-120 variety which, due to their geometry, allow measurements to be taken closer to welds than other varieties permit. There was no data reduction coefficient information available which varied with depth for the 062UM strain gauge rosettes which were used. The only data reduction coefficient information available was for full depth holes.

The finite element model of the benchmark test that was described previously was used to determine data reduction coefficients which could then be used later to consider the variation

of residual stress with depth for this strain gauge. The finite element model was used to derive this data rather than experimental techniques due to the increased accuracy that can be achieved.

The three element 45° rectangular rosette equations generally used to calculate residual stress and principal direction are given below.

$$\sigma_{max,\,min} = \frac{E}{2}\left\langle \frac{\varepsilon_1 + \varepsilon_3}{1-\nu} \pm \frac{Z}{1+\nu} \right\rangle \tag{4.3}$$

where

$$Z = \sqrt{(\varepsilon_1 - \varepsilon_3)^2 + (2\varepsilon_2 - \varepsilon_1 - \varepsilon_3)^2} \tag{4.4}$$

and

$$\beta = \frac{1}{2}\operatorname{atan}\left(\frac{2\varepsilon_2 - \varepsilon_1 - \varepsilon_3}{\varepsilon_1 - \varepsilon_3}\right) \tag{4.5}$$

Beaney and Procter (1974) modified these equations in order consider a sensitivity calibration factor, $1/K_1$ and a residual stress rosette Poison's constant, $\nu K_2/K_1$.

$$\sigma_{max,\,min} = \frac{1}{K_1} \bullet \frac{E}{2}\left(\frac{\varepsilon_1 + \varepsilon_3}{1-(\nu K_2)/K_1} \pm \frac{Z}{1+(\nu K_2)/K_1} \right) \tag{4.6}$$

For uniaxial stress calibration, the rosette constants are given by:

$$\frac{1}{K_1} = \frac{\varepsilon_A}{\Delta\varepsilon_A} \tag{4.7a}$$

$$\frac{\nu K_2}{K_1} = \frac{\Delta\varepsilon_T}{\Delta\varepsilon_A} \tag{4.7b}$$

where,

ε_A = Total axial strain before drilling at applied load

$\Delta\varepsilon_A$ = Total axial strain change after drilling at applied load

$\Delta\varepsilon_T$ = Total tangential strain change after drilling at applied load

In the ASTM Standard E837 the rosette equation uses calibration constants, $\bar{A}$ and $\bar{B}$ which were derived from a finite element study by Schajer (1981). $\bar{a}$ and $\bar{b}$ are data reduction coefficients used to account for the drilled hole dimensions. The stress is given by:

$$\sigma_{max,\,min} = \frac{\varepsilon_1 + \varepsilon_3}{4\bar{A}} \pm \frac{\sqrt{2}}{4\bar{B}}\sqrt{(\varepsilon_1 - \varepsilon_2)^2 + (\varepsilon_2 - \varepsilon_3)^2} \qquad \textbf{(4.8)}$$

where,

$$\bar{A} = \frac{\nu - 1}{2E} \cdot \bar{a} \qquad \textbf{(4.9a)}$$

$$\bar{B} = \frac{-1}{2E} \cdot \bar{b} \qquad \textbf{(4.9b)}$$

As stated in Pang (1989) the relationship between Equation (4.6) and (4.8) is given by:

$$\frac{1}{K_1} = \frac{1}{E(\bar{A} + \bar{B})} \qquad \textbf{(4.10a)}$$

$$\frac{\nu K_2}{K_1} = \frac{(\bar{B} - \bar{A})}{(\bar{B} + \bar{A})} \qquad \textbf{(4.10b)}$$

By equating relations (4.7a), (4.7b) with (4.10a), (4.10b), $\bar{A}$ and $\bar{B}$ could be calculated from the strain results in the finite element models used in this study for varying hole depths.

$$\bar{B} = \frac{K_1 + \nu K_2}{2E} \tag{4.11}$$

$$\bar{A} = \frac{K_1 - \nu K_2}{2E} \tag{4.12}$$

In turn the data reduction coefficients $\bar{A}$ and $\bar{B}$ could be calculated for varying hole depths using the relations (4.9a) and (4.9b) given in the ASTM Standard E837 and rearranging them to make $\bar{a}$ and $\bar{b}$ the subject of the formula.

$$\bar{a} = \frac{-2\bar{A}E}{1 + \nu} \tag{4.13}$$

$$\bar{b} = 2\bar{B}E \tag{4.14}$$

The results are presented in Figure 4.8.

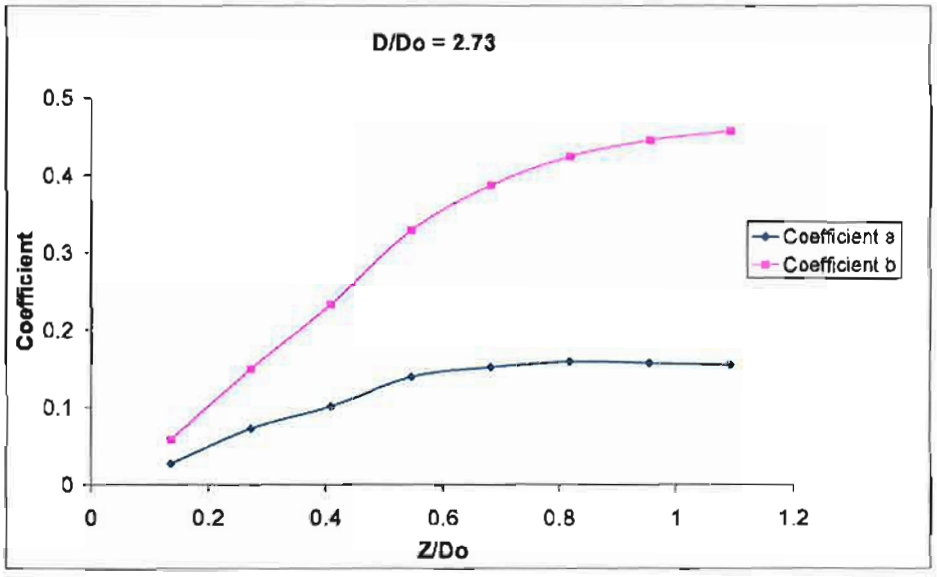

Figure 4.8: Data reduction coefficients for UM rosettes as functions of non dimensional hole depth and diameter calculated from finite element models.

These coefficients apply only to a certain hole diameter of 0.074in for the 062UM variety of rosette. This data allows calculation of residual stress at different hole depths. These results are used to calibrate the experimental measurements that were made on pipe girth welds as explained in section 4.3.

4.3 EXPERIMENTAL RESIDUAL STRESS MEASUREMENT

A girth weld was performed on a segment of X70 pipe, and the 'Blind Hole Drilling' technique of residual stress measurement was carried out on the weld. The pipe segments used had a vee-preparation machined onto the ends using a lathe. Once a vee-preparation had been placed on the pipe ends the pipe segments were 'tack welded' together in four locations around the girth. The specimen was then stress relieved in a furnace prior to welding.

Line pipe generally has locked-in stresses from the hot rolling process during fabrication and hydrostatic testing. These stresses cannot be accounted for in the modelling process but are expected to be low in relation to the welding residual stresses. Stress relieving was used to remove these locked-in stresses to ensure what is being modelled is as close to reality as possible. The experiment conducted was for the purpose of validating the modelling procedure used rather than to determine the stress experienced in a pipeline girth weld. Once the modelling procedure has been verified it can be used to highlight trends despite a small variation in results that may occur due to fabrication stresses that would occur in the field.

The specimen was heat treated by heating it to 600°C holding it at that temperature for two hours and allowing it to cool overnight to 300°C before removing it from the furnace. This procedure for stress relief of ferritic steel was taken from the Material Handbook (Brady et al (2002).

The pipe used was X70 pipe with an internal diameter of 350mm and a wall thickness of 5.4mm. The material was measured in tensile tests to have a proof stress of 525MPa. The weld preparation used was a 60° included angle with a 1mm root gap and a 1mm root face. The electrodes used were E6010 (Lincoln 5P) with a diameter of 3.2mm. A typical pipeline construction procedure was used with a 50% weld completion of the root pass with 90° of the girth welded on opposite sides of the pipe. The two weld segments carried out on opposite sides of the pipe consumed two electrodes each to complete.

A welding monitor was used during welding to record the voltage and current at one second intervals. The results were averaged to give an average voltage of 25 volts and an average current of 111 amperes. The length of a weld was measured and the time taken to produce the weld was gathered from the welding monitor. This information was used to calculate the welding speed, which was 4mm/s. From this information the heat input was calculated to be 0.69kJ/mm, which is not unusual for a root pass carried out in the field.

Using the 'Blind Hole Drilling' technique residual stress measurements were taken on the inside wall of the pipe in varying positions away from the weld centreline as shown in Figure 4.9. The gauges were placed on the inside wall of the pipe with gauge 2 opposite the weld. The strain gauges used were the CEA-XX-062UM-120 type as previously described in Section 4.2.1.1. The holes were introduced using an air powered drill with a diameter of 0.074 inches. The holes were drilled in 8 increments of 0.0101 inches to a maximum depth

of 0.0808 inches with strain gauge readings recorded at each increment. A photograph of the weld from which the measurements were taken is given in Figure 4.10.

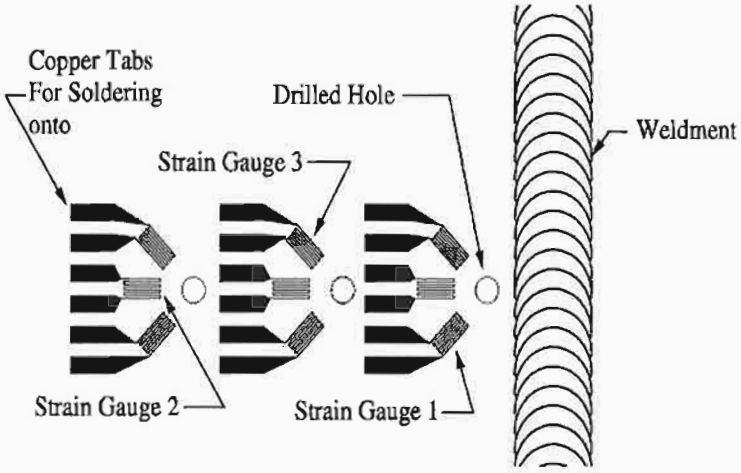

Figure 4.9: CEA-XX-062UM-120 Rosettes that were used for residual stress measurement, were aligned with strain gauge 2 perpendicular to the direction of the weld.

Figure 4.10: Inside pipe where residual stress measurements were made.

4.3.1 Results of Residual Stress Measurement

Incremental strain results were recorded for eight holes which were drilled on the inside surface of the pipe in varying locations from the weld centre line. In Appendix C, plots of strain verses depth are given for each strain gauge used and the incremental strain results, residual stresses and their directions are tabulated.

The strain results were plotted on the same axis as the strain scatter band used in ASTM E837. The scatterband gives a range of results inside which normalised strain results will fall if the residual stress field is uniform with depth. The measurements made close to the weld centreline, where the residual stress is the highest, had strain readings which fell predominately within the scatter band with very few outliers. This is encouraging as welding

residual stress fields are known to typically vary with depth. It is stated in ASTM 837, for this method to yield results with an accuracy better than 10% strain readings must fall within the scatterband. The residual stress results measured at the eight incremental depths were averaged for comparison with numerical results.

Measurements made further from the weld centreline, where the residual stress is lower, suffer from increased error. This error is because there is a constant amount of background noise experienced in the strain gauge bridge and other parts of the equipment which for higher readings become less significant. If residual stresses which approach zero are measured, this noise will produce proportionally more error in the results than regions of higher residual stress. This can be seen in the plots of strain verses depth for the measurements made further than 20mm from the weld centreline (see Appendix C).

Ideally the 'Blind Hole Drilling' technique should be carried out on a residual stress that does not exceed 50% of the yield strength of the material. Typically the residual stress associated with welding approaches the yield strength causing localised plasticity effects which introduce error in the results. This can be seen in Figure 4.11 where the results indicate that there is a residual stress that exceeds the yield strength of the pipe material. This problem however has been recognised by a number of researchers such as Beghini and Bertini (1998) and solutions have been proposed.

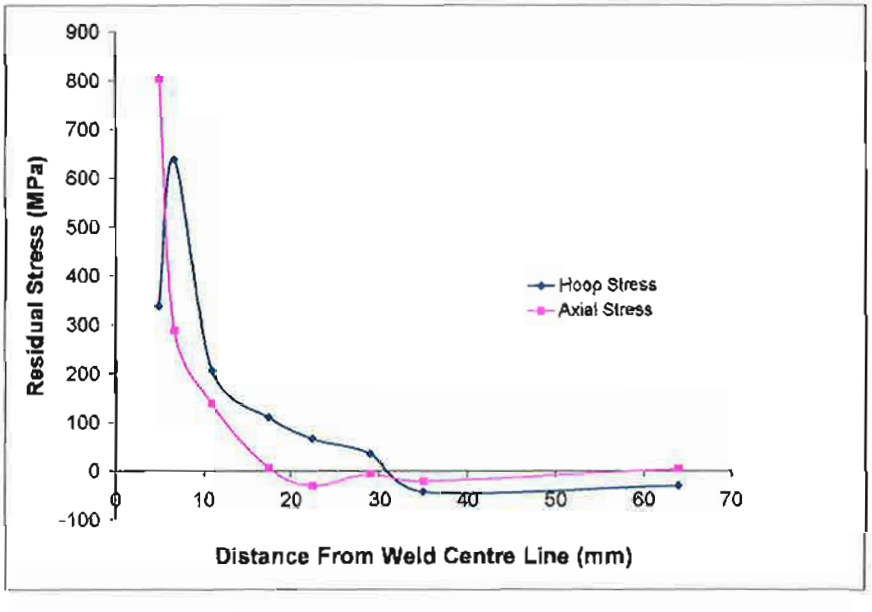

Figure 4.11: Residual stress results determined using the 'Blind Hole Drilling' technique with some results indicating a residual stress above the yield strength.

4.3.2 Localised Plasticity

The phenomena of localised plasticity was recognized by Weng and Lo (1992). They conducted a series of calibration tests from which they developed new calibration coefficients for when residual stress exceeds 70% of the yield strength for both RK and the UM rosette used in this study. The results after adjustment using the technique described by Weng and Lo (1992) are shown in Figure 4.11. The calibration coefficients they developed for the UM rosette were used in this study to correct the effect of localised plasticity.

$Stress \leq 70\ \%$ of σ_Y then $A = -0.363$

$$B = -0.799$$

$$Stress > 70\,\%\text{ of }\sigma_y \text{ then } A = -0.363 + 0.150X - 0.753X^2$$

$$B = -0.799 + 0.328X - 1.465X^2$$

where $$X = ((\sigma/\sigma_y) - 70)/30$$

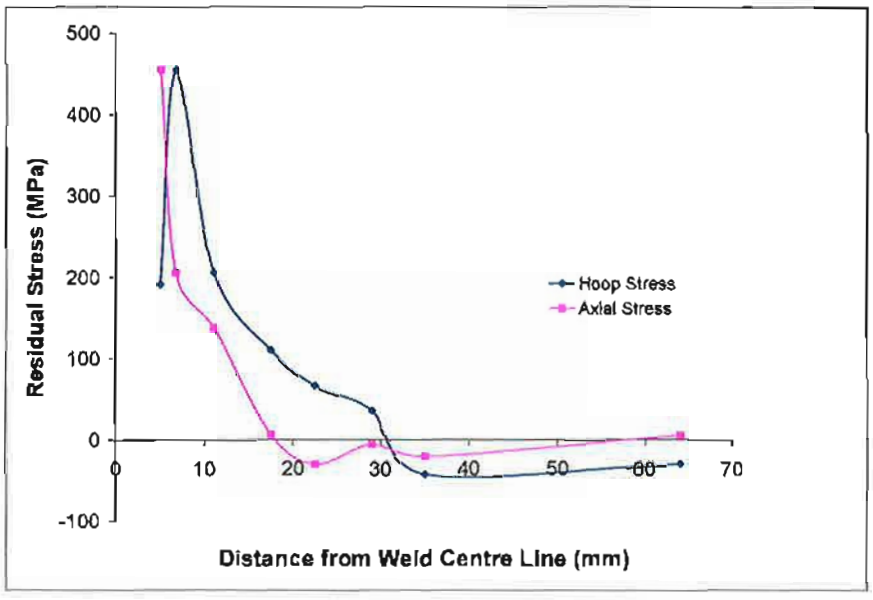

Figure 4.12: Residual stress results determined using the 'Blind Hole Drilling' technique. Results have been corrected for the effect of localised plasticity using the technique proposed by Weng and Lo (1992).

More recently however it has been demonstrated by Beghini et al (1998) and Vangi and Ermini (2000) that the calibration coefficients are also dependant on the biaxiality ratio (ratio of maximum and minimum residual stress) and the alignment of the strain gauge rosette with

respect to the residual stress field. A procedure was developed by Beghini et al (1998) to allow for the effect of localised plasticity. However the procedure required that the direction of the principal stress be known prior to drilling and that the number 1 strain gauge (see Figure 4.5) to be aligned with it. The typical residual stress field of a circumferential weld is known however magnitude and direction rapidly change further away from the weld centreline. It is therefore difficult to place a strain gauge in the correct location and direction in the near weld region.

In this work it was decided to align the gauges so that measurements could be taken as close to the weld centreline as possible, disregarding the principal stress direction. The technique proposed by Beghini et al (1998) was still able to be used including the effect of biaxiality however it is stated that by not having prior knowledge of the principal stress directions accuracy can only be expected to be within 20%. For further information on the procedure please see Beghini et al (1998). The results are shown in Figure 4.13.

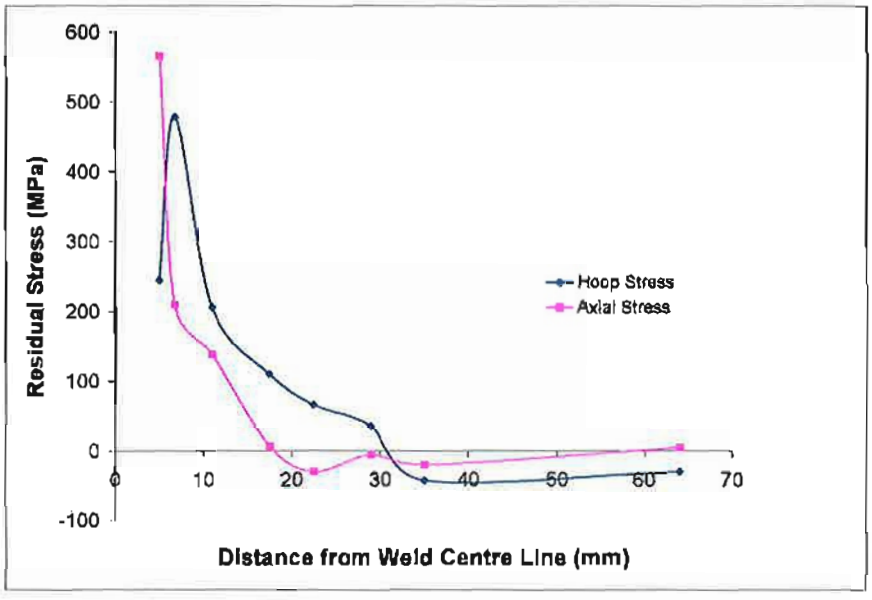

Figure 4.13: Residual stress results determined using the 'Blind Hole Drilling' technique. Results have been corrected for the effect of localised plasticity using the technique proposed by Beghini (1998).

4.4 NUMERICAL MODEL OF WELDING EXPERIMENT

For comparison with the experimental results produced using the 'Blind Hole Drilling' technique, residual stress finite element models of the same welding procedure were created. The finite element models were produced as described previously in Chapter 3. Both 2D and 3D models were created for comparison as both types of models are required to consider all process variables that occur during pipeline construction. The experimental results shown are corrected for localised plasticity using both the technique described by Weng and Lo (1992) and that of Beghini et al (1998) and are plotted on the same axis as the numerical results as shown in Figure 4.14 and Figure 4.15.

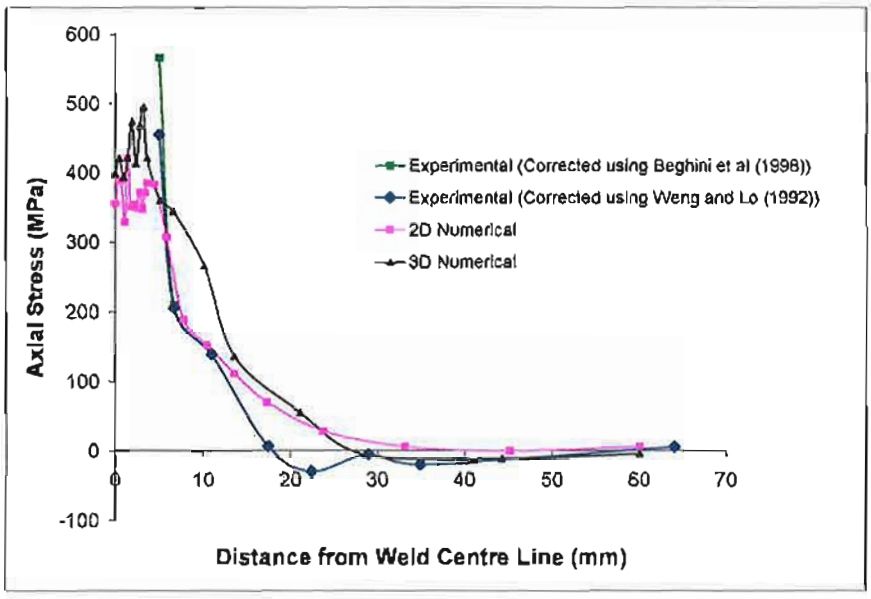

Figure 4.14: Comparison of finite element model residual stress prediction and 'Blind Hole Drilling' residual stress measurement technique results. The axial residual stress on the inside wall at varying locations away from the weld centre line are shown.

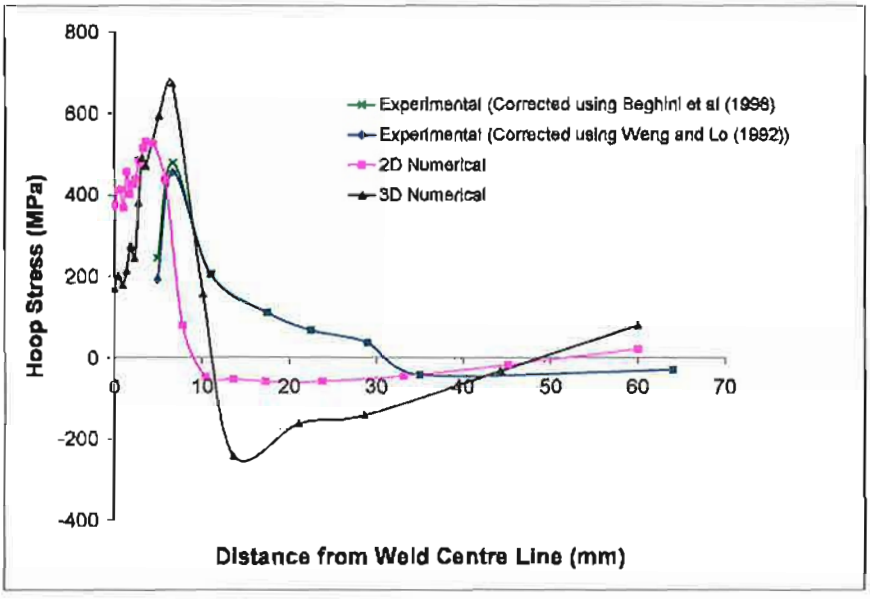

Figure 4.15: Comparison of finite element model calculated and experimentally determined residual stress results. The hoop residual stress on the inside wall at varying locations away from the weld centre line are shown.

4.5 SUMMARY

At best the 'Blind Hole Drilling' technique can be expected to achieve an accuracy within 10% provided the residual stress does not vary with depth. Welding residual stress fields are known to vary with depth so achieving accurate experimental results is difficult. Also further error is introduced when the effect of localised plasticity needs to be accounted for. With this in mind it can be seen that both the trend in the experimental and numerical results show excellent agreement. This also highlights the fact that finite element models are extremely useful to highlight trends despite the fact that there will always be an amount of error in the predictions made.

Finite element modelling offers the opportunity to efficiently and economically study pipeline construction. In this study, finite element models will be used therefore to investigate the effect of process parameters on the residual and transient stress.

Chapter 5

CONSTRUCTION PARAMETERS

5.1 INTRODUCTION

Both 2D axisymmetric and 3D models of the pipeline construction process have been created and produce results which are consistent with experimental results as outlined in Chapter 4. Numerical simulations using thermo-elastic plastic models are known to produce results which often have limited accuracy, but there is a benefit in using them. They demonstrate trends which are useful when designing a construction procedure. Numerical modelling also has the advantage that a large number of process parameters can be considered quickly and cost effectively. In this chapter the effect of varied construction parameters will be considered in relation to their effect on the transient and residual stresses in the weld zone.

Other researchers such as Higdon et al (1980) have considered the effect of lifting on the residual stress, however they considered it in terms of applying a force to a pre-existing stress field. This ignores the transient nature of the stress field and that the weld metal is at an elevated temperature during lifting. There were also other limitations within that work as outlined in Chapter 2.

Other work has also been carried out which considers the effect of welding heat input such as that conducted by Lin and Perng (1997). While process variables associated with construction have been considered in the past, few have been considered in relation to the complete construction process. In this study models have been developed which are capable of considering the transient stress due to both thermal and mechanical effects.

5.1.1 Region of Interest

When using numerical models the transient as well as the residual stress can be observed. The region which is of greatest interest is where the highest tensile residual stress occurs. Shown in Figure 5.1 is the axial residual stress on the inside pipe wall versus transverse distance from the weld centre line at the 6 o'clock and 12 o'clock positions that occurs during a typical pipeline construction procedure. Due to the lifting and lowering processes, the area which suffers the highest level of tensile residual stress is on the weld centre line at the 6 o'clock position. Therefore, when considering the influence of process parameters on the transient stress, the weld centre line at the 6 o'clock position will be used.

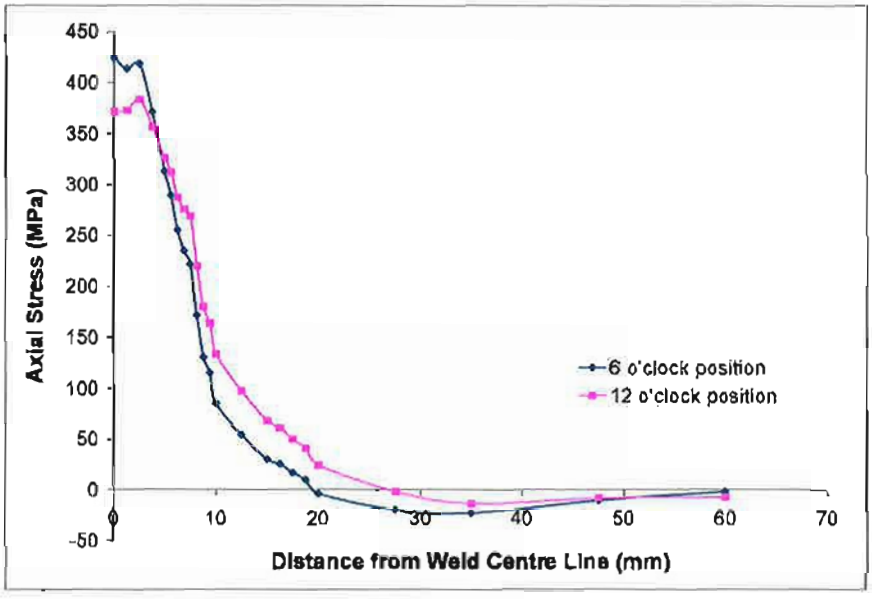

Figure 5.1: The residual axial stress verses the transverse distance from the weld centre line on the inside wall for the 6 o'clock and 12 o'clock positions.

5.2 INFLUENCE OF PARAMETERS ON RESIDUAL STRESS

The results given in this chapter demonstrate trends that occur when process parameters are altered. The process parameters that have been considered include:

- the height of lift during construction
- the timing of the lift
- the heat input
- the electrode used
- the parent material used
- the volume of the weld bead
- the wall thickness
- the proportion of the root run completed before lifting
- the diameter of the pipe

As previously demonstrated in Chapter 4, away from weld start and stop positions, axisymmetric models produce results which agree closely with those produced by 3D models. Therefore in some cases axisymmetric models have been used in this thesis because of the computational efficiency they offer. However axisymmetric models are not appropriate when investigating the effect of weld end effects, the effect of lifting and lowering the pipeline front end or incomplete root passes. When investigating the effect of heat input, pipe diameter, wall thickness, materials used and volume of the weld bead it is

advisable to model these effects in 2D due to the time saving it offers. When considering these parameters 2D models can be used without detriment to the results.

5.2.1 Heat Input Comparison

The heat input used during welding is an important factor to consider. It influences the welding speed that can be achieved, the bead height, the cooling rate of the material and the residual stress. Generally the heat inputs used when welding the root pass are fairly low when compared to those of the capping passes. This is because the welding speed used for the root pass is much greater than that of the capping passes. The faster the root pass is welded the faster the forward pace of construction, which is a major determinant of pipeline construction cost.

In the literature it is generally accepted that greater heat inputs result in greater residual stresses (Lim et al, 1998). Therefore using low heat inputs has the beneficial effect of keeping the residual stress in the root pass lower than it would otherwise have been. To give an indication of the extent to which the heat input influences the residual stress a numerical experiment was conducted using 2D models.

The heat input was varied by changing the current and voltage used, while the welding speed was kept constant. The size and shape of the bead was also altered depending on the heat input used. The greater the heat input the greater deposition rate and therefore bead volume.

Information was found from Lincoln Electric (1995) which related the deposition rate to the welding current used as shown Figure 5.2. This information was used to calculate a bead height, which was related to the heat input whilst maintaining a constant voltage, welding speed and joint preparation. Pipe segments are generally welded using a 60^{o} vee-preparation with a gap between the two pipe segments of 1.6mm and a 1.6mm root face. So using this basic geometry the height of the weld bead was varied while keeping other boundary conditions constant. The height of the weld bead was varied from 2mm, which is less than that of a typical root pass, to 4mm, which is greater than that of a typical root pass.

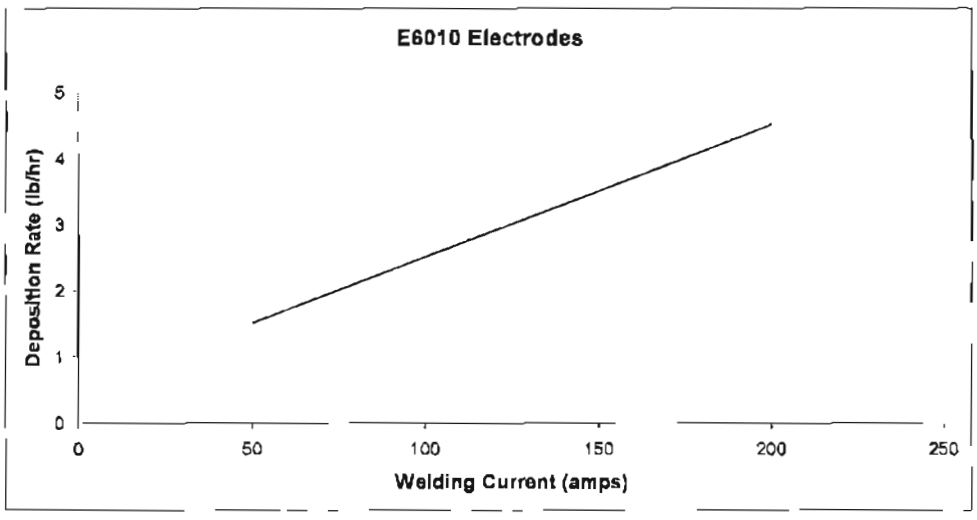

Figure 5.2: Relationship between the welding current and the weld metal deposition rate for E6010 electrodes. Lincoln Electric (1995)

As can be seen in Figure 5.3 the higher the heat input the greater the residual stress. It can also be seen however that the transient stress takes longer to develop with higher heat inputs. This is due to the extended cooling time that occurs with higher heat inputs.

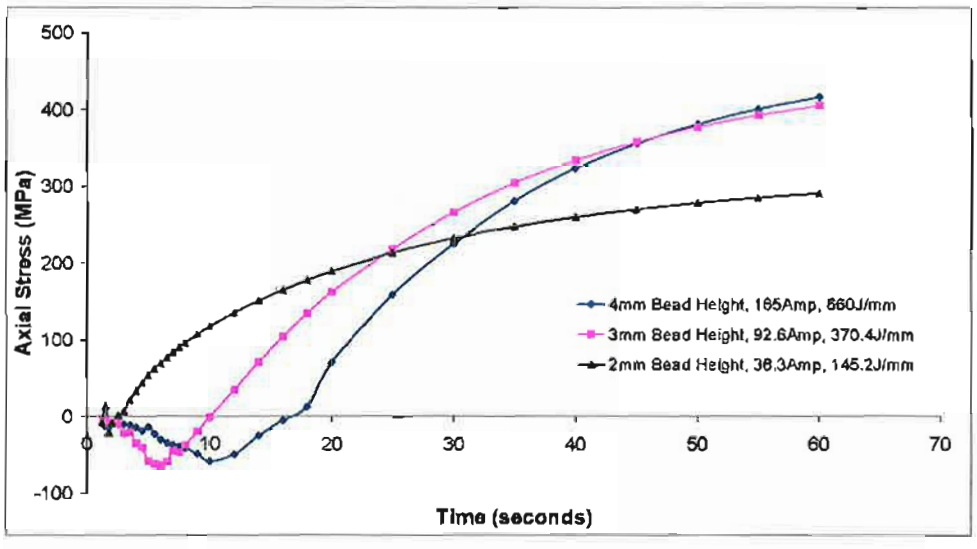

Figure 5.3: Transient axial stress at the root of the weld at the 6 o'clock position using different heat inputs while allowing for deposition rates.

The residual stress produced in a weld would be expected to be greater if the weld cooled very quickly. This is because the weld metal would experience greater restraint by the surrounding material. It is well known that increased restraint results in increased residual stress (Henderson et al, 1996). An investigation therefore was carried out to determine whether the increase in residual stress that occurs when increasing the heat input was actually related to the increased deposition rate of weld metal.

To test the theory that increased residual stress is related to increased bead volume rather than heat input some models with varying bead volumes were created. It can be seen in Figure 5.4 that by increasing the deposition rate alone a reduction in residual stress occurs.

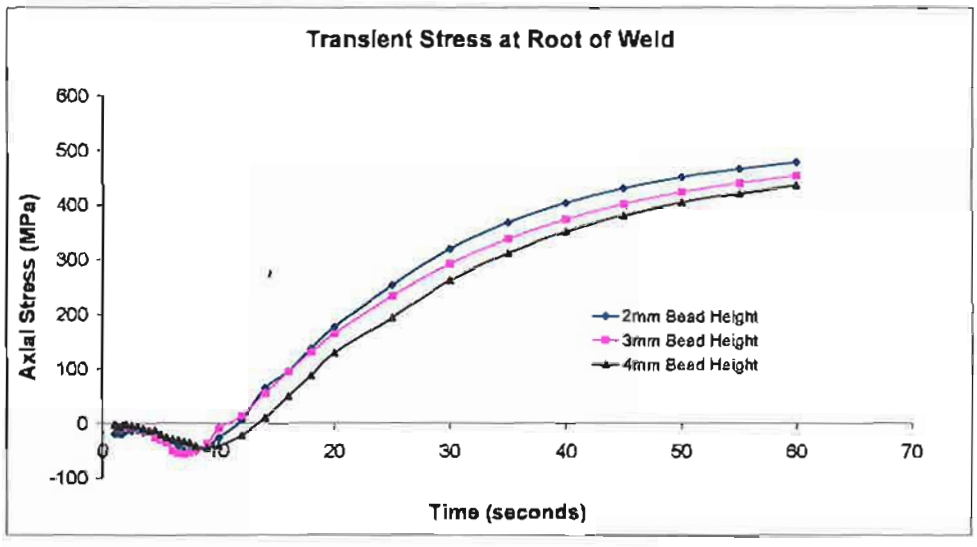

Figure 5.4: Transient axial stress at the root of the weld at the 6 o'clock position for varying bead heights for a constant heat input of 500J/mm.

While it has been previously reported by some researchers that increased heat input increases residual stress, it has not been made clear how to use this information. The author of this thesis proposes that for optimal performance of a root pass in relation to heat input, a low heat input should be used with an electrode with a high deposition rate for a given current. This recommendation is given because it will result in a low tensile residual stress while achieving a high rate of productivity.

5.2.2 Material Used

By using high strength materials thin walled pipes can be used to carry high pressure gas. With all other factors being equal the required wall thickness of a pipe is inversely proportional to the yield strength. Therefore using higher strength pipe has the benefit of allowing a material saving of up to one third if moving from say X65 to X100 grade material. When constructing pipelines there is a requirement that the strength of the weld must exceed that of the pipe itself. This requirement is known as over matching. This means that as the strength of the pipe increases the strength of the weld metal should also increase.

The greater the strength of the parent material used the greater the residual welding stresses that are induced in the root pass. Axisymmetric models were created using different material properties from X42 to X80 using E9010 electrodes. As the strength of the parent material increases so to does the residual stress as can be seen in Figure 5.5.

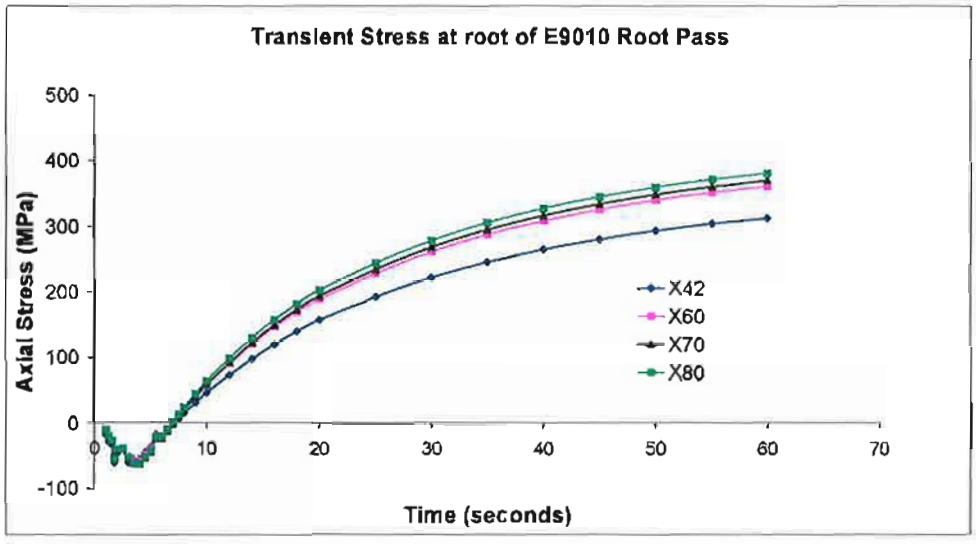

Figure 5.5: Transient axial stress at the root of the root pass for various parent materials while using E9010 electrodes.

The strength of parent material influences the restraint on the root pass material thereby altering the residual stress. The residual stress experienced in the root pass however is more dependant on the strength of the weld metal than that of the parent metal. This can be seen in the Figure 5.6. It would therefore be advisable to use lower strength material for the root pass than for the capping passes. By doing this a reduced residual stress would be produced at the root of the weld in the tensile region while still meeting the over matching requirements.

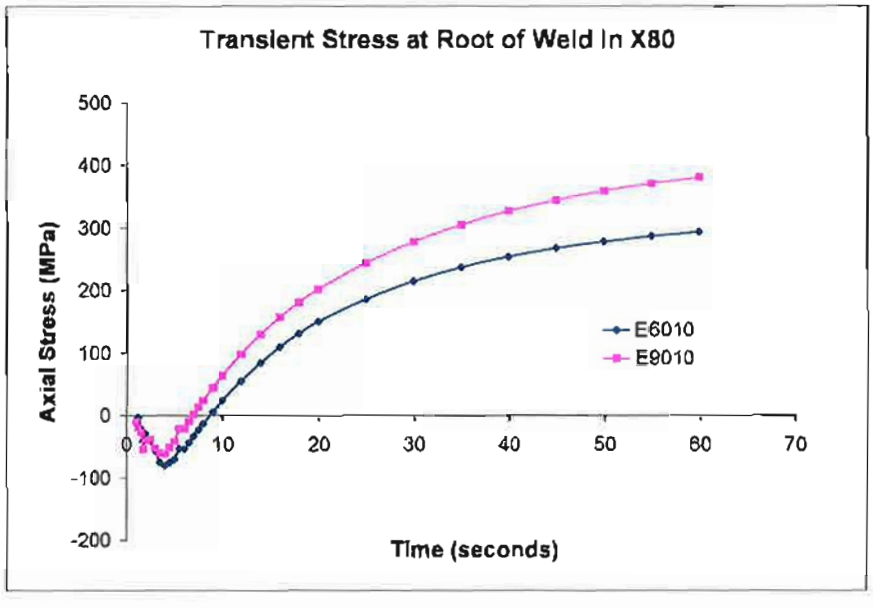

Figure 5.6: Transient axial stress at root of weld for E6010 and E9010 electrodes.

5.2.3 Pipe Wall Thickness to Diameter Ratio

The ratio between the pipe wall thickness and the diameter has a significant effect on the residual stress. In circumferential welds the stress field is capable of deforming in the radial direction, which reduces the restraint and residual stress in the weld. The amount of circumferential deformation depends on the wall thickness to diameter ratio.

Figure 5.7 shows the result of varying the wall thickness for a given diameter. The geometry of the root pass, the heat input (500J/mm) and other boundary conditions were kept consistent between the two models. Figure 5.8 shows the effect of varying the diameter for a constant wall thickness. As the diameter increases the residual stress is reduced. It is

interesting to note that the current move toward using thinner walled pipe will have the beneficial effect of reducing the residual stress.

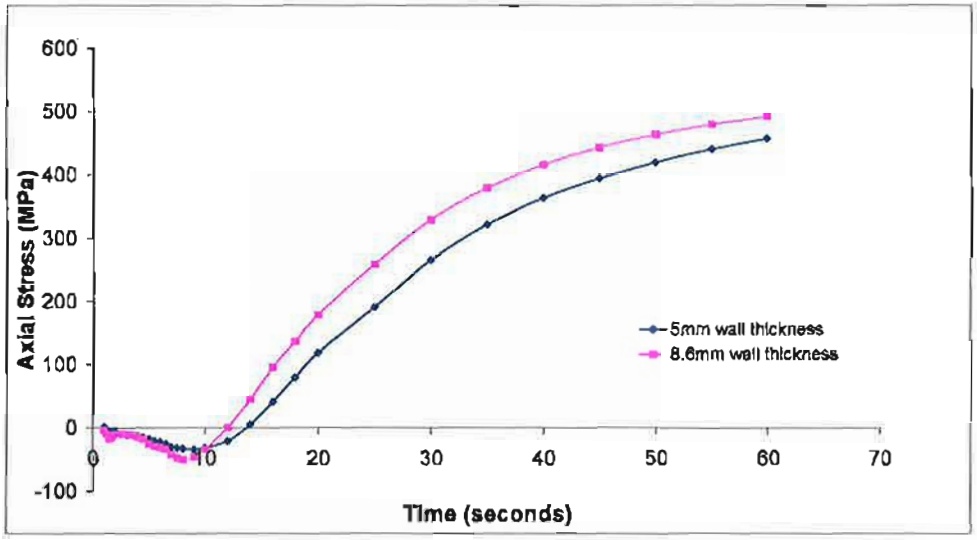

Figure 5.7: Transient stress at the root of weld for different wall thicknesses for the same weld bead geometry.

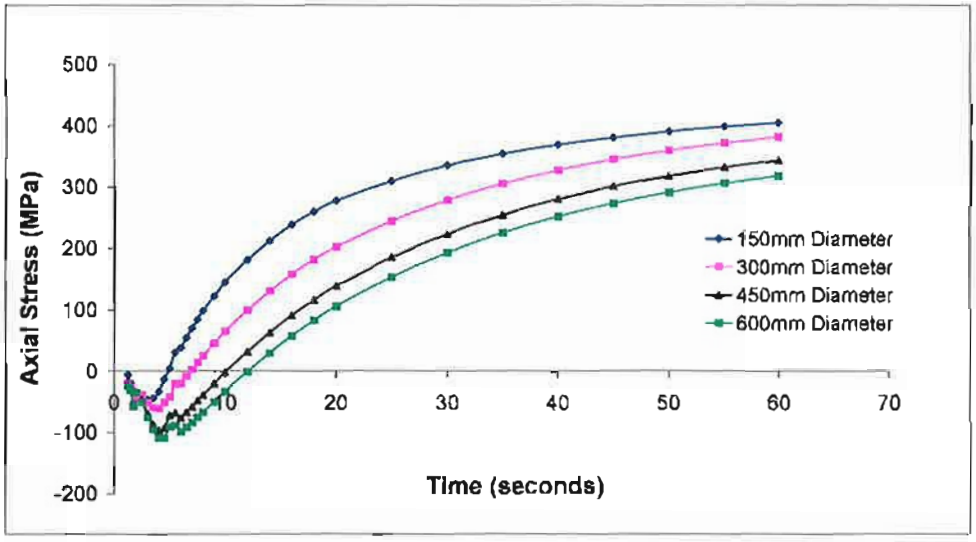

Figure 5.8: Transient axial stress at the root of weld for different pipe diameters.

5.2.4 Lifting Pipeline Front End

After welding of the root pass the pipeline front end is lifted to place it on a support skid. The lifting process places additional mechanical loading on the root pass which affects the resulting residual stress. During the lifting and lowering process, plastic deformation occurs in the root pass. This plastic deformation can result in leaving an increased residual stress in the root pass or it can be used to relieve some of the residual stresses in the root pass as demonstrated in preliminary models in Chapter 2. The particular effect of lifting and lowering is dependant on the height of lift, the material properties, the timing of the lift and the proportion of the root pass completed before lifting.

5.2.4.1 Height of Lift

The construction model described in Chapter 3 was run a number of times whilst only changing the height of the lift of the front end of the pipeline. Figure 5.9 shows the transient axial stress that resulted from this analysis. Only the axial stress is shown since the hoop stress experienced in the root pass shows similar trends, however the magnitude of the hoop stresses are lower due to the ability of the pipe to radially deform. Since the maximum residual stress occurs near the weld centre line as shown in Figure 5.9, the residual stress is compared at the weld centre line in this present work.

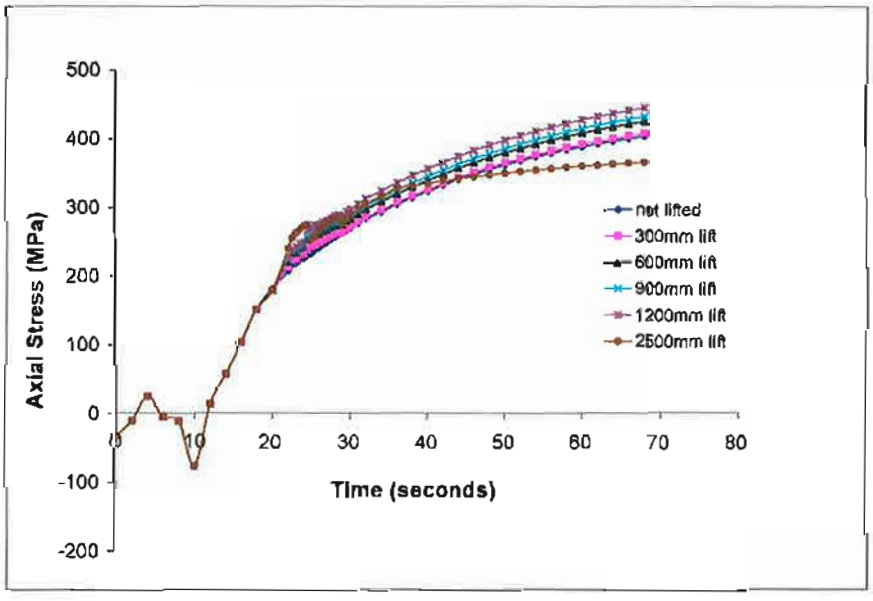

Figure 5.9: Transient stress at the root of weld for various lift heights. Parent material is X80 and the electrodes used are E9010.

In Figure 5.9, X80 grade material was used with a 50% completion of the root pass and E6010 electrodes. In this scenario lifting the front end for a normal lift (300mm) or an extreme lift (600mm) both result in an increased residual stress. However if the front end is lifted high enough and the root pass is stressed enough to produce enough plastic deformation in the root pass some of the residual stresses can be relieved. For enough plastic deformation to occur there are two factors other than increased lift height to consider. Firstly a pipe grade of lower strength can be used or the front end can be lifted earlier while the material is at a more elevated temperature.

5.2.4.2 Strength of Material

In the scenario used above a lift height greater than used in practice was required to produce enough plastic deformation in the root pass to relieve some of the residual stress. However if the strength of the pipe and electrodes were lower, the lift height of the pipe could be lower while still resulting in enough plastic deformation to relieve some of the residual stress.

This can be seen in Figure 5.10 where X42 pipe grade was used. A lift height of only 1200mm rather than 2500mm was required to induce enough plastic deformation to relieve some of the residual stress. While this numerical experiment has highlighted a trend that occurs when lifting the pipeline front end, the height of the lifts considered here are extreme and are unlikely to be used in practice.

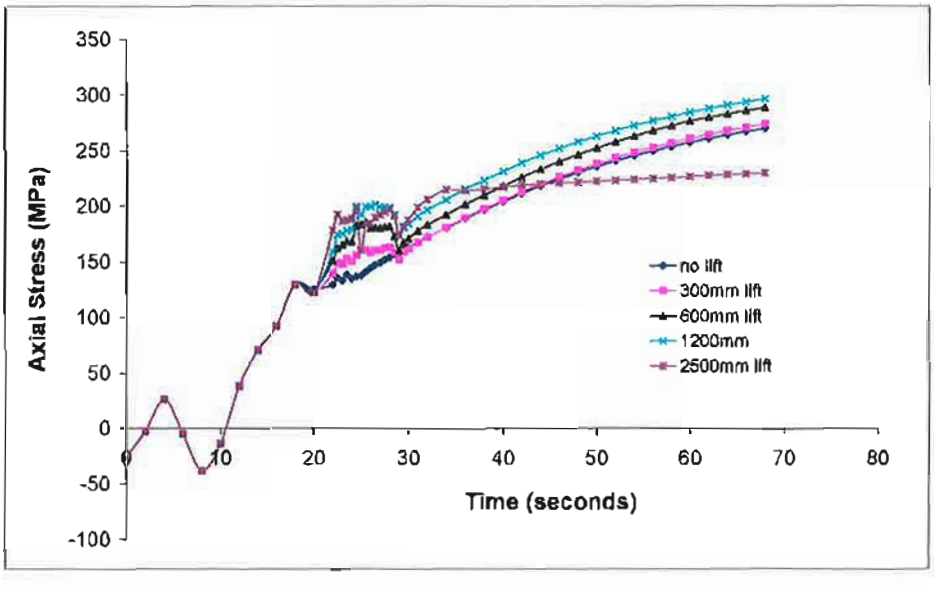

Figure 5.10: Transient stress at the root of weld for various lift heights. The pipe material is X42.

5.2.4.3 Timing of Lift

The pipeline front end is lifted shortly after welding the root pass so as to maximise the forward pace of construction. This means the weld metal is at an elevated temperature during lifting. It is therefore important to model the construction process using transient models.

By altering the timing of the lifting and lowering, the residual stress experienced in the root pass can be altered. This phenomena can be seen in the Figure 5.11. If the lift occurs early enough such that it results in significant plastic deformation in the weld zone then this can

have the effect of relieving some of the residual stresses in the root pass. However if the lift does not result in enough plastic deformation in the root pass the residual stress is increased.

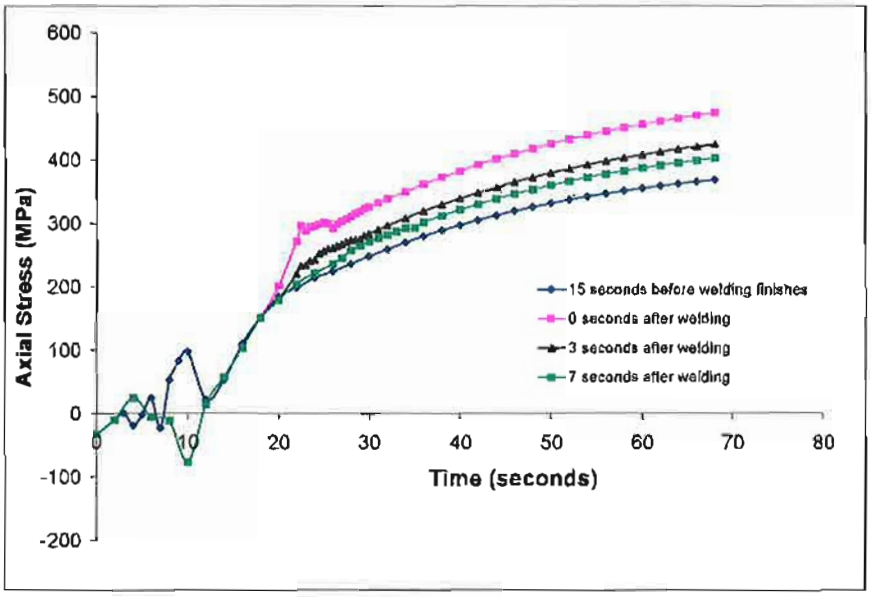

Figure 5.11: Variation of the transient axial stress at the root of the weld in the 6 o'clock position for different lift times.

It can therefore be seen that if the lifting does not result in sufficient plastic deformation for stress relief to occur it would be advisable to keep lift heights to a minimum and allow the weld metal to cool sufficiently before lifting. However lift heights that are currently used cause only a small increase in the residual stress of the order of 5-10%, which suggests current practice is overly conservative.

It could well be decided that out of conservatism lifting of the front end would not be used to relieve residual stresses in the root pass. In this case the lift height, the timing of the lift and the percentage completion of the root pass required can be specified for a given material grade and geometry using the modelling scheme developed. It would appear that current procedures are conservative and recommendations could be made to increase the forward pace of construction.

5.2.4.4 Proportion of Root Pass Completed

The benefit of allowing reduced root pass completion and earlier lifting of the pipeline front end would be increased forward pace of construction (one of the objectives of this research). An important improvement made to the pipeline construction process was suggested by Henderson et al (1996), which was that only a 50% completion of the root was required before lifting. This enabled the pace of front-end construction to increase from 4km per day to 8km per day, as demonstrated on the Carpenteria Pipeline (Chipperfield, 2002).

It has also been stated by Smart and Bilston (1995) that the section modulus of a root pass is dependant on the portion of the root pass welded in relation to the lifting axis. For example if the portions of the top and bottom pipe are welded, it will result in a greater section modulus than if portions of the two sides are welded. This suggested that less than 100% completion could be used if the correct portions were welded.

A numerical experiment was conducted to determine the difference in the resulting residual stress in the 6'oclock position for differing proportions of root pass completion. The welding start and stop position was 20° before top and bottom dead centre respectively for all models. A 600mm lift was carried out immediately after welding was completed.

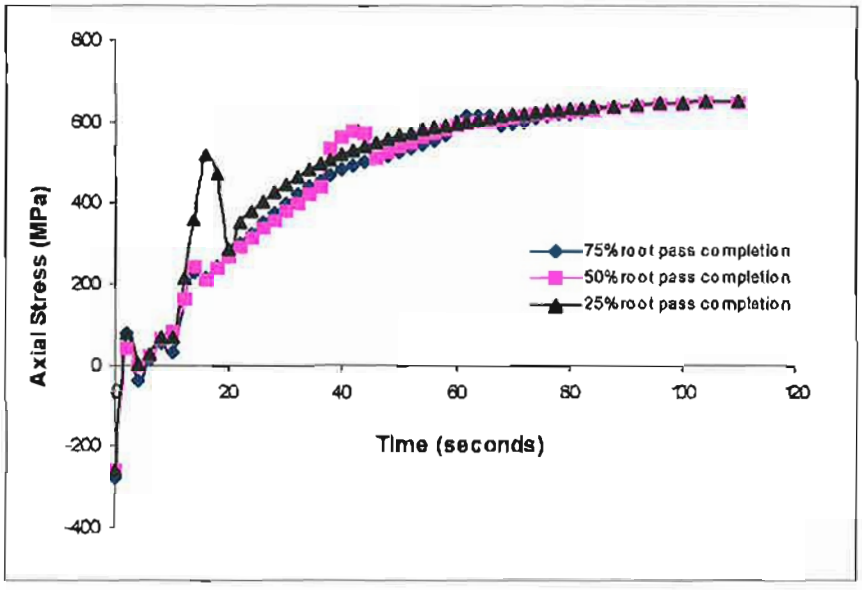

Figure 5.12: The transient stress at the root of the weld at bottom dead centre for different root pass completions.

It can be seen from Figure 5.12 that provided the root pass start and stop locations are 20° before the top and bottom dead centre, then as little as 25% of the root pass can be welded without increasing the residual stress. It can be seen however that the root pass is placed

under more stress during the lifting procedure than in the models with greater proportions welded before lifting.

The reduction in the proportion of the root pass completed before lifting did not result in enough plastic deformation to relieve some of the residual stresses for a 600mm lift height. If a greater lift height was used in combination with reduced root pass completion, stress relief would occur. This demonstrates how little root pass is required provided the appropriate parts of the girth are welded.

While this appears to suggest that only 25% of the root pass needs to be welded before lifting of the pipeline front end, it is assumed in these models that no weld mismatch occurs. In order for no weld mismatch to occur when only 25% of the root pass is completed before lifting, the line-up clamp may be required after the lifting process whilst the root pass was completed. Without early release of the line-up clamp the speed increase may not be achieved.

5.2.5 Effect of Welding Start / Stop Position

The location in which the girth is welded influences the section modulus of the girth weld. If the top and bottom portions of the pipe are welded the girth will have a greater section modulus than if the sides are welded. A numerical experiment was conducted where 50% of

the root pass was welded before lifting, while changing the location around the girth where the root pass was welded.

Three different scenarios were considered. In all scenarios only 50% of the girth was welded by two welders working simultaneously on opposite sides of the pipe. In the first case, the root pass was welded 45° after bottom dead centre (ABDC). In the second case, the root pass was welded 20° ABDC. In the third the root pass was welded until it reached bottom dead centre. The results are shown in Figure 5.13.

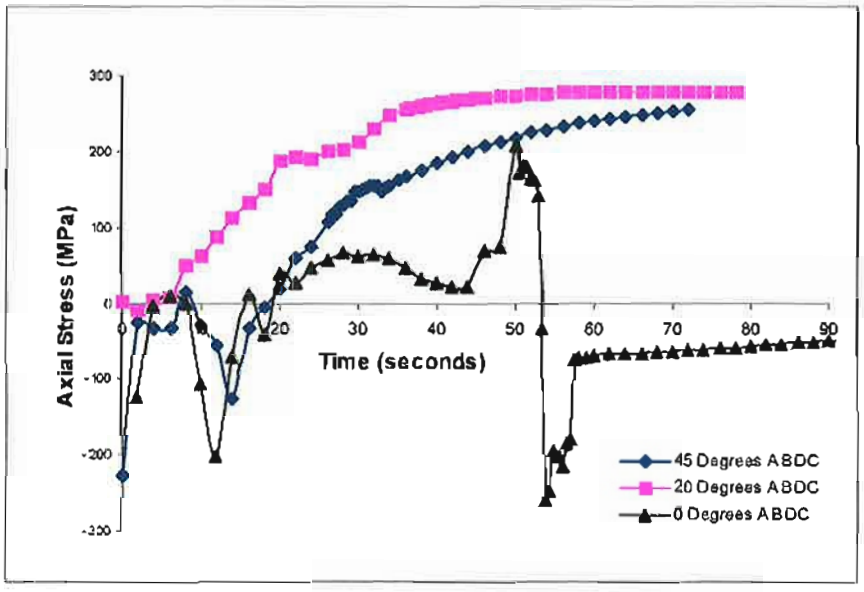

Figure 5.13: The transient stress at the root of the weld at bottom dead centre for a root pass of 50% completion with various start positions.

A similar trend can once again be observed. By increasing the amount of plastic deformation by a sufficient amount, some of the residual stress can be relieved. In this case the amount of plastic deformation is altered by varying the section modulus. It can also be seen however that if the weld is stressed to an insufficient level the residual stress can be increased.

5.3 SUMMARY

After investigating the influence of process parameters on the residual stress it can be seen that current practice does not adversely affect the residual stress. This is not unexpected as current procedures are based on past experience and trials that have been carried out. The work presented here however has developed an understanding of the influence of individual process parameters in relation to the induced transient and residual stress.

It has been shown that broadly speaking, the greater the heat input, the higher the residual stress. The effect of heat input however is also related to the weld deposition. It was found that the greater weld metal deposition for a given heat input, the lower the residual stress. An increase of 50% in deposition rate produced a reduction of axial stress of approximately 10%.

The strength of the electrode has a very strong influence on the resulting magnitude of the residual stress in the root pass. It was demonstrated that reducing the strength of the electrode by one third, had a corresponding effect of reducing the residual stress by one third. The parent material also influences the residual stress in the root pass but to a lesser extent than that of the electrode strength. The difference in the magnitude of the axial residual stress when moving from say X42 to X80 strength pipe material is approximately 20%.

It has been confirmed in this present study, that the higher wall thickness to diameter ratio the greater the residual stress. It was found that by doubling the diameter the axial residual stress was reduced by approximately 15%.

The proportion of the root pass completed before lifting can influence the maximum residual stress induced in a girth weld. It was demonstrated, however, that if the portions that are welded evenly cover the top and bottom dead centre of the girth, as little as 25% of the girth needs to be completed before lifting. This depends, however, on the pipe segments having no ovality, which is unlikely in reality. For this reason it would be unwise to recommend that only 25% of the girth needs to be welded before lifting.

It has been found that by lifting the pipeline front end higher than is the current practice, some of the welding residual stresses can be relieved. While this is a revelation not previously observed, it may not be an advisable approach. This is because increasing the amount of plastic deformation could also have the effect of initiating cracks. Until microscopic effects are also taken into account it would be unwise to recommend this approach for reducing the chance of HACC. It has been shown however that 'normal' lift heights (300mm) or even 'extreme' lift heights (600mm) are not going to adversely affect the residual stress.

The timing of the lifting of the pipeline front end can also influence the residual stress induced in the root pass. If the lift occurs early enough to induce additional plastic deformation, some of the residual stress can be relieved.

From this study it would appear that current practise is overly conservative and there is still room to increase efficiency without placing the pipeline at risk.

Chapter 6

HYDROGEN DIFFUSION MODELLING

6.1 INTRODUCTION

Previous chapters have been concerned with the development of tensile residual stress in the weld zone, which is the driving force behind HACC. The presence of hydrogen is also an important consideration. The transient hydrogen concentration is analysed in this chapter.

During welding hydrogen diffuses into the molten weld metal from the cellulose in the electrodes and moisture in the atmosphere. This hydrogen then diffuses throughout the weld metal and into the HAZ of the parent material. When the weld metal cools to ambient temperature the hydrogen diffuses very slowly and some hydrogen becomes trapped in regions of high stress and dislocations (features termed 'hydrogen traps'). As the material cools there comes a temperature when the hydrogen diffusion is sufficiently slow such that very little more escapes the material into the atmosphere. The time taken for hydrogen to diffuse out of the material is dependant on many factors such as the cooling rate, the geometry of the weld and time between weld passes. In this section, the opportunity for reduced risk of HACC is investigated with regard to hydrogen diffusion.

The procedure used to investigate hydrogen diffusion is explained with regard to currently available techniques. Results of the investigation are given which allow a quantitative view of the diffusion of hydrogen. The results of the modelling cannot be experimentally verified however well established numerical techniques are used which allow trends to be demonstrated.

6.2 MODELLING TECHNIQUE USED

The modelling of hydrogen diffusion has made many steps forward over the last 30 years. Models based on Fick's Second Law of diffusion have been commonly used in the past however, more advanced models such as that produced by Zhang et al (1991) have been developed which consider microstructural, plastic strain and trapping effects. There are also models that have been developed which consider stress assisted diffusion such as that of Krom et al (1999). As stated by Boellinghaus et al (1995), these advances in modelling of hydrogen diffusion have contributed to a greater qualitative understanding of hydrogen diffusion. However Boellinghaus et al (1995) also stated that for a quantitative analysis of hydrogen diffusion, simple diffusion models based on Fick's Second Law of diffusion are more advisable.

There are still differing opinions on whether stressed regions act as hydrogen traps or whether stress assisted hydrogen diffusion occurs, therefore more complex models are unlikely to give a more accurate result. When considering pipeline construction such issues do not need to be addressed because HACC is most likely to occur in the first few minutes after welding (Fletcher and Yurioka, 2000). It is therefore not necessary to model hydrogen accumulation over several hours.

Past work by Suzuki and Yurioka (1986) developed a cracking parameter to be used for the determination of the minimum preheating temperature required to prevent HACC. That

work demonstrated how the hydrogen content increases in critical areas with time and how the maximum concentration occurs several hours after welding. It was stated in that work however that, "*the formula (for determining critical preheat temperature) has been developed mostly for low-hydrogen electrodes*" (Suzuki and Yurioka, 1986 23-15). The calculated variation of hydrogen content with time is shown in Figure 6.1. The hydrogen concentration reaches a maximum several hours after welding. This is due to the location being considered (weld root) having a hydrogen trap simulated in that region.

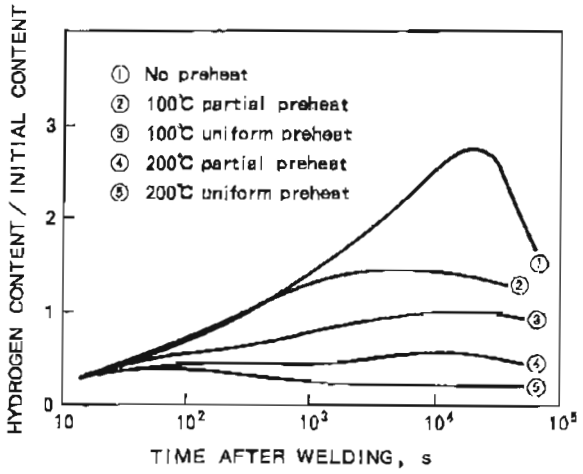

Figure 6.1: Time dependant change in hydrogen concentration at weld root of single bevel weld after welding under various preheat conditions calculated by finite difference method. Suzuki and Yurioka (1986).

In pipeline construction however high hydrogen welding processes are used. It is stated in the Australian Standard, Pipelines - Gas and liquid petroleum (AS 2885.2, 2002 pp.103),

"cellulosic electrodes are commonly employed, leading to very high levels of hydrogen in the weld metal of 30ppm or more."

One of the aims of this investigation is to highlight the linked effects of transient temperature, stress and hydrogen diffusion immediately after welding. As previously demonstrated it only requires several minutes after welding for the temperature of the material to reach ambient and the transient stress to reach a residual level. Therefore the diffusion of hydrogen during the first few minutes after welding is of primary interest in this work. As stated by Fletcher and Yurioka (2000), "*Pipeline girth welding is unique in contrast to welding of other steel structures usually conducted by low hydrogen consumables. HACC occurs some hours after completion of welding in low hydrogen welding, because it takes time for hydrogen to diffuse and accumulate at the site where HACC is initiated. However, pipelines are often welded with cellulosic electrodes which produce welds completely saturated in hydrogen, and HACC in a root weld is reported to be initiated several minutes after welding*" (Fletcher and Yurioka, 2000 pp.25)

Due to saturation of the weld metal with hydrogen in pipeline welding, the diffusion of hydrogen in the first few minutes after weld deposition is assumed to be unaltered by the existence of hydrogen traps. Also since HACC is reported to typically occur several minutes after welding there is no need to model accumulation of hydrogen over several hours. Fick's second law of diffusion allows modelling of the diffusion due to the large chemical potential that exists immediately after welding with cellulosic electrodes. This chemical potential is

assumed to be the predominant driving force behind the distribution of hydrogen throughout the weld zone when saturated. Hydrogen diffusion that occurs due to the welding of pipelines can therefore be modelled using Fick's Second Law of diffusion.

The diffusivity of hydrogen in steel is dependant on the temperature of the steel. For this reason, within the transient model the material properties are altered depending on the temperature of the material. The temperature history of the material is predicted via an axisymmetric thermal model as described in Chapter 3. As the material cools after welding there is a temperature gradient throughout the material. Since the diffusivity of the material is dependant on the temperature of the material every element is assigned a new hydrogen diffusivity each time step.

It is stated in Easterling (1992) there is a wide scatter of diffusivity measurements for hydrogen in ferritic steels below 200°C. Although there is a wide scatter of results, it is typical to assume two diffusivity coefficients for hydrogen in ferritic steels. The diffusion coefficient used for temperatures below 200°C is given in Equation 6.1 and the diffusion coefficient used for temperatures above 200°C is given in Equation 6.2.

$$d = 0.14\exp\left(\frac{-13400}{RT}\right) \text{ mm}^2\text{s}^{-1} \qquad \text{(Temperature} < 200^\circ\text{C)} \qquad \textbf{(6.1)}$$

$$d = 12\exp\left(\frac{-32700}{RT}\right) \text{ mm}^2\text{s}^{-1} \qquad \text{(Temperature} > 200^\circ\text{C)} \qquad \textbf{(6.2)}$$

where:

d = Diffusivity

R = Constant used to calculate diffusivity

T = Temperature

The surfaces exposed to the atmosphere are assigned a hydrogen concentration equal to zero. This causes the hydrogen concentration to have a gradient which promotes diffusion out of the material. This is a valid assumption as hydrogen at the surface of the material will diffuse into the atmosphere. This approach is consistent with past models of hydrogen diffusion. One such example is Boellinghaus et al (1995).

The material properties in the model were changed continuously between time steps, which is costly in terms of computation time. An external computer program was written to reassign diffusivity of each element between time steps by determining the temperature of the element from a thermal model that had been run previously. Therefore a new solution had to be run for each time step. This meant that at each time step the mesh and other model parameters had to be reread into memory and a new wave front minimisation procedure had to be carried out. This procedure was necessary however, given that the commercial finite element package, 'NISA' does not allow material properties to be changed during a solution if the cause of the change is decoupled from the current solution. A schematic diagram of the procedure used to model hydrogen diffusion is given in Figure 6.2.

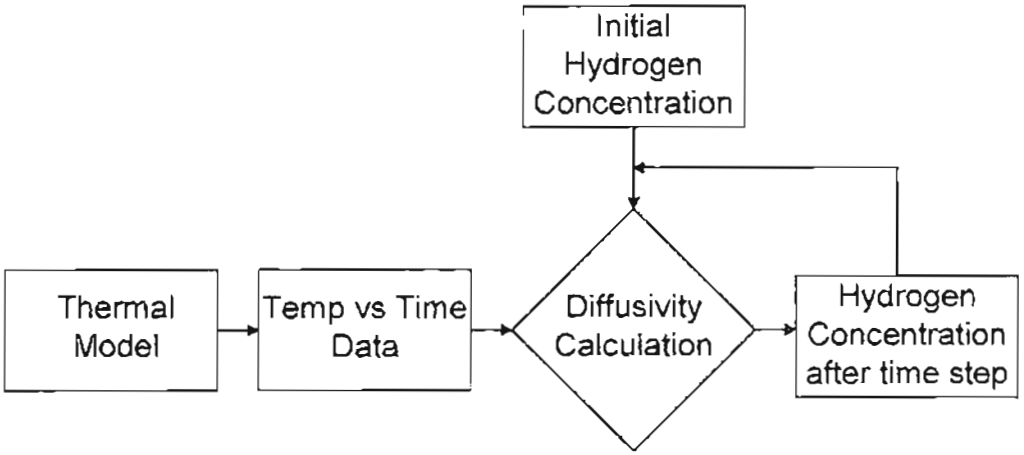

Figure 6.2: Flow diagram of procedure used to model hydrogen diffusion.

6.3 NUMERICAL EXPERIMENT

Using Fick's Second Law of Diffusion and ignoring the existence of hydrogen traps and stress assisted diffusion means the reduction in hydrogen diffusion is only dependant on the geometry of the weld, the temperature of the weld and the time elapsed since welding. It does however mean that during girth welding with cellulosic electrodes, the predominant methods for altering the rate of hydrogen diffusion are via changes to the temperature. This can be achieved by pre-heating, post-heating or altering the timing of the hot and capping passes.

A numerical experiment was conducted whereby four scenarios were considered.

- In the first, the girth weld was allowed to cool to ambient temperature after welding with no modification to the cooling rate.
- In the second, pre-heating was simulated by assuming an initial temperature of the near weld region of 300°C before welding.
- In the third, solution the near weld region was allowed to cool for the length of time the root pass takes to complete. Then the temperature of the near weld region was raised to 300°C to simulate post-heating and allowed to cool.
- Finally, the effect of the hot pass on the transient hydrogen concentration was examined. A model was created where a hot pass was laid five minutes after the root pass. This model was created to simulate the hot pass with a different mesh, which included elements for the hot pass.

6.4 RESULTS

The hydrogen concentration 11 minutes after welding, which was calculated using a model based on Fick's Second law of diffusion can be seen in Figure 6.3. When making comparisons the location considered in this work is shown in Figure 6.4 and the nominal dimensions are given in Figure 3.2. This is because the root of the weld is exposed to the atmosphere and therefore has a low hydrogen concentration in that region. The location shown in Figure 6.4 is typically where hydrogen cracks are initiated when welding high strength steels such as is used today for pipeline construction (Kufner, 2003).

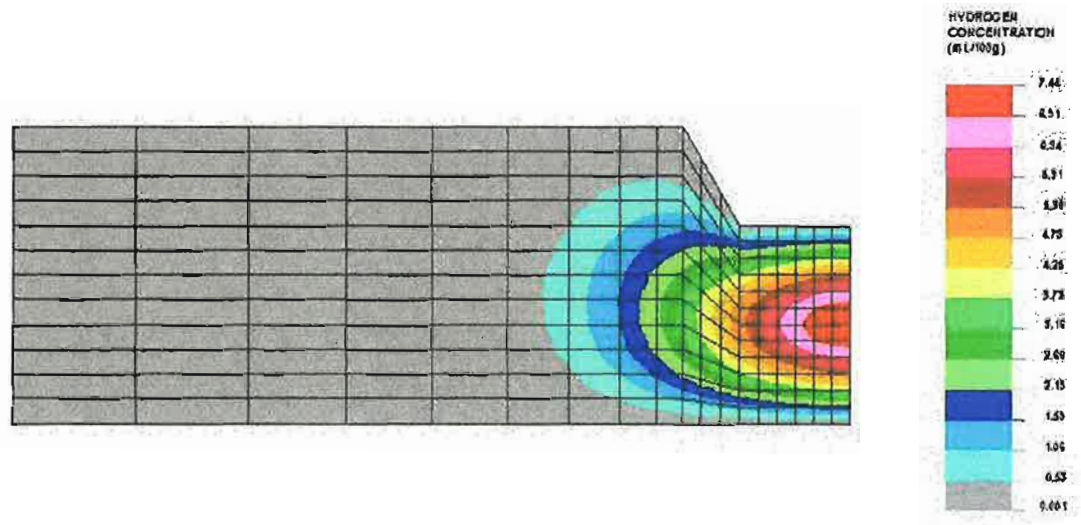

Figure 6.3: The calculated hydrogen distribution 11 minutes after welding.

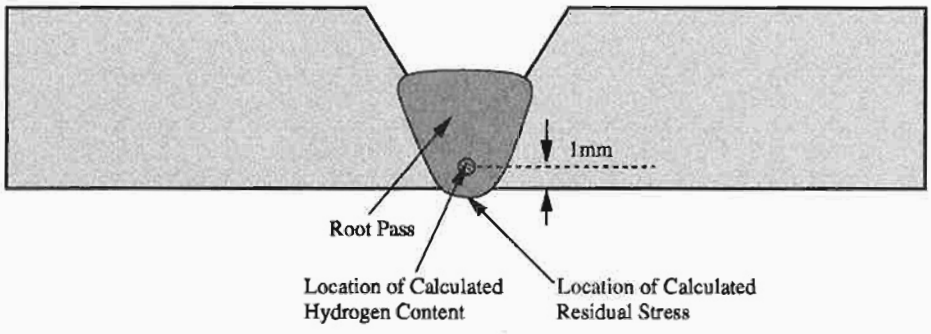

Figure 6.4: Location where the calculations are considered in the present study.

The rate of hydrogen diffusion is highly dependant on the temperature cycle of the material. At elevated temperature the hydrogen diffuses out of the material quickly whereas at ambient temperature the hydrogen diffuses so slowly it almost becomes trapped in the material. This phenomena means that the effect of pre-heat or post-heat can greatly increase the rate of hydrogen diffusion.

The effect of pre-heating or post-heating the weld on the rate of hydrogen diffusion was examined. This can be seen to have a significant and beneficial effect on reducing the hydrogen concentration as shown in Figure 6.5. Both pre-heating and post-heating of the near weld region result in a very similar rate of diffusion.

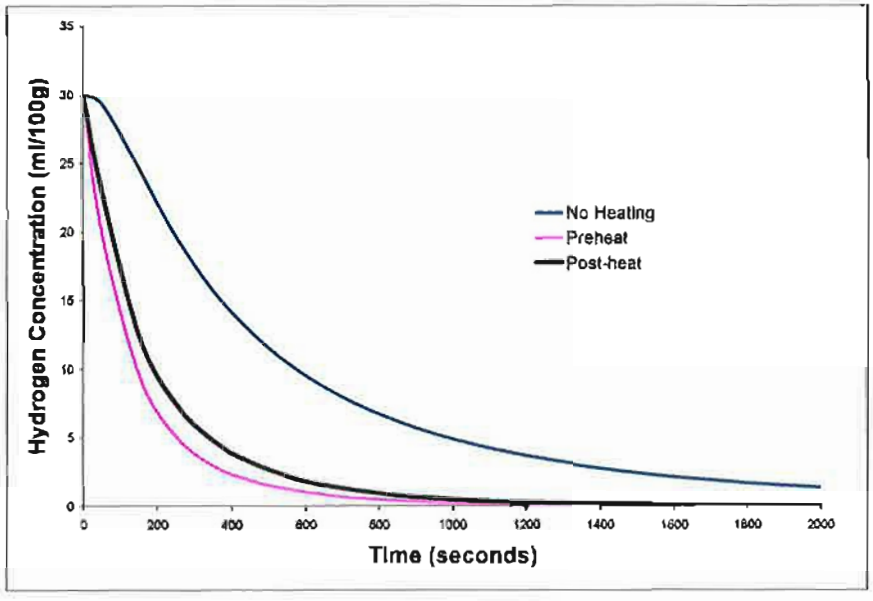

Figure 6.5: Transient hydrogen concentration after welding of root pass.

The rate of hydrogen diffusion is increased by pre-heating and post-heating of the near weld region because the material spends longer at an elevated temperature which promotes diffusion. This can be seen in Figure 6.6 where the temperature history is shown for the three scenarios.

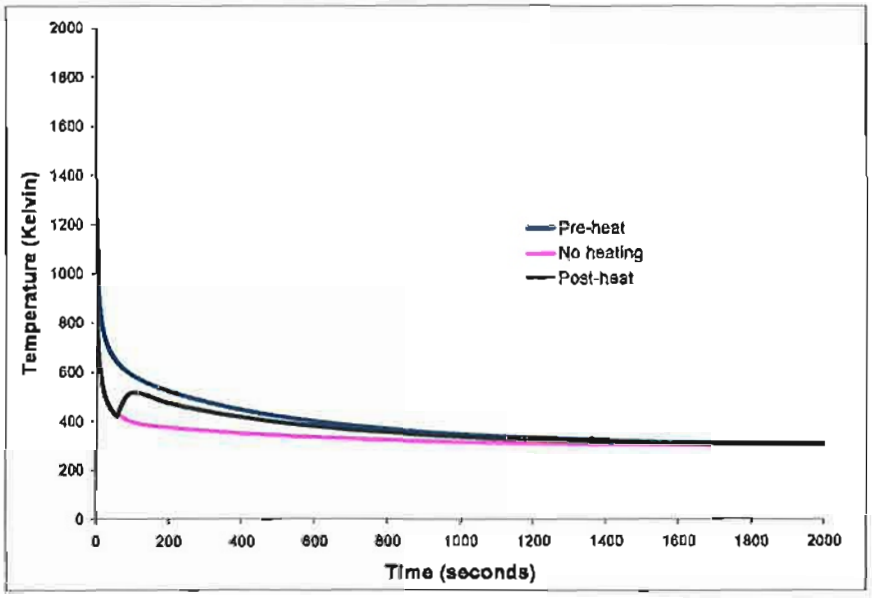

Figure 6.6: Temperature history for a node in the root pass including scenarios where pre-heating and post-heating are used.

In order to simulate the hot pass, a thermal model was created to predict the temperature history using the temperature field from the previous model after five minutes as an initial temperature boundary condition. A hydrogen diffusion model was then created using an initial concentration of 30mL/100g (which was suggested by Fletcher and Yurioka, 2000) in the hot pass weld metal.

When the hot pass is laid on top of the root pass typically with a dwell time of five minutes between passes, the temperature of the root pass is once again elevated, increasing the rate of hydrogen diffusion, but more hydrogen is also introduced within the weld metal of the

second pass. In Figure 6.7 the transient hydrogen concentration is shown for the two scenarios for a node in the location shown in Figure 6.4.

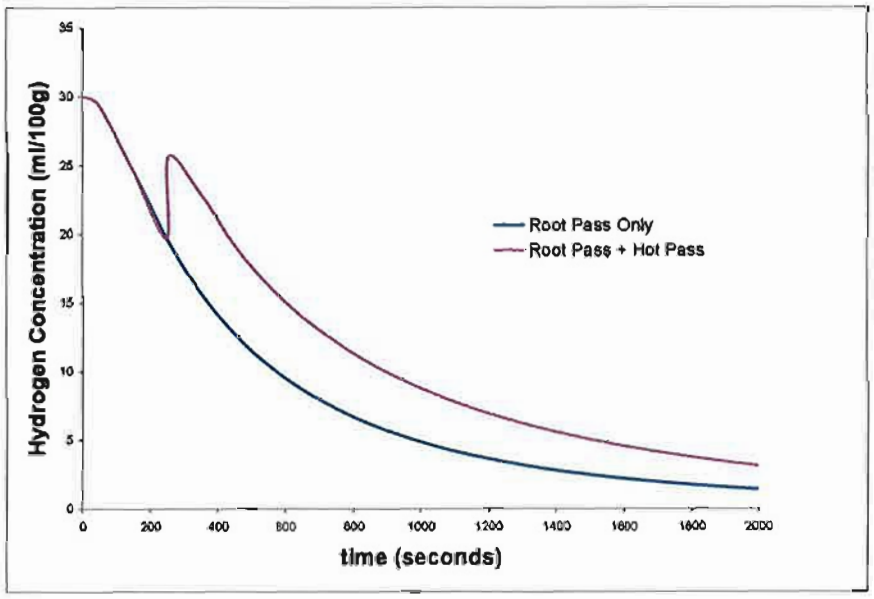

Figure 6.7: Transient hydrogen concentration after welding of root pass and hot pass.

In Figure 6.8 the temperature history for the node in the location shown in Figure 6.4 which was considered in Figure 6.7 is shown. It can be seen that when the hot pass is laid on top of the root pass the temperature of the root pass is elevated and then cools more slowly than it would have without the hot pass. As the root pass stays at a higher temperature for longer, hydrogen diffuses out more quickly.

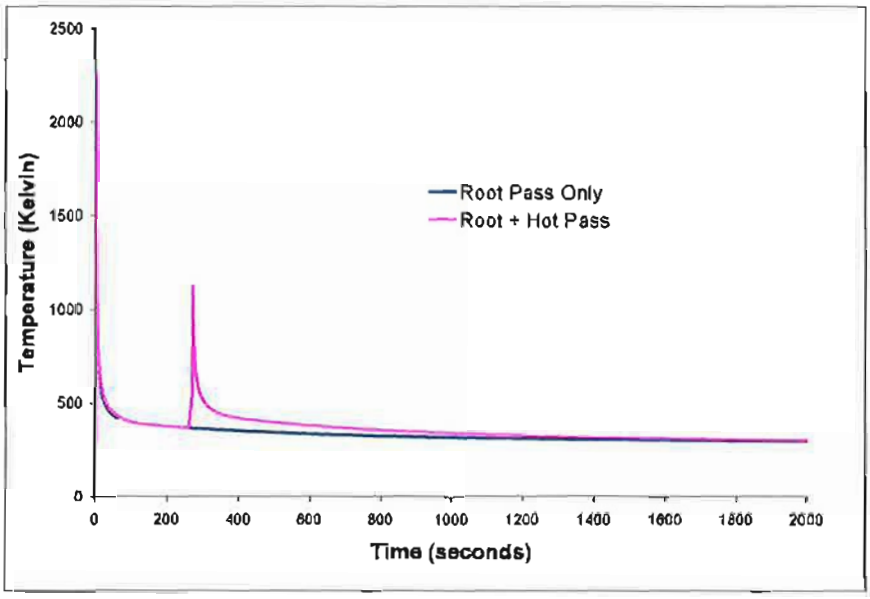

Figure 6.8: Temperature history of a root pass with and without a hot pass laid on top.

By adding a hot pass shortly after the root pass, increases the concentration of hydrogen. This would suggest that by adding a number of passes in short succession would cause a build up of hydrogen. Also it would make it more difficult for the hydrogen to escape as it would need to travel further to reach the atmosphere. The more weld metal deposited in a single pass the greater the hydrogen content in the near weld region because the hydrogen has to travel further to escape.

6.5 CONCLUSION

The investigation into transient hydrogen concentration has highlighted two points. Firstly, it is generally recognised that in order to move toward using X80 or higher strength materials factors such as pre-heating or post-heating of the material need to be considered. It is therefore interesting to see the effectiveness of this approach in rapidly reducing hydrogen concentration. Pre-heating of the near weld region appears to be the most appropriate and effective method of reducing hydrogen in the near weld region when using cellulosic electrodes.

Secondly, the requirement that the hot pass be added within a certain time constraint does not appear to be related to its influence on the hydrogen concentration. It is most likely that the benefit in controlling the dwell between root and hot pass welds would be in terms of reduction in residual stress and material hardness.

Chapter 7

TRANSIENT HACC RISK

Pipeline construction procedures are primarily governed by how the speed of front end construction can be maximised. However the timing of the various processes involved in construction also influence the residual stress as demonstrated in Chapter 5. Using a typical pipeline construction procedure the variation of the risk of HACC with time has been investigated in this chapter.

It has been reported in AS 2885.2-2002 that HACC is most likely to occur several minutes after welding during pipeline construction which is in contrast to low hydrogen welding processes in which it is most likely to occur after several hours. An explanation of this phenomena is offered in this chapter and recommendations are given to avoid HACC based on the timing of the process.

7.1 EVOLUTION OF STRESS, TEMPERATURE AND HYDROGEN

In order to understand the transient risk of HACC the evolution of the stress, temperature and hydrogen concentration need to be considered in unison. These factors have been calculated for a typical girth weld using the techniques described in this thesis and are shown in Figure 7.1. It should be noted that the transient stress reaches its maximum and final residual stress when the temperature reaches ambient. It can also be seen that the temperature and stress reach constant values well before the hydrogen concentration.

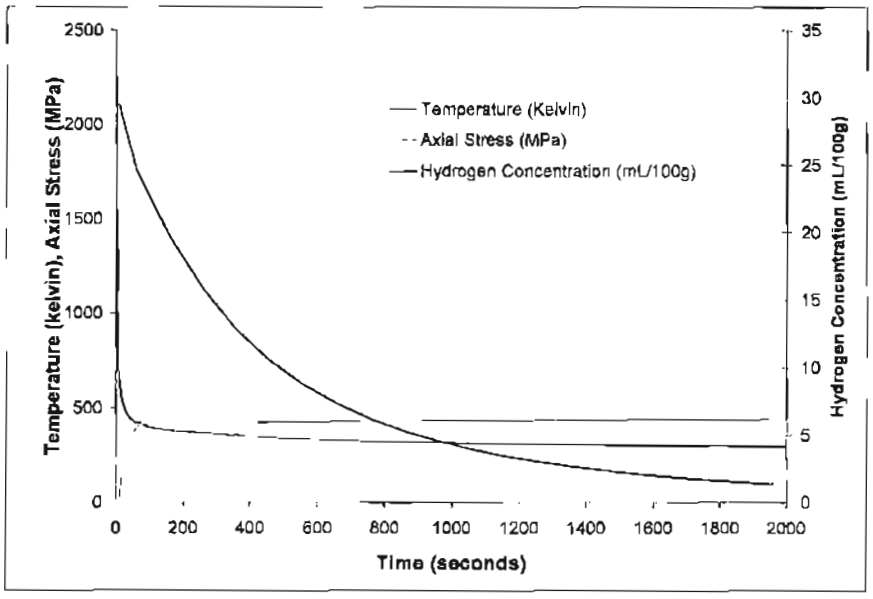

Figure 7.1: Typical transient stress, temperature and hydrogen concentration in the root pass of a pipeline girth weld.

7.2 TRANSIENT HACC RISK

In order to gain a general understanding of the transient risk of HACC it was assumed that the risk was related to stress, temperature and hydrogen concentration in the manner shown in Equation 7.1, which was developed by the author of this thesis. This allowed a conceptual understanding to be developed which coincides with past experience with HACC in pipeline girth welds. A schematic diagram of the transient risk of HACC for pipeline welding and for low hydrogen welding processes based on Equation 7.1 is given in Figure 7.2.

$$Risk \sim \frac{Stress \times Hydrogen}{Temperature} \tag{7.1}$$

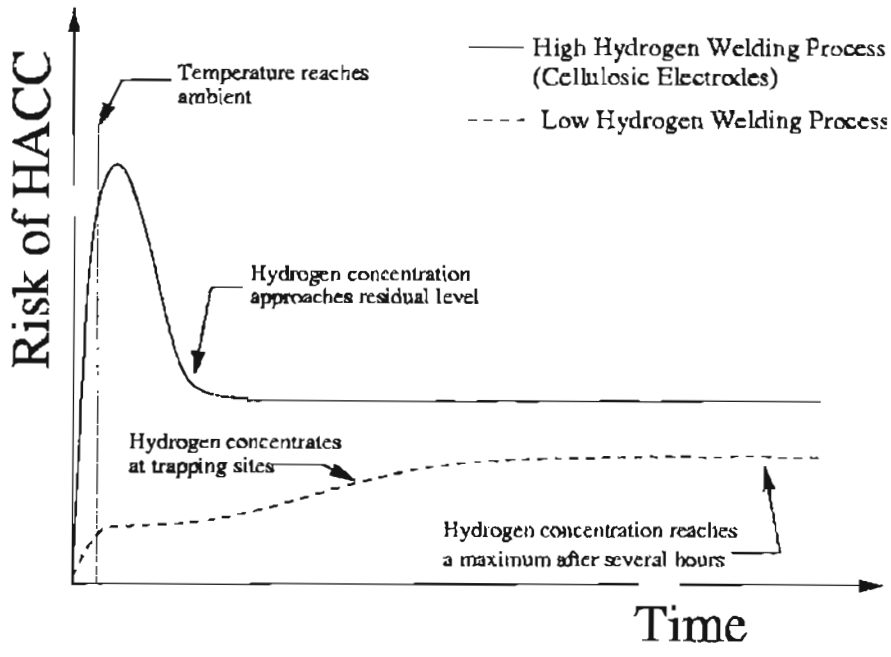

Figure 7.2: Schematic diagram showing the transient risk of HACC.

It is known that in order for HACC to occur the temperature of the material must fall to below 50°C (Kobayashi and Aoshima, 1971). It is also known that the residual stress is also not developed fully until the temperature falls to ambient. Once the temperature has fallen to ambient (several minutes after welding) the residual stress stays constant. The hydrogen however still diffuses out of the material.

Pipeline construction generally uses cellulosic electrodes due to the high productivity and robust nature of the process. Cellulosic welding is a high hydrogen process and the weld metal is saturated in hydrogen after welding. Due to this saturation of hydrogen, HACC generally occurs several minutes after welding as compared with low hydrogen welding processes where HACC occurs several hours after welding (Fletcher and Yurioka, 2000).

It can be seen in Figure 7.2 that the time when HACC is most likely to occur is when the material first reaches ambient temperature and the residual stress reaches its maximum and residual level. After several hours the majority of the hydrogen gas diffuses out of the material leaving only the residual hydrogen trapped in voids and stress concentrations. This leaves the material with a residual HACC risk.

Contrast the previously described trend with that of low hydrogen electrodes, in which the hydrogen that is introduced into the material is in a low concentration. Once again the material reaches ambient temperature and the residual stress reaches its maximum and final level several minutes after welding. However the hydrogen diffusing through the material

collects at 'hydrogen traps' and increases in concentration in localised areas until it reaches a maximum after several hours. At this time the risk of HACC reaches its maximum. The residual HACC risk for cellulosic electrodes is greater than for low hydrogen electrodes because the residual hydrogen level is greater.

7.3 INFLUENCE OF HOT PASS ON THE RISK OF HACC

It is generally accepted that the application of a hot pass reduces the risk of HACC when welding pipelines. In the Australian Standard, Pipelines - Gas and liquid petroleum AS 2885.2-2002 it is stated, "*Delays of more than about 6 minutes between the completion of the root pass and the deposition of the hot pass greatly increase the risk of HACC occurring.*" The reasons given for this reduced risk are that, "*the hot pass increases the weld throat thickness, reduces the notch effect strain concentration in the wagon track region, refines and tempers the microstructure, and most importantly raises the temperature of the weld cooling rate to enhance hydrogen effusion.*"

The schematic diagram given in Figure 7.2 is modified in Figure 7.3 to demonstrate the transient risk of HACC with the addition of a hot pass with a delay time of less than 6 minutes. By adding a hot pass, immediately the risk of HACC is reduced as the temperature of the material is raised above 50°C where HACC is reported not to occur (Suzuki and Yurioka, 1986). This reduction in risk of HACC immediately after application of the hot pass is shown in Figure 7.3.

Once the material cools again however tensile residual stresses increase in the near weld region. The hot pass weld metal is saturated with hydrogen from the cellulosic electrodes which diffuses into the surrounding HAZ and root pass weld metal. A peak risk of HACC

once again occurs several minutes after welding of the hot pass and a residual risk is reached several hours after welding as shown in Figure 7.3.

However, the level of risk is much lower than it would have been with a root pass only. The reduced risk is due to the residual stresses in the root of the weld being reduced by the application of the hot pass. This is supported by Radaj (1992) who states that, "*the longitudinal residual stresses of the layers deposited first are relieved, however, by the layers placed over them*" (Radaj, 1992 pp. 260).

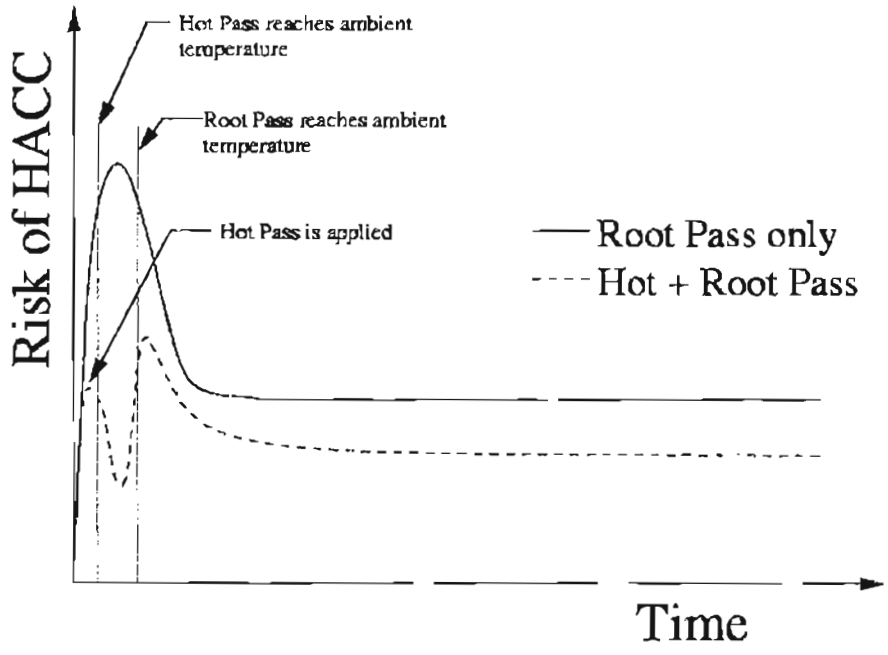

Figure 7.3: Schematic diagram showing the transient risk of HACC when a root pass is laid and for when a root and hot pass are laid for a high hydrogen welding process.

7.4 SUMMARY

By understanding the transient risk of HACC it can be seen that factors such as the timing of the lifting of the pipeline front end are important. Generally the lift occurs almost immediately after welding while the material is at an elevated temperature. This is an appropriate time for lifting to occur but if it was to occur several minutes after the root pass was completed when it reached room temperature the lifting of the front end would increase the potential for HACC.

To summarise the methods available for the reduction of HACC risk while using cellulosic electrodes the following statement can be made:

- Reduce the tensile residual stresses in the material.
- Slow the cooling rate to increase the rate of hydrogen diffusion and reduce the hardness of the material.
- Avoid applying loads to the welds during times of high HACC risk.

Chapter 8

DISCUSSION AND CONCLUSIONS

8.1 DISCUSSION

The cost of building a pipeline is strongly related to:

- the strength of the pipe material. Using higher strength pipe material with thinner walls can provide a material saving of up to one third if moving from say X65 to X100.
- the forward pace of front end construction, which is a major determinant of construction cost.

Both of these cost saving measures can potentially increase the likelihood of HACC so a greater understanding of the influence of various process parameters is needed.

An efficient modelling procedure has been developed in this study, which can simulate the stress cycle endured by a girth weld during construction. The model has been experimentally verified using the 'Blind Hole Drilling' method of residual stress measurement. A variety of different process variables have been investigated. This highlighted the risk factors and potential areas for greater efficiency.

The evolution of temperature, stress and hydrogen concentration was calculated for a typical pipeline construction procedure. This enabled an understanding of the transient risk of hydrogen assisted cracking to be developed. The importance of the timing of events was demonstrated, the critical events were revealed and explained with the aid of science rather than anecdotal evidence.

Cellulosic electrodes are generally used for welding of pipelines in Australia. This is due to the ability to weld at high speeds and the addition of alloying elements in the flux create desirable running characteristics and material properties. Cellulosic electrodes however introduce a high concentration of hydrogen into the weld metal. Fick's second law of diffusion was used to model the hydrogen diffusion due to the welding process.

8.1.1 Pipeline Construction Modelling

The stress cycle in the girth weld during front end pipeline construction has been modelled in a complete, time dependant manner allowing for the effects of material non-linearity. This incorporates simulation of both thermal and mechanical effects in 3D, and considers all elements of construction thought to influence the transient stress in the girth weld.

Calculating the stress induced in a weld due to the welding thermal cycle is a computationally intensive process. It is not economically feasible to model the effect of the lifting and lowering process with three pipe lengths (which are required to simulate lifting)

and include the effect of the welding thermal cycle. To combat this problem a sub-modelling technique was developed to simulate the affect of lifting and lowering the pipeline front end on the near weld region.

Goldak's (1985) double ellipsoidal heat source was modelled, passing around the girth in a transient manner to calculate the temperature cycle induced due to welding. An external program was written to transfer the temperature history from a fine first order mesh as used in the heat transfer model to a coarse second order mesh as used in the stress analysis model. Mesh refinement and grading allowed an efficient model to be set up for analysis of numerous process parameters as described in Chapter 5. Complex non-linear material properties including the effect of transformation plasticity were allowed for in the modelling procedure.

A preliminary investigation into the effect of lifting of the pipeline front end was carried out. The lifting process appeared to have a detrimental effect on the residual stress induced into the girth weld when an 'extreme' lift of 600mm was carried out, however a lift of 1200mm appeared to relieve some of the residual stress. This relief is due to additional plastic deformation induced into the root pass during lifting. This result is dependant on numerous other parameters however, such as the strength of the material, the electrodes used, the geometry of the pipe and the timing of the lift. These other parameters are considered in Chapter 5.

The operation of the line up clamp was also simulated in the construction model developed. This was achieved by simulating an internal pressure inside the pipe in the region where the line up clamp is applied. The pressure that was used was estimated using a schematic diagram of a typical line up clamp and knowledge of the pneumatic pressure used to actuate it. It was found that provided no weld mismatch occurs during welding, the line up clamp has no influence on the residual stress induced in the root pass.

8.1.2 Experimental Verification Issues

The 'Blind Hole Drilling' measurement technique and the finite element models have demonstrated consistent residual stress results. They gave confidence that the numerical modelling scheme developed is capable of investigating pipeline construction.

Some measurements indicated that the residual stress exceeded the yield strength of the material, which was measured to be 525MPa in tensile tests. It is not likely that the residual stress will significantly exceed the yield strength of the pipe since the material will deform plastically. This is a problem with this measurement technique that was outlined by Weng and Lo (1992) and Beghini et al (1998). When measuring residual stress which is greater than 50% of the yield strength of the material, localised plasticity effects in the material cause inaccuracies in measurement. Beghini et al (1998) found that when the stress exceeds 50% of the yield strength the calibration coefficients increase non-linearly. The UM rosette as

used in this study was found to be more sensitive to the effects of local plasticity than the RK rosette used by Weng and Lo (1992).

The experimental results corrected using the technique suggested by Weng and Lo appears to agree with the numerical results better than those corrected using the technique suggested by Beghini et al (1998) despite the fact that the effect of biaxiality was not accounted for. This is also highlighted by the fact that the results produced by the Beghini et al (1998) technique exceed the yield strength of the material. This obvious inaccuracy is most probably due to the strain gauge rosette not being aligned with the residual stress field. Without knowing the direction of the residual stress prior to measurement inaccuracy of up to 20% should be expected with the Beghini et al (1998) technique.

Each measurement of residual stress was made at varying depths to determine the variation of residual stress with depth. Ideally the residual stress field would not vary with depth as inaccuracies are introduced when they do. The measurements made further away from the weld centre line appeared to vary significantly with depth. This is predominately due to the fact that there is a constant amount of noise in the measurements and when the measurements are smaller the amount of error is proportionally greater. Measurements made closer to the weld centre line appeared to vary with depth to a more acceptable level.

Welding residual stress fields in cylinders are known to vary with depth, typically with a tensile stress on the inside wall and a compressive stress on the outside wall of the cylinder.

The results achieved therefore are reasonably accurate considering the limitation of this method.

The closest measurement to the weld centre line was made at 5mm. It was not possible to take measurements directly on the weld centre line as the weldment re-enforcement must firstly be ground off which results in an altered residual stress field. 20mm and further away from the weld centre line the variation of stress with depth increases. The greater consistency of residual stress with depth gave increased confidence in the results close to the weld centre line which is the area of interest. Further away from the weld centre line the residual stress approaches zero so accuracy in this region is less important.

8.1.3 Residual Stress

The pipeline construction process has many variables which influence the tendency for HACC and pipeline construction cost. The important ones were identified and investigated in relation to their influence on the residual stress produced in the root pass of a girth weld in Chapter 5. The modelling scheme developed is capable of analysing any given set of process parameters. Trends were investigated while considering individual process parameters.

The manner in which the residual stress develops was observed by consideration of the transient stress. As the transient stress develops into a residual stress the weld metal is

cooling toward ambient temperature. While at an elevated temperature the material is more susceptible to mechanical handling loads altering the residual stress.

The predictions of the resulting stress due to the welding thermal cycle cannot be expected to achieve high levels of accuracy. The level of agreement that can be expected was demonstrated in Chapter 4 using the 'Blind Hole Drilling' method of residual stress measurement. The manual metal arc welding process however is far from perfectly consistent in terms of welding speed, heat input and other parameters. Due to this variability it would be pointless to develop a scheme capable of modelling the perfect process as this would be unachievable in reality. Instead a model capable of observing trends due to process parameters has been created and used with success by the author of this thesis.

It was found that the resultant residual stress field in a pipeline girth weld is influenced not only by the process parameters but also their timing. Factors such lifting of the pipeline front-end before welding of the root pass can have a significant effect on the residual stress. However if the weld is allowed to cool for only a few seconds, the weld develops enough strength to endure typical lift heights (300-600mm) with only a small increase in tensile residual stress in the root pass.

It was also shown that the tensile residual stress in the root pass can be reduced by lifting of the pipeline front end. This relief of tensile residual stress was achieved by plastically deforming the material while still at an elevated temperature. However in order to create the

required circumstances needed to achieve this relief of residual stress, impractical lift heights were required. As lift heights become greater the force required to lift the pipeline also becomes greater since more and more of the pipeline is lifted off supports. This method would also require very strict timing of the process to ensure that failure of the weld did not not occur during the stress relief process.

It is interesting to explore the possibilities for alteration of the construction process as a number of opportunities have been demonstrated. Not all opportunities are feasible, however a number of recommendations are given later in Section 8.3.

8.1.4 Hydrogen Diffusion

As higher strength pipe material such as X80 is used factors such as pre-heat and post-heat will become increasingly important. The use of pre-heat or post-heat will slow the cooling of the HAZ, reduce hardness, as well as reducing the concentration of hydrogen. Pre-heating is used during pipeline construction in some countries due to the low ambient temperatures that exist. In Australia pre-heat is not currently required to achieve appropriate HAZ hardness nor to avoid HACC. As the industry moves toward the use of higher strength pipe such as X80 the use of pre-heat may become critical.

In the United Kingdom specialised equipment is used to pre-heat the pipe. It has been shown in Chapter 6 that post-heat, which could be simply applied using flame torches, also can

achieve a significant increase in hydrogen diffusion. The use of pre-heat however has the added benefit of increasing the $T_{8/5}$ cooling time (time taken for material to cool from 800°C to 500°C). This will result in a lower hardness and therefore a lower susceptibility to HACC. Post-heating has the effect of tempering the near weld region however it does not affect the $T_{8/5}$ cooling time.

In most pipeline construction procedures there is a requirement that the hot pass is laid after the root pass within a certain time constraint. This constraint is designed to reduce the risk of HACC. The reasons given in the Australian Standard, Pipelines - Gas and liquid petroleum, for the risk reduction are that, "*the hot pass increases the weld throat thickness, reduces the notch effect strain concentration in the wagon track region, refines and tempers the microstructure, and most importantly raises the temperature of the weld cooling rate to enhance hydrogen effusion*" (AS 2885.2, 2002 pp.104). It was shown in this present work that by laying a hot pass, the rate of hydrogen diffusion was increased by a small but insignificant amount, however the hydrogen content was increased. This would suggest that any reduction in HACC risk obtained by the application of a hot pass is not due to an enhanced hydrogen effusion.

8.1.5 Transient Risk of HACC

In the past anecdotal evidence was used to avoid times of high risk when performing operations such as lifting the pipeline front end. Through this present investigation, a good

understanding of the evolution of stress, temperature and hydrogen concentration that occurs during pipeline construction has been developed. With this understanding a view of the transient risk of HACC that occurs during pipeline construction has also been developed. This allowed schematic representation of the transient HACC risk.

8.2 CONCLUSIONS

First Model of Stress Evolution During Pipeline Construction

The first model published capable of simulating the stress evolution experienced in the root pass of a pipeline girth weld during construction has been created. The root pass is of critical importance in relation to the likelihood of HACC as it is at the root of the weld where tensile residual stress is induced due to the welding thermal cycle. This tensile stress is the driving force behind HACC. Subsequent passes have the effect of reducing some of the residual stresses and tempering the material.

Experimentally Validated

This research has demonstrated the level of agreement achieved between the numerical model produced and the 'Blind Hole Drilling' method of residual stress measurement. It has taken into account the problems experienced in relation to stress varying with depth such as occurs in welding residual stress fields, which is a source of error when using the 'Blind Hole Drilling' method. The effect of localised plasticity also had to be allowed for in the situation where the residual stress exceeded 50% of the yield strength of the material. It was found that the modelling scheme developed was capable of making reasonable predictions of residual stress.

Construction Parameters

Construction parameters were analysed using the model developed with respect to their influence on the transient and residual stress. This highlighted trends to be expected when altering construction parameters. It was found that:

- Lifting of the pipeline front end with 'normal' and 'extreme' lifts will result in an increased tensile residual stress, however the increase is only in the order of 5-10% when using X70 pipe, 300mm in diameter, 6mm in wall thickness with 12m lengths.
- Lifting of the pipeline front end during construction will increase the residual stress unless it results in enough plastic deformation to relieve some of the stresses. For the above pipe only extreme lifts could generate this level of plastic deformation.
- Additional plastic deformation can be produced in the root pass without lifting the pipeline higher by: using lower strength material; lifting earlier while the material is at a higher temperature; reducing the proportion of the root pass completed; or altering the section modulus by changing the welding start and stop positions.
- The lifting of the front end can be conducted immediately after welding of the root pass without adversely affecting the residual stress.
- Provided no weld mismatch occurs the line-up clamp has no effect on the residual stress.
- Completing as little as 25% of the root pass before lifting will not adversely affect the residual stress in the root pass, provided the top and bottom portions of the girth are welded and no weld mismatch occurs.
- Using greater heat input results in higher residual stress.

- An electrode which has a higher deposition rate for a given heat input will produce a lower residual stress.
- Residual stress approaches the yield strength of the material, so the stronger the material being welded the greater the resulting residual stress.
- Similarly, higher strength electrodes result in a greater residual stress.
- The greater the diameter to wall thickness ratio the lower the resulting residual stress.

Hydrogen Diffusion

- Pre-heating and Post-heating dramatically increase the rate of hydrogen diffusion.
- The hot pass increases the temperature of the root pass, thereby increasing the rate of diffusion. The hot pass however also introduces more hydrogen into the material and traps the hydrogen in the root pass, preventing it from escaping quickly as the path it has travel to reach the atmosphere increases.
- The reduction of HACC risk resulting from adding a hot pass as reported in AS 2885.2-2002 is not related to reduced concentration of hydrogen.

Transient HACC risk

The transient temperature, stress and hydrogen diffusion have been calculated for a typical pipeline construction procedure. By understanding the evolution of these parameters a transient risk of HACC has been suggested:

- The highest risk of HACC occurs when the material reaches ambient temperature and the residual stress is fully developed. This occurs several minutes after welding of the root pass.
- A residual HACC risk is reached several hours after welding when the hydrogen concentration reaches a residual level.

8.3 RECOMMENDATIONS TO PIPELINE INDUSTRY

Reduce Risk of HACC

- Lifting and other mechanical loads to be applied to the pipe during construction should be carried out before the temperature in the root pass falls to ambient. This is because the maximum risk of HACC occurs after the near weld region reaches ambient temperature as explained in Chapter 7.
- The hot pass should be laid before the temperature of the root pass falls to ambient. By doing this, some of the residual stresses in the root pass will be relieved and it will prevent the maximum level of HACC risk being reached.
- The welding should be carried out by two welders working simultaneously. The sections of the girth welded should include the 6 o'clock and 12 o'clock positions. This will reduce the stresses induced in the root pass due to the lifting and lowering process.
- When welding the root pass a low heat input should be used with an electrode that produces a high deposition rate for a given current. This will result in a lower residual stress in the root pass than would otherwise be achieved.
- The root pass should be welded with a lower strength electrode than the capping passes. By using a lower strength electrode for the root pass will reduce the residual stress at the root of the girth weld which is typically where the tensile residual stresses occur.

- A lift height for the pipeline front end should not exceed 1m to prevent adversely affecting the residual stress. This requirement is based on a typical pipeline and will obviously vary depending on the pipeline sizes and grades used.
- When the use of high strength pipe material increases the risk of HACC to an unacceptable level, pre-heating of the root pass should be used.

Increase Forward Pace of Construction

- Lifting of the pipeline front end should be carried out shortly after welding of the root pass. It was shown in Section 5.2.4.3 that after a short period (15 seconds) after welding the residual stress would not be adversely affected by lifting the pipeline front end. Therefore to maximise the forward pace of construction lifting should take place shortly (15 seconds) after welding.
- Only 50% of the root pass should be completed before lifting of the front end. The 6 o'clock and 12 o'clock positions of the root pass should be welded. Welding 50% of the root pass is adequate to prevent any weld mismatch after removal of the line-up clamp and will not result in an increased residual stress in the root pass as shown in Section 5.2.4.4.
- The line-up clamp should be removed immediately after welding of the root pass and placed at the new pipeline front end. This is because the line up clamp is not required to counter the lifting stresses induced in the pipeline front end.

8.4 SIGNIFICANCE OF WORK

This research has shown it is possible to develop 3D models of pipeline construction using currently available computer technology and to use such models to analyse the stress induced during the pipeline construction process.

This work has shown that the final state of residual thermal stress is influenced by the lifting and lowering of the pipeline front end. Previously it was assumed that the lifting process only altered the stress induced in the girth weld during the lifting and lowering process (Higdon et al, 1980). In contrast to this notion it has been shown that under some circumstances the lifting process can be used to relieve welding residual stresses.

This work has determined the influence of a large number of process parameters on transient stress in the weld during construction. While certain parameters have been considered by researchers in the past, this is the first time a large number of parameters have been tested using the same model. This indicated trends and the relative importance of the various parameters.

The hydrogen diffusion due to pipeline welding was modelled which allowed a transient view of temperature, stress and hydrogen concentration for a typical pipeline construction procedure. A discussion on the transient HACC risk based on these factors is provided.

8.5 FUTURE WORK

In this work, the residual stress and hydrogen concentration in pipeline welds were considered with a view toward minimisation. Understanding the evolution of residual stress and hydrogen concentration enabled a transient view of the risk of HACC to be constructed. Future work which would be useful would be the development of a model capable of predicting when cracking is likely to occur by relating the residual stress, microstructure and hydrogen concentration to experiments where cracking has occurred.

REFERENCES

Anderson B.A.B (1978) *Thermal Stresses In A Submerged Arc Welded Joint Considering Phase Transformation.* Journal of Engineering Materials and Technology. Trans AMSE vol. 100

Anderson B.A.B. (1980) *Diffusion and Trapping of Hydrogen in a bead on plate weld.* Journal of Engineering Materials and Technology, vol. 102

ASTM (American Society for Testing Materials) (2003) *Standard Test Method for Determining Residual Stresses by the Hole Drilling Strain-Gauge Method.* ASTM Standard E837-01, Philadelphia, Pa.

Australian Standard (2002) *Pipelines - Gas and liquid petroleum* AS 2885.2-2002.

Bailey, N., Coe., Gooch T.G., Hart P.H.M., Jenkins N. and Pargeter R, J. (1993) *Welding Steels Without Hydrogen Cracking.* Book. Second Edition. Publ: Abington, Cambridge CB1 6AH, UK; Abington Publishing.

Beaney, E. M. and Procter, E. (1974) *A critical evaluation of the centre hole technique for the measurement of residual stresses.* Strain, vol. 10, no. 1, pp. 7-14.

Beghini, M., Bertini, L. and Vitale, E. (1994) *Fatigue crack growth in residual stress fields: experimental results and modelling.* Fatigue Fract. Eng. Mater. Struct., vol. 17, no. 12, pp. 1433-1444.

Beghini, M. and Bertini, L. (1998) *Recent advances in the hole drilling method for residual stress measurement.* Journal of Materials Engineering and Performance (USA), vol. 7, no. 2, pp. 163-172.

Boellinghaus T., Hoffmeister H. and Schubert C. (1995) *Finite Element Analysis of Hydrogen Diffusion in Butt Joints.* Trends in Welding Research, Proceedings of the 4th International Conference.

Boellinghaus, T. and Hoffmeister, H. (2000) *Numerical model for hydrogen-assisted cracking.* Corrosion (USA), vol. 56, no. 6, pp. 611-622

Brady, G.S., Clauser, H.R. and Vaccari, J.A (2002) *Materials handbook: An encyclopedia for managers, technical professionals, purchasing and production managers, technicians, and supervisors.* McGraw-Hill, Inc.

British Standard PS/P2 (1974) *Specification for Field Welding of Steel Pipelines for High Pressure Gas Transmission.*

Brust, F.W. and Kanninen, M.F. (1981) *Analysis of Residual Stresses in Girth Welded Type 304 Stainless Steel Pipes* ASME Journal of Materials in Energy Systems, vol. 3, no. 3.

Burst, F.W. and Stonesifer, R.B. (1981) *Effect of Weld Parameters on Residual Stresses in BRW Piping Systems.* Electric Power Research Institute, Inc., Palo Alto , Calif., NP-1743.

Carslaw, H. S. and Jaeger, J. C. (1947) *Conduction of Heat in Solids.* O. U. P., pp. 219.

Cerjak, H., Enzinger, N. (1998) *The development of residual stresses due to welding.* ASM International, Trends in Welding Research (USA), pp. 937-942.

Chandra, U. (1985) *Determination of residual stresses due to girth-butt welds in pipes.* Transactions of the ASME, Journal of Pressure Vessel Technology, vol.107, no. 2, pp. 178-184.

Cheng, W. and Finnie, L. (1985) *A method for measurement of axisymmetric axial residual stresses in circumfrentially welded thin walled cylinders.* Journal of Engineering Materials and Technology, 107, pp. 181-185.

Chew, B. and Kyte W.S. (1975) *Diffusion of hydrogen in fillet welds.* Metals Technology, vol. 2, no. 2, pp. 66-72.

Chipperfield, C. (2002) Private conversation.

Chong, L.M. (1982) *Predicting Weld Hardness.* M.Eng.Thesis, Department of Mechanical and Aeronautical Engineering, Carleton University, Ottowa, Canada

Chrenko, R.M. (1978) *Weld Residual Stress Measurement on Austenitic Stainless Steel Pipes.* Weldments: Physical Metallurgy and Failure Phenomena. Proceedings, 5th Bolton Landing Conference, General Electric Corporate Research and Development Centre, Lake George Conference, pp. 195-205.

Davies, M.H. (1995) *Numerical Modelling of Weld Pool Convection in Gas Metal Arc Welding.* PhD Thesis, University of Adelaide, Australia.

Dike, J.J., Ortega, A.R., Cadden, C.H., Rangaswamy, P. and Brown, D. (1998) *Finite element modelling and validation of residual stresses in 304L girth welds.* ASM International, Trends in Welding Research (USA), pp. 961-966.

Dong ,Y., Hong J.K., Tsai C.L. and Dong P. (1997) *Finite element modelling of residual stresses in austenitic stainless steel pipe girth welds.* Welding Journal, vol.76, no.10, pp. 442-449.

Dong, P., Hong J.K., Zhang J., Rogers P., Bynum J. and Shah S., (1997) *Effects of repair weld residual stresses on wide-panel specimens loaded in tension.* ASME, vol. 347, pp. 125-139.

Dong, P, (2001) *Residual stress analyses of a multi-pass girth weld: 3-D special shell versus axisymmetric models.* Battelle Memorial Institute, Journal of Pressure Vessel Technology (Transactions of the ASME) (USA), vol. 123, no. 2, pp. 207-213.

Easterling K. (1992) *Introduction to the Physical Metallurgy of Welding.* Oxford [England]; Boston : Butterworth-Heinemann.

Edwards, L., Dutta, M; Fitzpatrick, M.E. and Bouchard P.J. (1998) *Direct measurement of residual stresses at a repair weld in an austenitic steel tube.* Integrity of High-Temperature Welds. Proceedings, International Conference, Nottingham, pp.181-191.

Ellingson, W.A. and Shack W.J. (1979) *Residual Stress Measurements on Multi-pass Weldments of Stainless-steel Piping.* Experimental Mechanics, pp. 317-323.

Enzinger, N. and Cerjak, H. (1998) *On the Development of residual stresses in a circumfrential butt joint.* Mathematical Modelling of Weld Phenomena, vol. 4, pp 669-678.

Fletcher, L. and Yurioka, N. (2000) *A Holistic Model of Hydrogen Cracking in Pipeline Girth Welding.* Welding in the World, vol. 44, no. 2, pp. 23-30.

Friedman, E. (1975) *Thermomechanical Analysis of the Welding Process Using the Finite Element Method.* ASME Journal of Pressure Vessels and Piping. Paper no. 75-PVP 27.

Glover, A. and Rothwell, B. (1999) *Specifications and Practises for Hydrogen Crack Avoidance in Pipeline Girth Welds.* Proc WTIA "First International Conference on Weld Metal Hydrogen Cracking in Pipeline Girth Welds," Wollongong, Australia.

Goldak, J., Chakravarti, A. and Bibby, M. (1984) *A new Finite Element Model For Welding Heat Sources.* Metallurgical Transactions B, vol. 15B, pp. 299.

Goldak, J., Chakravarti, A. and Bibby, M. (1985) *A Double Ellipsoid Finite Element Model for Welding Heat Sources.* IIW Doc 212-603-85.

Goldak, J. and Zhang, C.(1991) *Computer Simulation of 3D-Hydrogen Diffusion of Low Alloy Steel Weld.* IIW Doc. IX-1662-92.

Hart, P.H.M. (1999) *Hydrogen Cracking - Its Causes, Costs and Future Occurance.* Proc WTIA "First International Conference on Weld Metal Hydrogen Cracking in Pipeline Girth Welds" Wollongong, Australia.

Higdon, H.I., Weickert, C.A., Pick, R.J. and Burns, D.J. (1980) *Root Pass Stresses in Pipeline Girth Welds Due to Lifting.* Conference proceedings "Pipeline and Energy Plant Piping - Fabrication in the 80's", Calgary, Pergamon.

Henderson, I.D., Krishan, K.N. and Cantin, D. (1996) *Investigation of Field Welding Practise Limits for Girth Welding of Thin-Walled, High-Strength Pipes.* Final Report on CRC Project 96.32.

Hong, J.K., Tsai, C.L. and Dong, P. (1998) *Assessment of Numerical Procedures for Residual Stress Analysis of Multipass Welds.* Welding Journal, vol.77, no.9, pp.372-382.

Jonsson, M. and Joesfson, B.L. (1988) *Experimentally determined transient and residual stresses in a butt-welded pipe.* Journal of Strain Analysis, vol 23, no.1.

Josefson, B. L. (1985) *Effects of transformation plasticity on welding residual stress fields in thin walled pipes and thin plates.* Materials Science and Technology, pp. 904-908.

Josefson, B.L. (1982) *Residual Stresses and Their Redistribution During Annealing of a Girth Butt Welded Thin-Walled Pipe.* Journal of Pressure Vessel Technology, vol. 104, pp. 245.

Karlsson, L. (1986) *Thermal stresses in welding.* Thermal Stresses I. Mechanics and Mathematical Methods Handbook. 2nd Series, Thermal Stresses, Ed: R.B.Hetnarski. Publ: 1000BZ Amsterdam, Netherlands; Elsevier Science Publishers B.V.; ISBN 0-444-87728-2.

Karlsson, C.T. (1989) *Finite Element Analysis of Temperatures and Stresses in a single-pass butt-welded pipe - influence of mesh density and material modelling.* Eng. Comput, vol.6.

Karlsson, R.I. and Josefson, B.L. (1990) *Three dimensional finite element analysis of temperatures and stresses in a single -pass butt-welded pipe.* Journal of Pressure Vessel Technology, vol.112, pp. 76-84.

Kikuta, Y., Ochiai, S.I. and Horie, J. (1980) *Computer Simulation of Hydrogen Redistribution Behaviours in Weldment.* Transaction from the Japan Welding Society, vol 2.

Kobayashi, T. and Aoshima, I. (1971) *Welding Cracks In Low-Alloy Steels.* Proceedings, 1st International Symposium Of The Japan Welding Society. Tokyo, vol. 2.

Krautz, G.W. and Segerind, L.J. (1978) Welding Journal Research Supplement, vol. 57, pp. 211-16.

Krom, A.H.M., Maier, H.J., Koers, R.W.J. and Bakker, A. (1999) *The effect of strain rate on hydrogen distribution in round tensile secimens.* Material Science and Engineering, pp. 22-30.

Kufner, A. (2003) *Relationship Between Hollow Bead Defects and Hydrogen Assisted Cold Cracking in the Root Runs of Pipeline Welds.* MSc Thesis, University of Adelaide, Australia.

Li M, Atteridge D.G., Anderson W.E., West S.L. (1993) *Modelling of Residual Stress Mitigation in Austenitic Stainless Steel Pipe Girth Weldment.* Proceedings, International Conference, Orlando

Li, M., Atteridge, D.G., Meekisho, L.L. and West, S.L. (1995) *A 3D Finite Element Analysis of Temperature and Stress Field in Girth Welded 304L Stainless Steel.* Trends in Welding Research, 5-8, Gatlinburg, Tennessee.

Lim, C.H.K., Anami, K. and Miki, CH, (1998) *Evaluation and reduction of welding residual stress.* Structural Engineering & Construction: Tradition, Present and Future. Vol. 3, Taipei, Taiwan, National Taiwan University, Sixth East Asia-Pacific Conference on Structural Engineering & Construction, vol. 3, pp. 1965-1970.

Li, M., Atteridge, DG, Anderson, WE. and West, SL. (1993) *Modelling of residual stress mitigation in austenitic stainless steel pipe girth weldment.* Modelling and Control of Joining

Processes. Proceedings, International Conference, Orlando, FL, 8-10. Ed: T.Zacharia. Publ: Miami, FL 33126, USA; American Welding Society; ISBN 0-87171-440-X, pp. 430-437.

Lin, Y.C. and Perng, J.Y. (1997) *Effect of welding parameters on residual stress in type 420 martensitic stainless steel.* Science and Technology of Welding an Joining, vol. 2, no. 3.

Lincoln Electric Co. (1995) *Procedure Handbook Of Arc Welding Design And Practice*, 13th Edition.

Lindgren, L. and Karlson, L. (1988) *Deformations and stresses in welding of shell structures.* Journal of Numerical Methods in Engineering, vol. 25, pp. 635-655.

Mahin, K.W., Shapiro, A.B. and Hallquist J. (1986) *Assessment of Boundary Condition Limitations on the Development of a General Computer Model for Fusion Welding.* Proceedings: Advances in Welding Science and Technology, ed S.A. David, pub. ASM International, pp. 215-223.

Makhnenko, J.I., Shekera, V.M. and Izbenko, L.A., (1970) *Special Features of the Distribution of Stresses and Strains Caused by Making Circumferencial Welds in Cylindrical Shells.* Autimatic Welding, no. 12, pp. 43-47.

Mangonon, P.L. and Mahimkar, M.A. (1986) *A Three Dimensional Heat Transfer Finite Element Model of the SAW of HSLA Steels.* Proceedings: Advances in Welding Science and Technology, ed S.A. David, pub ASM International, pp. 35-47.

Mansell, D. (1994) *Looking back without anger - revisiting two bridge collapses in Melbourne.* Welding Technology in Action. Proceedings, 42nd National Welding Conference 1994, Melbourne. Publ: Silverwater, NSW 2128, Australia; Welding Technology Institute of Australia. vol.3, Paper 48.

Masubuchi, K. (1981) *Analysis of Welded Structures.* Pergamon Press, International series on Materials Science and Technology, vol. 33.

Mc Dill, J.M.J., Oddy, A.S. and Goldak, J.A. (1992) *Comparing 2D Plane Strain and 3D Analyses of Residual Stresses in Welds.* Proceedings: International Trends in Welding Science and Technology," ed. David, S.A & Vitek, J.M., pub. ASM International, pp. 105-108.

Mc Nabb, F. (1963) *Residual Stress Measurement.* Transactions of the Metallurgical Society of the AIME, 227, pp. 618-627.

Measurements Group Tech Note TN-503-3.

Michaleris, P., Kirk, M. and Laverty, K. (1996) *Incorporation of Residual Stresses into Fracture Assessment Models.* MPC FC-30, Materials Properties Council.

Michaleris, P. (1996) *Residual Stress Distributions for Multipass Welds in Pressure Vessel and Piping Components.* Residual Stress in Design, Fabrication, Assessment and Repair ASME, vol. 327.

Mohr, W.C. (1996) *Internal Surface Residual Stress in Girth Butt-Welded Steel Pipes.* Proceeding of the ASME Pressure Vessel and Pipe Conference, vol. 327, Residual Stresses in Design, Fabrication, Assessment and Repair.

Mohr, W.C., Michaleris, P. and Kirk, M. (1997) *An Improved Treatment of Residual Stresses in Flaw Assessment of Pipes and Pressure Vessels Fabricated From Ferritic Steels.* Fitness for Adverse Enviroments in Petroleum and Power Equipment, ASME, vol. 359.

Myers, P. S., Uyehara, O.A. and Borman, G.L. (1967) *Fundamentals of Heat Flow in Welding.* Welding Research Council Bulletin, New York, NY, no. 123.

Nguyen, N.T., Mai, Y.W. and Ohta, A. (2000) *A new hybrid double-ellipsoidal heat source heat source in semi-infinite body and weld pool simulation.* IIW Asian Pacific Welding Congress. Proceedings, NZIW 2000 Annual Conference and WTIA 48th Annual Conference, Melbourne.

North, T.H., Rothwell, A.B., Ladanyi, T.J., Pick, R.J. and Glover, A.G. (1981) *Full scale field weldability testing of high strength line pipe.* Presented at conference on: "Steels for Line Pipe and Pipeline Fittings", Grosvenor House, London.

Oddy, A.S., Goldak, J.A. and McDill, J.M.J. (1990) *Transformation Effects in the 3D Finite Element Analysis of Welds.* ASM International, pp. 97-101.

Paley, Z. and Hibbert, P.D. (1975) Welding Journal Research Supplement, vol. 54, pp. 385-392.

Pang, H.L. (1989) *Residual stress measurements in a cruciform welded joint using hole drilling and strain gauges.* Strain, vol. 25, no. 1, pp. 7-14.

Pardo, E. and Weckman, D.C. (1990) *The Interaction between Process Variables and Bead Shape in GMA Welding: A Finite Element Analysis.* Proceedings: Recent Trends in Welding Science and Technology, ed S.A. David and J.M. Vitek, pub. ASM International, pp 391-397.

Pavelic, v., Tanbakuuchi, R., Uehara, O.A. and Myers, P.S. (1969) Welding Journal Reasearch Supplement, vol. 48, pp. 295-305.

Phelps, B. (1977) *Weldability testing of High-Strength Microalloyed Pipeline Steel.* Microalloying 75, 570, New York, Union Carbibe Corp.

Pick, R.J., North, T.H. and Glover, A.G.. (1982) *Full-scale weldability testing of large diameter line pipe*. CIM Bulletin.

Popelar, C.H., Barber, T. and Groom, J. (1982) *A Method for Determining Residual Stress in Pipes*. Journal of Pressure Vessel Technology, vol. 104, pp. 223.

Roberts, O. F. T. (1923) Proc. Roy. Soc., Series A, 104, 604.

Rosenthal, D. (1935) Trans. A.S.M.E., 68, 849 (1946). (See also 2ieme Congres National des Sciences, Brussels,1277).

Rybicki, E.F., Roadabaugh, E.D. and Groom, J.J. (1977) *Residual Stresses in Girth Butt Welds in Pipes and Pressure Vessels*. Final Report to U.S. Nuclear Regulatory Commission. Report NUREG-0376.

Rybicki, E.F., Schmumeuser, D.W., Stonesifer, R.W., Groom, J.J. and Mishler, H.W. (1978) *A Finite Element Model for Residual Stress and Deflections in Girth-Butt Welded Pipes*. Transactions of the ASME, vol. 100.

Rybicki, E.F. and Stonesifer, R.W. (1979) *Finite Element Analysis of Multipass Welds in Piping Systems*. Journal of Pressure Vessel Technology. vol. 101, pp. 149-154.

Rybicki, E.F., McGuire, P.A. and Stonesifer, R.W. (1980) *Applications of Computational Models for Controlling Weld Residual Stresses in BRW Piping.* Seminar on Countermeasures for BRW Pipe Cracking, EPRI Session 3.

Rybicki, E.F., McGuire, P.A., Merrick, E. and Wert, J. (1982) *The Effect of Pipe Thickness on Residual Stress Due to Girth Welds.* ASME Journal of Pressure Vessel Technology, pp. 204-209.

Rybicki, E.F. and Shadley, J.R. (1986) *A Three-Dimensional Finite Element Evaluation of a Destructive Experimental Method for Determining the Through Thickness Residual Stresses in Girth Welded Pipes.* Journal of Eng. Mat. & Tech., vol. 108, pp. 99.

Sabapathy, P.N., Wahab, M.A. and Painter, M.J. (2001) *Numerical methods to predict failure during the in-service welding of gas pipelines.* Journal of Strain Analysis for Engineering Design, vol.36, no.6, pp.611-619.

Scaramangas, A. (1984) *Residual Stresses in Girth Weld Butt Welded Pipes.* Ph.D. Dissertation, University of Cambridge, UK.

Schajer, G.S. (1981) *Application of Finite Element Calculations to Residual Stress Measurements.* Journal of Engineering Material and Technology, vol.103, pp. 157-163.

Smart, R., and Bilston, K. (1995) *Stresses upon Partially Completed Girth Welds During Line-up Clamp Removal and Lowering Off.* WTIA / APIA Panel 7 Research Seminar. Welding high strength thin walled pipelines. Wollongong.

Spiller, K.R. (1970) *Stovepipe Welding.* Metal Construction and British Welding Journal, pp. 439-440.

Suzuki, H. and Yurioka, N. (1986) *Weldability of Line pipe Steels and Prevention of Cracking in Field Welding.* 7th Symposium on Linepipe Research, American Gas Association, Houston.

Sykes, C., Burton, H.H. and Gegg, C.C. (1947) *Hydrogen in Steel Manufacture.* Journal of the Iron and Steel Institute, vol. 156, pp. 155-180.

Tang, M., Huang, L., Meng, F. and Liu, M. (1988) *A Study on Welding Residual Stress Formation During Multilayer Girth Welding of Pipes.* Proceedings, IIW Asian Pacific Regional Welding Congress, and 36th Annual AWI Conference, Hobart.

Tekriwal, P. and Mazumder, J. (1988) *3D Finite Element Analysis of Multi-pass GMAW.* Proceedings; Modelling and Control of Castings and Welding Processes 4, ed. A.F. Giamei and G.J.Abbaschian, pub. Minerals, Metals and Materials Soc. pp. 167-177.

Teng T. and Chang P. (1997) *A study of residual stresses in multi-pass girth-butt welded pipes.* Journal of Pressure Vessels and Piping, vol. 74, pp. 59-70.

Ueda, Y. and Nakacho, K. (1982) *Simplifying Methods for Analysis of Transient and Residual Stresses and Deformations Due to Multipass Welding.* Trans. JWRI, vol. 11, no. 1, pp. 95-103.

Vaidyanathan, S., Todoro, A.F. and Finnie, I. (1973) *Residual Stresses Due To Circumferential Welds.* Transactions Of The Asme, Series H, Journal Of Engineering Materials And Technology, vol. 95, no. 4, pp. 233-237.

Vangi, D. and Ermini, M. (2000), *Plasticity effects in residual stress measurement by the hole drilling method.* Universita di Firenze; Universita di Firenze, Strain (UK), vol. 36, no. 2, pp. 55-59.

Vishay Measurement Group Bulletin B-129 (2000) *Surface preparation for Strain Gauge Bonding.*

Weckman, D.C., Mallory L.C. and Kerr H.W. (1989) *Technique for the Prediction of Average Pool Width and Depth for GTA welds on Stainless Steels.* Zeitschrift fur Metallkunde v80, n7, pp459-468.

Westby, O. (1968) *Temperature Distribution in the Workpiece by Welding.* Department of Metallurgy and Metals Working, The Technical University, Trondheim, Norway.

Weickert, C.A., Pick, R.J. and Burns, D.J. (1984) *The Effect of Welding Residual Stress in Root Pass Welds of Pipelines.* Journal of Pipelines, pp. 267-277.

Wells, A.A. (1953) *The mechanics of notch brittle fracture.* Welding Research (London), 7 (4) 34r-56r.

Weng, C.C. and Lo, S.C. (1992) *Measurement of residual stresses in welded steel joints using hole drilling method.* Materials Science and Technology, vol.8, no.3, pp.213-218.

Yurioka, O. (1980) Asano, IIW-Doc. NO. IX-1161-80.

Zhang, C. and Goldak, J. (1991) *Computer Simulation of 3D-Hydrogen Diffusion of Low-Alloy Steel Weld.* IIW Doc. IX-1662-92.

Zhang, J., Dong, P. and Brust, F.W. (1997) *A 3D composite shell element model for residual stress analysis of multi-pass welds.* 14th International Conference on Structural Mechanics in Reactor Technology.

Zhang, J., Dong, P., Brust, F.W., Shack, W.J., Mayfield, M.E. and McNicl, M. (1998) *Modelling of weld residual stresses in core shroud structures.* Nuclear Engineering and Design, pp. 171-187.

Zhao, H., Shi, Y., Pei, Y., Lei, Y. and Chen, Y. (1996) *On the correction of plasticity effect at the hole edge when using the centre hole method for measuring high welding residual stress.* Strain, pp.125-129.

APPENDICES

A. SIMULATION OF LINE-UP CLAMP

Shown below in Figure A.1 is a schematic diagram of the operation of a typical internal line-up clamp.

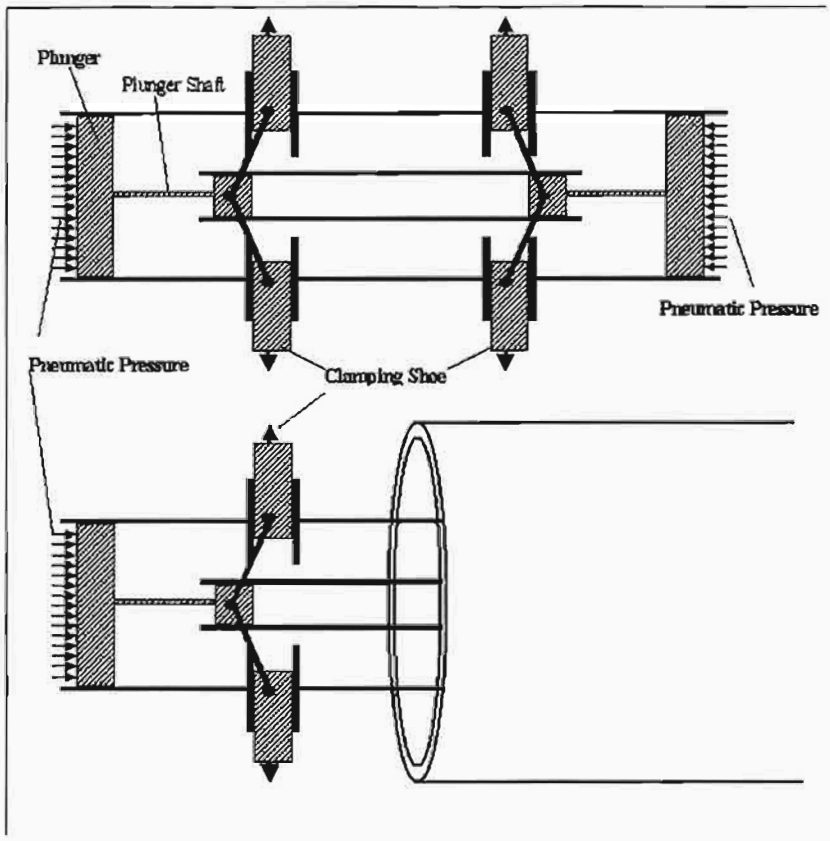

Figure A.1: Schematic diagram of the operation of the internal line-up clamp.

In order to model the effect of the internal line-up clamp, the force applied by the line-up clamp was approximated from the pneumatic pressure of the clamp. The line-up clamp operates approximately 20mm from the weld centre line, which is also where the internal pressure boundary conditions are applied.

The force on the plunger shaft is:

$$F_H = A_P \times P$$

$$= \frac{\pi}{4} D_P^2 \times P$$

$$= 25.77 \text{ kN}$$

where

F_H = Force on line up clamp plunger

A_P = Area of line up clamp plunger

P = Pneumatic pressure

D_P = Diameter of plunger

The clamping force applied to the inside of the pipe can be calculated by resolving the force into the direction normal to the pipe wall.

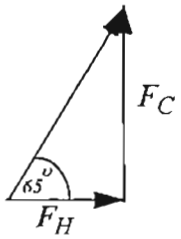

Figure A.2: Vector diagram of forces applied to the inside wall of a pipe by the line-up clamp.

$$F_C = F_H \times \tan(65^o)$$
$$= 53.95 \text{ kN}$$

where

F_C = Clamping force

F_H = Force on line up clamp plunger

By calculating the area over which the force is applied the internal pressure applied to the pipe by the line up clamp can be approximated.

$$A_C = \pi D_i \times W$$
$$= 0.0414 m^2$$
$$P_C = \frac{F_C}{A_C}$$
$$= 3.8 MPa$$

where

A_C = Area over which clamp is applied

D_i = Inside diameter of pipe

W = Width over which clamp is applied

P_C = Clamping pressure

B. BLIND HOLE DRILLING EXPERIMENTAL RESULTS

5mm from weld centre line

Depth	E1	E2	E3	a	b	A	B	Rsmin (MPa)	Rsmax (MPa)	Angle (rads)
0.001	-58	-18	-69	0.027	0.058	-5.8E-04	-9.7E-04	213	539	0.73
0.002	-130	-43	-146	0.072	0.149	-1.6E-03	-2.5E-03	174	438	0.74
0.003	-212	-66	-241	0.101	0.233	-2.2E-03	-3.9E-03	216	502	0.74
0.004	-305	-95	-345	0.139	0.329	-3.0E-03	-5.5E-03	229	520	0.74
0.005	-409	-110	-444	0.152	0.387	-3.3E-03	-6.4E-03	281	620	0.76
0.006	-473	-96	-516	0.159	0.424	-3.4E-03	-7.1E-03	304	694	0.76
0.007	-535	-83	-576	0.157	0.445	-3.4E-03	-7.4E-03	347	787	0.76
0.008	-575	-61	-627	0.155	0.457	-3.3E-03	-7.6E-03	376	865	0.76

6.7mm from weld centre line

Depth	E1	E2	E3	a	b	A	B	Rsmin (MPa)	Rsmax (MPa)	Angle (rads)
0.001	-84	-24	-40	0.027	0.058	-5.8E-04	-9.7E-04	200	416	-0.58
0.002	-149	-32	-114	0.072	0.149	-1.6E-03	-2.5E-03	152	432	-0.70
0.003	-222	-44	-169	0.101	0.233	-2.2E-03	-3.9E-03	173	446	-0.70
0.004	-298	-69	-238	0.139	0.329	-3.0E-03	-5.5E-03	182	436	-0.71
0.005	-364	-73	-310	0.152	0.387	-3.3E-03	-6.4E-03	214	498	-0.73
0.006	-433	-79	-354	0.159	0.424	-3.4E-03	-7.1E-03	242	552	-0.72
0.007	-498	-80	-402	0.157	0.445	-3.4E-03	-7.4E-03	286	633	-0.72
0.008	-545	-82	-430	0.155	0.457	-3.3E-03	-7.6E-03	318	689	-0.71

11mm from weld centre line

Depth	E1	E2	E3	a	b	A	B	Rsmin (MPa)	Rsmax (MPa)	Angle (rads)
0.001	-2	-1	-7	0.027	0.058	-5.8E-04	-9.7E-04	11	42	0.48
0.002	-9	-17	-28	0.072	0.149	-1.6E-03	-2.5E-03	28	54	0.08
0.003	-27	-47	-56	0.101	0.233	-2.2E-03	-3.9E-03	52	80	-0.18
0.004	-49	-85	-93	0.139	0.329	-3.0E-03	-5.5E-03	65	98	-0.28
0.005	-71	-133	-127	0.152	0.387	-3.3E-03	-6.4E-03	81	128	-0.44
0.006	-95	-172	-162	0.159	0.424	-3.4E-03	-7.1E-03	103	156	-0.46
0.007	-114	-223	-192	0.157	0.445	-3.4E-03	-7.4E-03	119	193	-0.53
0.008	-121	-241	-212	0.155	0.457	-3.3E-03	-7.6E-03	132	211	-0.51

17.5mm from weld centre line

Depth	E1	E2	E3	a	b	A	B	Rsmin (MPa)	Rsmax (MPa)	Angle (rads)
0.001	0	-10	-1	0.027	0.058	-5.8E-04	-9.7E-04	-31	37	-0.76
0.002	-5	-35	-10	0.072	0.149	-1.6E-03	-2.5E-03	-22	55	-0.74
0.003	-15	-63	-22	0.101	0.233	-2.2E-03	-3.9E-03	-10	69	-0.75
0.004	-24	-88	-35	0.139	0.329	-3.0E-03	-5.5E-03	-3	71	-0.74
0.005	-32	-109	-49	0.152	0.387	-3.3E-03	-6.4E-03	6	80	-0.72
0.006	-41	-137	-58	0.159	0.424	-3.4E-03	-7.1E-03	7	93	-0.74
0.007	-45	-152	-61	0.157	0.445	-3.4E-03	-7.4E-03	8	100	-0.75
0.008	-46	-171	-67	0.155	0.457	-3.3E-03	-7.6E-03	6	110	-0.74

22.5mm from weld centre line

Depth	E1	E2	E3	a	b	A	B	Rsmin (MPa)	Rsmax (MPa)	Angle (rads)
0.001	4	-12	-2	0.027	0.058	-5.8E-04	-9.7E-04	-53	41	-0.67
0.002	0	-36	-16	0.072	0.149	-1.6E-03	-2.5E-03	-23	58	-0.65
0.003	-8	-7	-20	0.101	0.233	-2.2E-03	-3.9E-03	14	30	0.43
0.004	-10	-75	-23	0.139	0.329	-3.0E-03	-5.5E-03	-18	56	-0.73
0.005	-11	-94	-24	0.152	0.387	-3.3E-03	-6.4E-03	-23	60	-0.74
0.006	-13	-108	-26	0.159	0.424	-3.4E-03	-7.1E-03	-24	63	-0.75
0.007	-9	-118	-27	0.157	0.445	-3.4E-03	-7.4E-03	-28	65	-0.74
0.008	-9	-124	-26	0.155	0.457	-3.3E-03	-7.6E-03	-30	66	-0.75

29mm from weld centre line

Depth	E1	E2	E3	a	b	A	B	Rsmin (MPa)	Rsmax (MPa)	Angle (rads)
0.001	-6	-9	-12	0.027	0.058	-5.8E-04	-9.7E-04	43	64	0.00
0.002	-13	-19	-14	0.072	0.149	-1.6E-03	-2.5E-03	22	38	-0.74
0.003	-10	-31	-14	0.101	0.233	-2.2E-03	-3.9E-03	2	36	-0.73
0.004	-11	-34	-15	0.139	0.329	-3.0E-03	-5.5E-03	2	28	-0.74
0.005	-12	-44	-13	0.152	0.387	-3.3E-03	-6.4E-03	-4	30	-0.78
0.006	-11	-47	-13	0.159	0.424	-3.4E-03	-7.1E-03	-5	29	-0.77
0.007	-11	-59	-13	0.157	0.445	-3.4E-03	-7.4E-03	-10	34	-0.77
0.008	-14	-60	-15	0.155	0.457	-3.3E-03	-7.6E-03	-6	36	-0.78

35mm from weld centre line

Depth	E1	E2	E3	a	b	A	B	Rsmin (MPa)	Rsmax (MPa)	Angle (rads)
0.001	2	7	10	0.027	0.058	-5.8E-04	-9.7E-04	-20.9	-50	-0.12
0.002	4	14	18	0.072	0.149	-1.6E-03	-2.5E-03	-13.9	-35	-0.20
0.003	21	10	10	0.101	0.233	-2.2E-03	-3.9E-03	-17.7	-31	-0.39
0.004	31	17	13	0.139	0.329	-3.0E-03	-5.5E-03	-18.9	-32	-0.25
0.005	34	12	15	0.152	0.387	-3.3E-03	-6.4E-03	-17.5	-34	-0.46
0.006	36	15	16	0.159	0.424	-3.4E-03	-7.1E-03	-19.0	-33	-0.42
0.007	38	9	22	0.157	0.445	-3.4E-03	-7.4E-03	-20.2	-41	-0.60
0.008	40	6	21	0.155	0.457	-3.3E-03	-7.6E-03	-19.6	-43	-0.60

64mm from weld centre line

Depth	E1	E2	E3	a	b	A	B	Rsmin (MPa)	Rsmax (MPa)	Angle (rads)
0.001	6	6	-2	0.027	0.058	-5.8E-04	-9.7E-04	-32	8	0.39
0.002	11	18	-7	0.072	0.149	-1.6E-03	-2.5E-03	-30	21	0.53
0.003	3	13	-6	0.101	0.233	-2.2E-03	-3.9E-03	-11	16	0.63
0.004	5	19	-18	0.139	0.329	-3.0E-03	-5.5E-03	-10	25	0.57
0.005	8	24	-14	0.152	0.387	-3.3E-03	-6.4E-03	-12	19	0.59
0.006	13	37	-8	0.159	0.424	-3.4E-03	-7.1E-03	-20	15	0.64
0.007	18	43	-5	0.157	0.445	-3.4E-03	-7.4E-03	-24	11	0.63
0.008	22	51	2	0.155	0.457	-3.3E-03	-7.6E-03	-31	6	0.66

Benchmark Test

Depth	E1	E2	E3	a	b	A	B	Rsmin (MPa)	Rsmax (MPa)	Angle (rads)
0.002	-47	0	3	0.072	0.149	-1.6E-03	-2.5E-03	3	95	-0.36
0.003	-63	-26	-5	0.101	0.233	-2.2E-03	-3.9E-03	27	81	-0.13
0.004	-74	-28	-4	0.139	0.329	-3.0E-03	-5.5E-03	22	68	-0.15
0.005	-82	-22	10	0.152	0.387	-3.3E-03	-6.4E-03	12	64	-0.15
0.006	-80	-12	17	0.159	0.424	-3.4E-03	-7.1E-03	6	57	-0.19
0.007	-87	-16	20	0.157	0.445	-3.4E-03	-7.4E-03	8	60	-0.16
0.008	-104	-19	20	0.155	0.457	-3.3E-03	-7.6E-03	13	73	-0.18

C. STRAIN VERSES DEPTH

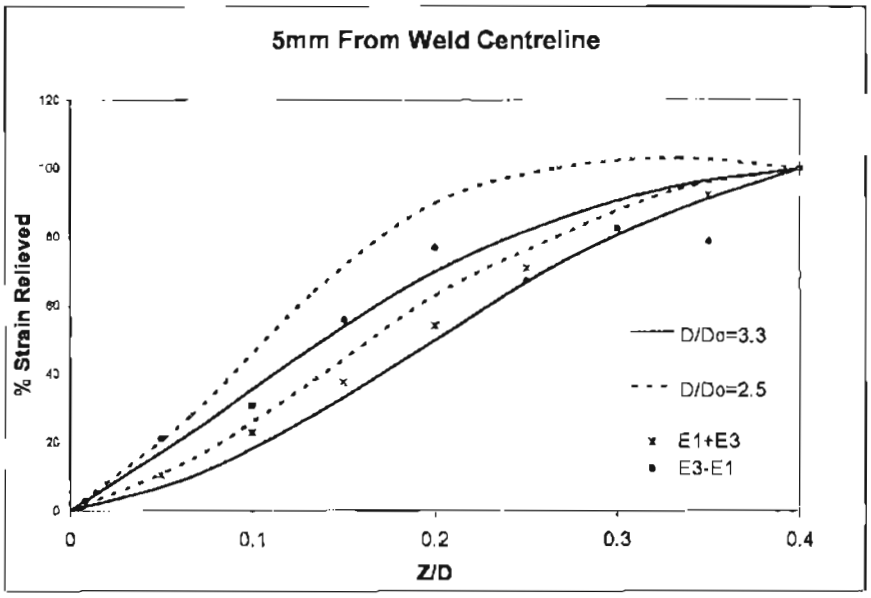

Figure C.1: Strain verses depth data for a measurement made 5mm from the weld centreline, plotted on the ASTM Standard E837 scatterband.

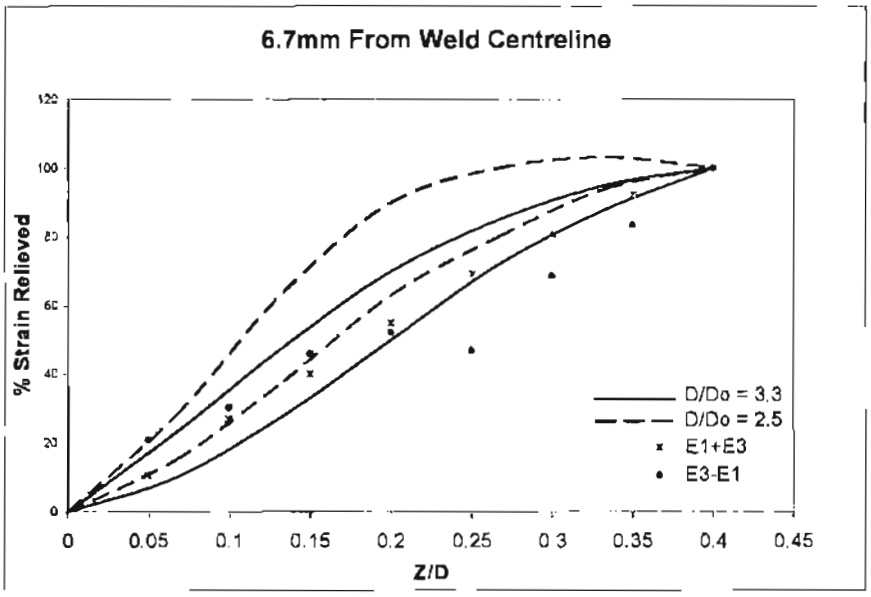

Figure C.2: Strain verses depth data for a measurement made 6.7mm from the weld centreline, plotted on the ASTM Standard E837 scatterband.

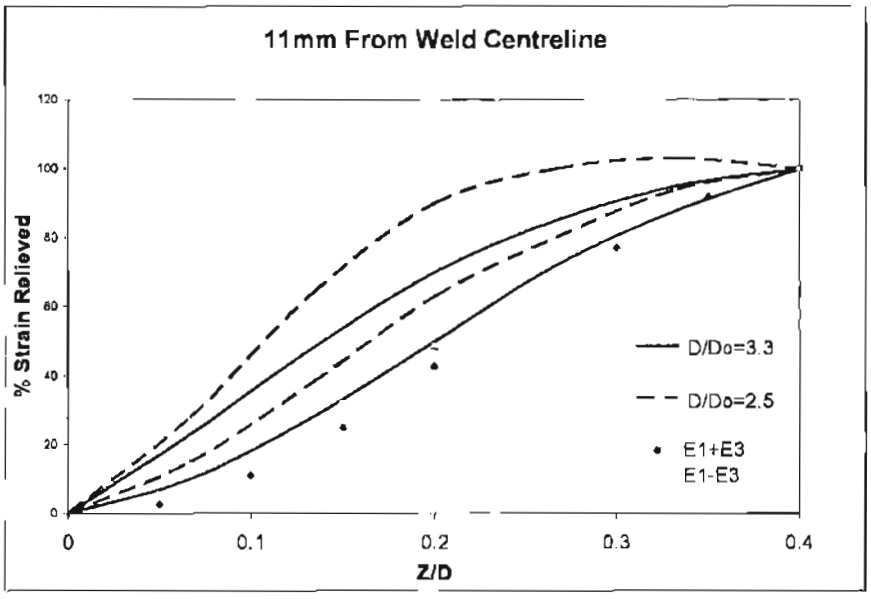

Figure C.3: Strain verses depth data for a measurement made 11mm from the weld centreline, plotted on the ASTM Standard E837 scatterband.

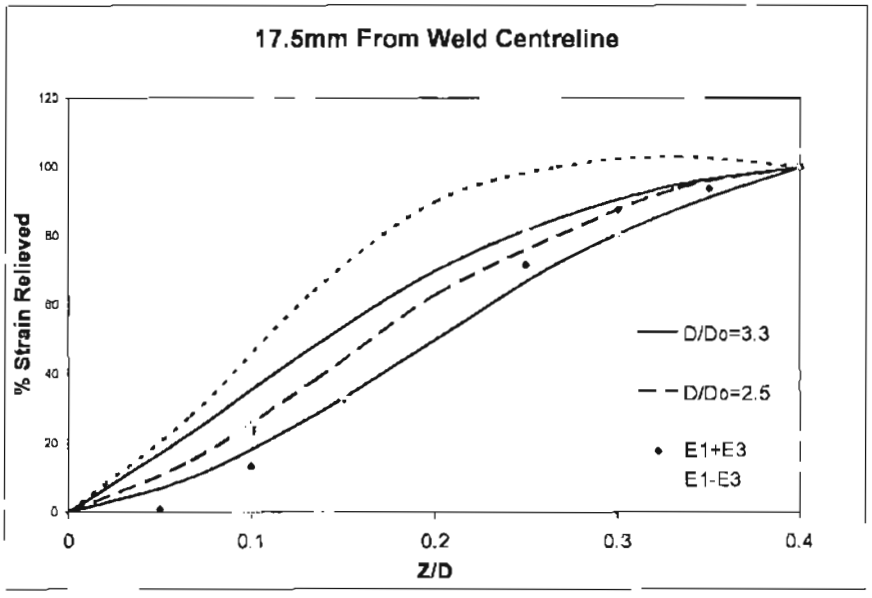

Figure C.4: Strain verses depth data for a measurement made 17.5mm from the weld centreline, plotted on the ASTM Standard E837 scatterband.

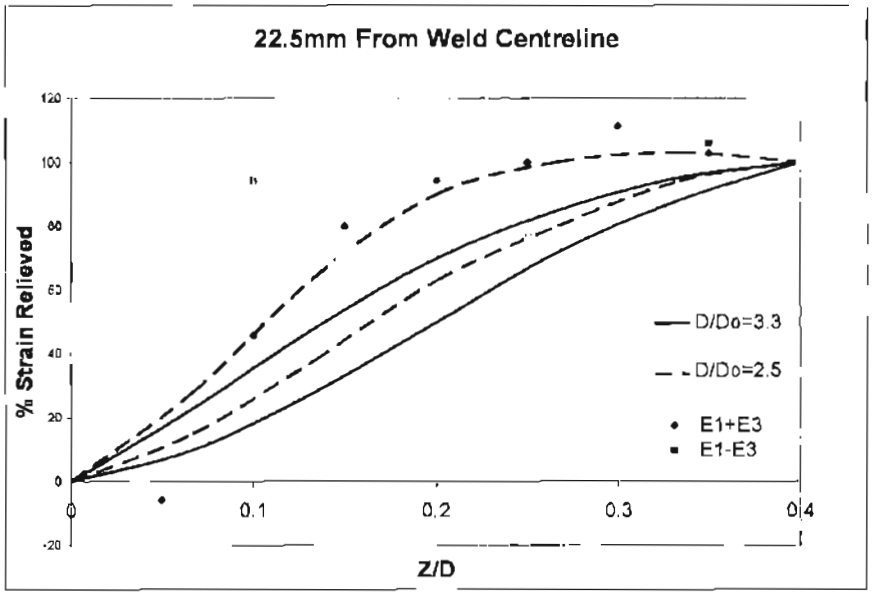

Figure C.5: Strain verses depth data for a measurement made 22.5mm from the weld centreline, plotted on the ASTM Standard E837 scatterband.

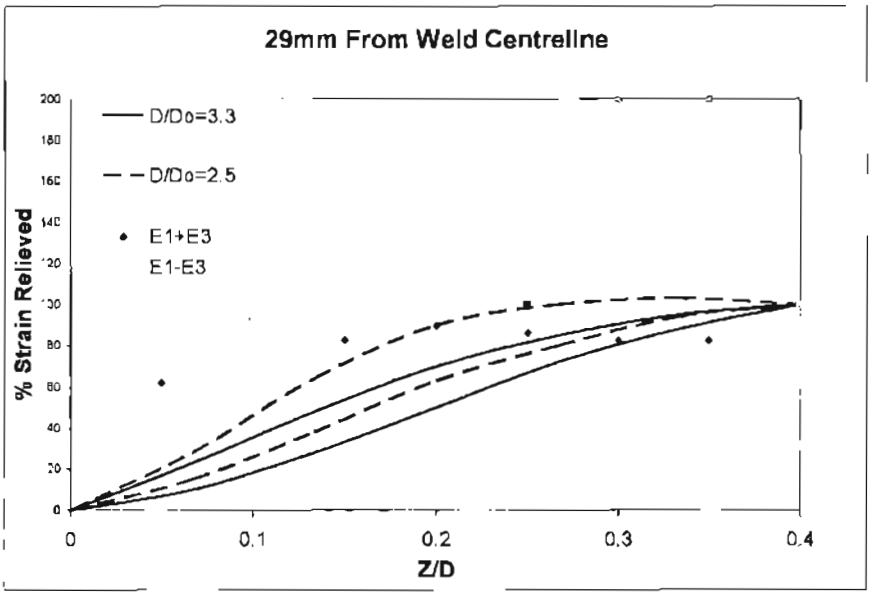

Figure C.6: Strain verses depth data for a measurement made 29mm from the weld centreline, plotted on the ASTM Standard E837 scatterband.

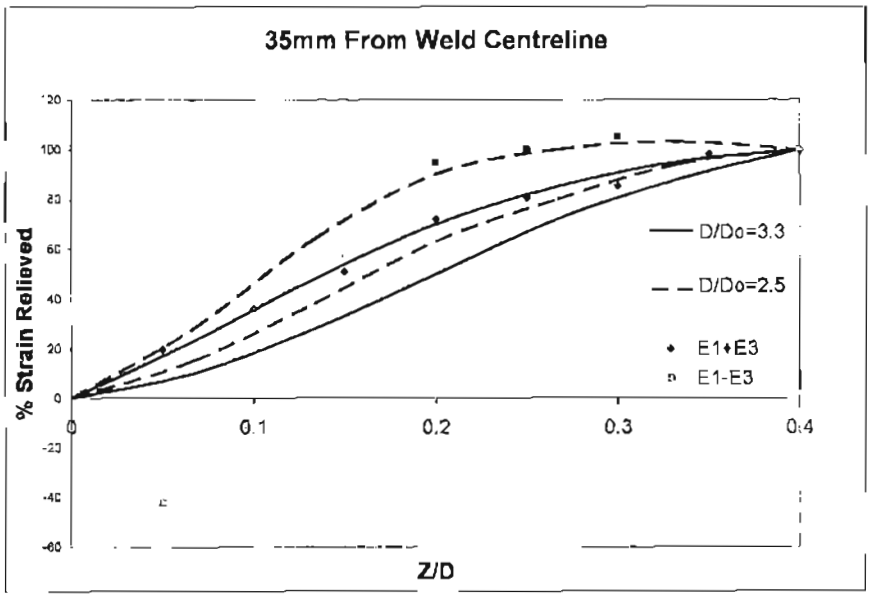

Figure C.8: Strain verses depth data for a measurement made 35mm from the weld centreline, plotted on the ASTM Standard E837 scatterband.

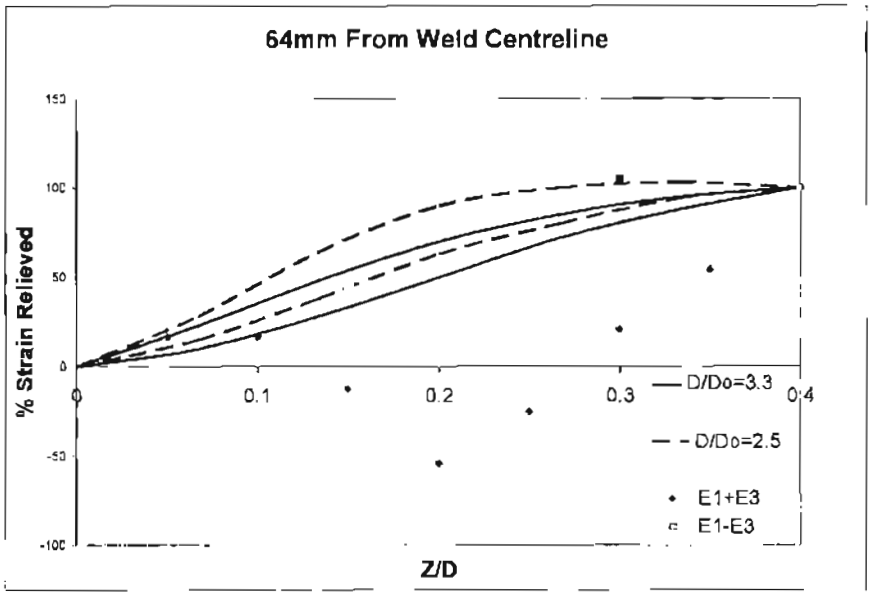

Figure C.9: Strain verses depth data for a measurement made 64mm from the weld centreline, plotted on the ASTM Standard E837 scatterband.

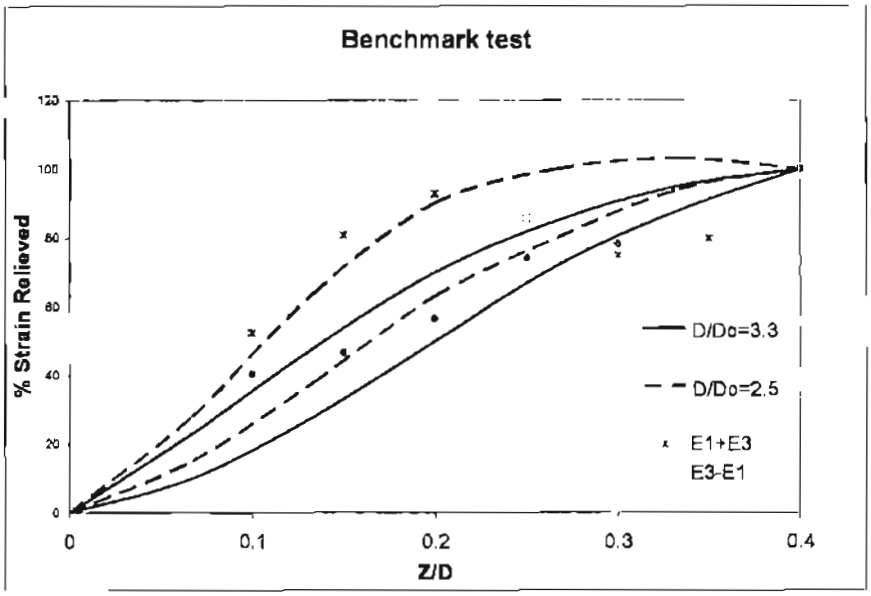

Figure C.10: Strain verses depth data for a measurement made on the benchmark test, plotted on the ASTM Standard E837 scatterband.

D. PUBLICATIONS ARISING FROM THIS THESIS

Dunstone, A.J., Wahab, M.A. and Painter, M.J. (2003) *An Experience in Residual Stress Modelling and Verification*, Submitted to the Journal of Strain Analysis for Engineering Design

Dunstone, A.J., Wahab, M.A. and Painter, M.J. (2002) *Computer Simulation of Pipeline Construction*, Welding Technology Institute of Australia (WTIA) Conference, Sydney

Dunstone, A.J., Wahab, M.A. and Painter, M.J. (2001) *Stress Development of Pipeline Girth Welds*. International Conference on Advanced Materials Processing Technologies (AMPT), Spain

Dunstone, A.J., Wahab, M.A. and Painter, M.J. (2000) *Stress Development of Pipeline Girth Welds*. Welding Technology Institute of Australia (WTIA) Conference, Melbourne